STUDY OF THE WHOLE CELIAC GANGLION AND OF ARTERY-PROJECTING AND VEIN-PROJECTING PATHWAYS IN THE CELIAC GANGLION

By

Amit Harendra Shah

A DISSERTATION

Submitted to
Michigan State University
in partial fulfillment of the requirements
for the degree of

Neuroscience—Doctor of Philosophy

2014

ABSTRACT

STUDY OF THE WHOLE CELIAC GANGLION AND OF ARTERY-PROJECTING AND VEIN-PROJECTING PATHWAYS IN THE CELIAC GANGLION

By

Amit Harendra Shah

The rat celiac ganglion (CG) contains ~10,000 sympathetic postganglionic neurons that innervate abdominal organs and the corresponding splanchnic vascular bed that supplies these organs. Splanchnic circulation holds approximately one-third of total blood volume and is a major source of blood redistribution to other vascular beds. In hypertension, blood from the high-capacitance splanchnic circulation may get redistributed to the low-capacitance central compartment, increasing arterial pressure. Surgical removal of the whole CG attenuates the development of hypertension, which suggests that the sympathetic innervation of the splanchnic circulation functions to regulate systemic arterial pressure. However, the pattern of hypertension-related increase in sympathetic activity of the ganglionic neurons that innervate the splanchnic vasculature is not known. Furthermore, the distribution of postganglionic sympathetic axons to the mesenteric vasculature is not fully understood. The studies reported in this dissertation address these two deficits in our knowledge by 1) comparing the levels of activation of CG neurons in normotensive rats to levels in hypertensive rats; 2) examining the extent and distribution of CG neuron innervation of mesenteric arteries and veins. Collectively, these studies suggest that there is not widespread increased activation of CG neurons in hypertension; in fact, neurons show a reduced sensitivity to activation by nicotine. Also, 72% of neurons that innervate mesenteric arteries and veins distribute their axons to widely separated vessels. This suggests that activation of relatively small number of ganglionic neurons can constrict the entire mesenteric circulation.

In Chapters two and three of this dissertation, factors in the whole CG that are influenced by hypertension are studied. In Chapter two, 5-HT was measured in the whole CG as it can activate sympathetic postganglionic neurons. It was found to be synthesized in a substrate-independent manner in the CG. While 5-HT levels were not different between normotensive and hypertensive CGs, lower gene expression was measured for TPH2 and for 5-HT_{3A} in hypertensive compared to normotensive CGs. In Chapter three, higher c-fos expression was observed at 6 Hz than 2 Hz preganglionic nerve stimulation indicating that c-fos expression is a good marker of neuronal activation. Basal levels of neuronal activation were similar between normotensive and hypertensive CGs but following preganglionic nerve stimulation and nicotine treatment, a smaller increase in c-fos expression was observed in hypertensive than normotensive sympathetic ganglia. Thus, these findings together question whether sympathetic activity is higher in the whole ganglion and instead, whether specific pathways in the CG may be overactive in hypertension.

Artery-projecting and vein-projecting sympathetic pathways were studied in Chapters four and five using a novel, *in vivo* preparation where tracers were applied to small segments of adjacent mesenteric arteries and veins. Two PRVs were initially used but control experiments indicated that they competed for productive replication in a given neuron and instead, PRV was used with CTb. A majority of labeled CG neurons (60%) projected to both arteries and veins while the remainder projected to either arteries or veins. Moreover, a majority of labeled neurons (72%) projected widely to either arteries or veins that supplied different segments of the small intestine while the remainder of neurons had narrower projection fields. Hence, arteries and veins can be both separately and jointly regulated and also, different subsets of neurons may project to widely separated blood vessels or to more narrowly spaced targets.

ACKNOWLEDGEMENTS

This endeavor was only possible through a great deal of support from my advisor, Dr. Kreulen, collaborators, family, and friends. I would like to thank Dr. Kreulen for introducing me to the study of autonomic ganglia, which after microscopically researching for several years has led to a better understanding of the broader fields of Neuroscience and Physiology. Also, thank you for encouraging me to find the questions that I found interesting and for guiding me in my pursuit of answers. The individual support, technical guidance, and helpful ideas of all my committee members, Drs. Keith Lookingland, Cynthia Jordan, and Gregory Fink, are also deeply appreciated.

I was very privileged to work alongside such excellent colleagues: thank you Dr. Timothy Houchin, Dr. Casey Henley, Bradley Hammond, Dr. Lynnette Gerhold, AnnaLiese Durling, and Amy Porter for your support. In addition, Dr. Timothy Houchin provided invaluable help with anatomy and nerve stimulation of sympathetic ganglia, Dr. Lynnette Gerhold kindly reviewed dissertation chapters, and Bradley Hammond did all cell counts of c-fos immunoreactivity. Work with viral tracers was conducted in collaboration with Drs. Alan Sved, Patrick Card, and Georgina Cano at University of Pittsburgh.

My parents, Meena and Harendra Shah, inspire me to challenge myself and to persist through these challenges and I am grateful to them for that. Last, but not least, I would like to thank my dear companion, Aisha, for her continual faith, love, and encouragement that motivate me to move forward and to do better in so many aspects in my life.

TABLE OF CONTENTS

LIST OF TABLES

LIST OF FIGURES

KEY TO ABBREVIATIONS

2-DG	2-deoxy-D-glucose
5-HT	5-hydroxytryptamine or serotonin
5-HIAA	5-hydroxyindoleacetic acid
AAD	amino acid decarboxylase
AAV	adeno associated virus
ACH	acetylcholine
ATP	adenosine triphosphate
CG	celiac ganglion
CGRP	calcitonin gene related protein
CTB	cholera toxin subunit b
DAPI	diamidinophenylindol
DOCA	deoxycorticosterone acetate
DRG	dorsal root ganglion
EGFP	enhanced green fluorescent protein
FC	frontal cortex
HBSS	Hanks' balanced salt solution
H&E	hematoxylin and eosin
HPLC	high performance liquid chromatography
HRP	horseradish peroxidase
HSV	herpes simplex virus
IMG	inferior mesenteric ganglion
IR	immunoreactive
MAO	monoamine oxidase
MCFP	mean circulatory filling pressure

NE	norepinephrine
NPY	neuropeptide Y
NSD-1015	3-Hydroxybenzylhydrazine dihydrochloride
PFA-LP	paraformaldehyde-lysine-periodate
PPIA	cyclophilin A
PRV	pseudorabies virus
PVN	paraventricular nucleus
RFP	red fluorescent protein
RT-PCR	real time reverse transcription-polymerase chain reaction
SERT	serotonin reuptake transporter
SHR	spontaneously hypertensive rats
SOM	somatostatin
TPH	tryptophan hydroxylase
WKY	Wistar Kyoto rats

CHAPTER ONE: GENERAL INTRODUCTION

Splanchnic sympathetic nerves originate from the celiac ganglion (CG) and innervate abdominal organs including the stomach, spleen, liver, pancreas, kidneys, small intestine, and colon (Li et al., 2010). These nerves also innervate the blood vessels supplying these organs and collectively, splanchnic circulation contains approximately one-third of total blood volume (Rothe, 1983). As this is the largest reservoir of blood in our bodies, it is an important source of blood redistribution. For instance, during exercise, blood gets redistributed from splanchnic circulation to muscles (Rowell, 1973, Perko et al., 1998). Also, redistribution of blood is thought to be an underlying mechanism behind hypertension. Venous capacitance is decreased in animal models of hypertension (Samar and Coleman, 1979, Young et al., 1980, Martin et al., 1998, King et al., 2007) and in human patients (London et al., 1978), which shifts blood into the arterial side of circulation, thereby increasing arterial pressure.

The CG plays an important role in arterial pressure regulation but how sympathetic postganglionic neurons within the CG is not fully understood. Celiac ganglionectomy attenuates the development of hypertension in several animal models of hypertension (King et al., 2007, Kandlikar and Fink, 2011b, Ye et al., 2011). Surgical sectioning of the splanchnic nerves was also used to successfully treat hypertension in human patients several decades ago (Hoobler et al., 1951). However, how sympathetic postganglionic neurons in the CG contribute to hypertension is unknown. One possibility is that neurotransmitter levels in the CG are altered in hypertension. Another possibility is that neuronal activation of sympathetic postganglionic neurons is increased in hypertension. Chapters two and three of my dissertation will examine these two possibilities by comparing the 5-HT system and c-fos expression, respectively, in normotensive and hypertensive CGs.

Specific neuronal populations in the CG may contribute to hypertension distinctly. It may be that mesenteric arteries and veins are innervated by separate, overlapping, or a mixture of separate and overlapping populations of sympathetic postganglionic neurons in the CG. If all vascular-projecting neurons innervate both arteries and veins, then resistance and capacitance, respectively, would not be differentially regulated. However, in the instance of hemorrhage, capacitance is decreased but resistance is not affected (Price et al., 1966). Alternatively, if artery-projecting neurons are altogether distinct from vein-projecting neurons, then there is no common mechanism of constricting both arteries and veins together. Instead, with a mixture of separate and overlapping sympathetic postganglionic neurons projecting to arteries and veins, there would be a common mechanism for constricting all blood vessels and also, a way to separately influence resistance and capacitance. The sympathetic innervation of mesenteric arteries and veins will be studied using two pseudorabies viruses (PRVs) in Chapter four and using a PRV and cholera toxin subunit b (CTb) tracer combination in Chapter five.

The divergence of vascular-projecting neurons and convergence of sympathetic innervation to mesenteric blood vessels are not known. It is possible that vascular-projecting neurons do not diverge at all and each neuron innervates a unique section of blood vessel. In this case, blood flow can be altered within small regions of the splanchnic circulation. However, such fine control may not be necessary and indeed, there are no known reports showing changes in blood flow within blood vessels to a single organ. Alternatively, it is possible that a single neuron diverges to cover all of splanchnic circulation. However, this would allow for no regional differences in blood flow to different abdominal organs and such differences are noted to occur (Perko et al., 1998). Lastly, it is possible that for blood vessels going to any one organ in the splanchnic vascular bed, there are some neurons that diverge widely to all these blood vessels

and some neurons that diverge more narrowly. The divergence of vascular-projecting neurons innervating blood vessels supplying the small intestine is investigated in Chapter five.

SYMPATHETIC NERVOUS SYSTEM

Sympathetic control of arterial pressure originates at blood vessels, continues in sympathetic ganglia, in the spinal cord, and concludes in the brainstem (**Fig. 1.1**). The nucleus tractus solitarius receives input from baroreceptor sensory nerves that project from the carotid sinus and aortic arch, via the IXth and Xth cranial nerves, respectively (reviewed in Sved et al., 2003, Guyenet, 2006). This input is excitatory to second order sensory neurons in the nucleus tractus solitarius, and increases in arterial pressure are shown to increase activity of these neurons. The nucleus tractus solitarius provides excitatory, glutamergic projections to the caudal ventrolateral medulla, which provides inhibitory, gamma-aminobutiric acid-ergic projections to presympathetic neurons in the rostral ventrolateral medulla. The rostral ventrolateral medulla, in turn, provides excitatory, glutamergic projections to preganglionic neurons in the spinal cord, which then provide excitatory, cholingeric projections to postganglionic neurons in paravertebral and prevertebral ganglia. The brainstem and spinal cord are important in generating (Barman et al., 2001) and relaying, respectively, tonic sympathetic vasomotor tone but it is the sympathetic postganglionic neurons in sympathetic paravertebral and prevertebral ganglia that directly innervate arteries and veins. Paravertebral ganglia innervate the central vascular compartment while prevertebral ganglia, namely the CG, innervates the splanchnic vascular compartment (Hsieh et al., 2000). All the above regions are integral for both short-term and long-term regulation of arterial pressure.

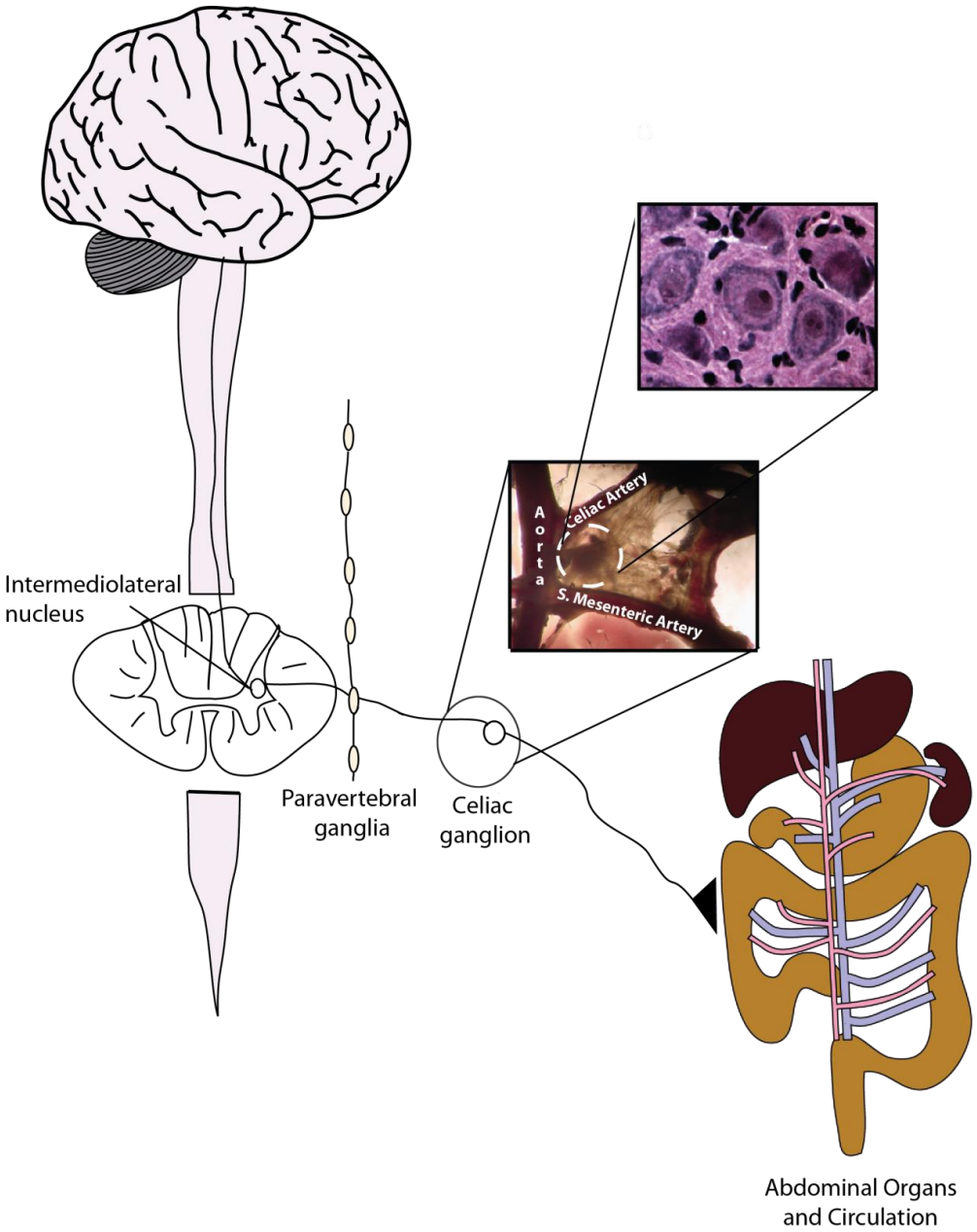

Figure 1.1. Diagram of the central and peripheral branches of the sympathetic nervous system with an emphasis on the CG, a prevertebral sympathetic ganglion. The sympathetic pathway is shown from brainstem to IML (central branches) to paravertebral and prevertebral ganglia (peripheral branch). The anatomical location of the CG is shown under an image taken with a dissecting microscope. The cell morphology within a CG is shown with an H&E micrograph showing sympathetic postganglionic neurons and satellite cells. A schematic is shown of the main innervated targets of the CG.

SYMPATHETIC GANGLIA

Sympathetic ganglia include paravertebral and prevertebral ganglia that are structurally and functionally different from each other (reviewed in McLachlan, 1995). Paravertebral ganglia form a bilateral chain that lie on either side of the spinal cord. Prevertebral ganglia form a single lobe or multiple fused lobes that lie on the ventral part of the aorta caudal to the diaphragm (**Fig. 1.2**). Paravertebral and prevertebral ganglia both receive innervation from preganglionic neurons in the interomediolateral nucleus of the thoracic and lumbar spinal cord. In addition, prevertebral ganglia receive innervation from sensory neurons and enteric neurons. Paravertebral ganglia provide sympathetic innervation to cranial and thoracic targets, while prevertebral ganglia provide sympathetic innervation to abdominal and pelvic targets, including the splanchnic vascular compartment.

The CG plexus (henceforth referred to as CG) is made up of two lobes of the CG and the superior mesenteric ganglion. It innervates the stomach, small intestine, proximal large intestine, liver, pancreas, spleen, and partially innervates both kidneys (Li et al., 2010). The inferior mesenteric ganglion (IMG) innervates the distal large intestine, rectum, bladder, and genitals (Langley and Anderson, 1895). The splanchnic ganglion (also referred to as the greater splanchnic ganglion) innervates the kidneys (Sripairojthikoon and Wyss, 1987).

Structurally, paravertebral and prevertebral ganglia are similar: they are encapsulated by a sheath of connective tissue, contain blood vessels and connective tissue within them, and contain clusters of sympathetic postganglionic neurons that are individually surrounded by satellite cells (reviewed in McLachlan, 1995). In addition to neurons and satellite cells, small intensely fluorescent (SIF) cells are also observed in sympathetic ganglia.

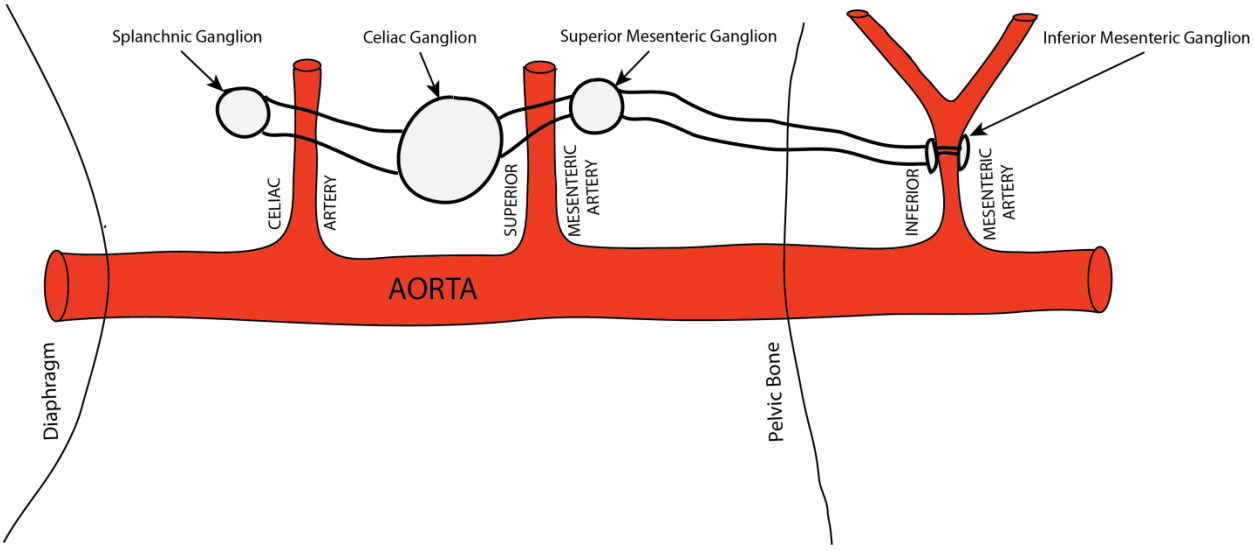

Figure 2.2. Illustration of the anatomical location of prevertebral ganglia in proximity to major blood vessels. Prevertebral ganglia are located parallel to the abdominal aorta. The splanchnic ganglion is rostral to the celiac artery; the CG is caudal to the celiac artery but rostral to the superior mesenteric artery; the superior mesenteric ganglion lobe of the CG plexus is caudal to the superior mesenteric artery; and the inferior mesenteric ganglion is located on either side of the inferior mesenteric artery. The relative size of the ganglia are also indicated in the illustration with the CG being the largest in size and the inferior mesenteric ganglion being the smallest in size.

Sympathetic Postganglionic Neurons

Most sympathetic postganglionic neurons synthesize and release norepinephrine but some neurons, mainly in paravertebral ganglia, are cholinergic and project to sweat glands (reviewed in McLachlan, 1995). In addition, many other neurotransmitters have been identified in ganglia including 5-HT, neuropeptide Y (NPY), somatostatin (SOM), substance P, calcitonin gene related protein (CGRP), and adenosine triphosphate (ATP). Some of these, including NPY, SOM, substance P, and ATP act as cotransmitters; others, including substance P and CGRP, are released in sympathetic ganglia from cell bodies located in sensory ganglia; and 5-HT is thought to be synthesized and released from SIF cells in sympathetic ganglia.

The size and complexity of dendritic fields and soma size of sympathetic postganglionic neurons are influenced by the target size. This was determined by surgically manipulating the size of the submandibular salivary duct and then measuring dendritic arborization and soma size of neurons projecting to this target (Voyvodic, 1989). Smaller and less complex dendritic fields and smaller soma sizes were found in neurons innervating ligated submandibular salivary ducts than intact ducts. This may mean that sympathetic neurons projecting to different targets may differ in size according to target size or innervation density of the target.

Sympathetic postganglionic neurons can be classified as tonic or phasic neurons based on their electrophysiological response (reviewed in McLachlan, 1995). In response to a sustained stimulus, tonic neurons fire action potentials throughout the stimulus duration, whereas phasic neurons fire a burst of action potentials at the onset of the stimulus. The exact proportion of phasic and tonic neurons varies between different sympathetic ganglia (**Table 1.1**) and this

	Tonic	Phasic
Activation response to depolarization	Sustained	Burst
Location of relative predominance	Prevertebral ganglia (~60%)	Paravertebral ganglia (~80%)
Synaptic input type	Weak	Strong, some weak (~16%) in prevertebral ganglia
Dominant potassium channel	M-channel: open slowly after depolarization	A-channel: transient outward currents, not inactivated at potentials > resting membrane potential
Relative soma size	Larger	Smaller
Total dendritic length	Larger	Smaller
Average length of dendrites	Larger	Smaller

Table 1.1. Tonic-firing and phasic-firing sympathetic postganglionic neurons differ in anatomical location, morphology, and ion channel expression. Tonic-firing neurons have a sustained activation response to depolarization whereas phasic-firing neurons have a burst response to depolarization. The anatomical, electrophysiological response, and morphological differences between tonic and phasic neurons is summarized above (Janig and McLachlan, 1992a, Boyd et al., 1996).

presumed to reflect the different subpopulations of neurons going to different targets (discussed in detail below).

SIF Cells

SIF cells are named based on the strong catecholamine fluorescence they exhibit (reviewed in Tanaka and Chiba, 1996, Hanani, 2010). They are spherical in shape and smaller than neurons but larger than glial cells in size. There is considerable evidence suggesting that SIF cells function as interneurons. For instance, some SIF cells are observed to be directly innervated by preganglionic neurons and send out processes that synapse with neighboring neurons. SIF cells can also synthesize neurotransmitters like serotonin (5-HT) that are not synthesized elsewhere in sympathetic ganglia (Happola, 1988). Many sympathetic neurons are responsive to 5-HT (Knoper et al., 1992), suggesting that SIF cells can modulate synaptic transmission in sympathetic ganglia. Additionally, SIF cells are located in close proximity to blood vessels in sympathetic ganglia, indicating that SIF cells may also have a paracrine function.

Satellite Cells

Satellite cells serve as glial cells in autonomic and sensory ganglia. Each sympathetic neuron is surrounded by several satellite cells. Striking characteristics of satellite cells include: small volume of satellite cells relative to sympathetic neurons and relatively large size of satellite cell nuclei relative to neuronal nuclei (**Fig. 1.1**). In sympathetic ganglia, satellite cells act as a blood-ganglion barrier preventing large molecules from penetrating to sympathetic neurons (reviewed in Hanani, 2010). In addition, satellite cells cover axon terminals on or near somata of sympathetic postganglionic neurons, which may allow satellite cells to influence synaptic

transmission. Gap junctions are present on satellite cells of sympathetic ganglia allowing the passage of ions and small metabolites. As in astrocytes (reviewed in Kielian, 2008), gap junctions on satellite cells may play an important role in regulating pH, potassium, and neurotransmitter levels. Gap junctions in the central nervous system are also important targets of modulation during pathophysiological conditions like inflammation by pathogenic stimuli and cytokines.

Convergence and Divergence of Preganglionic and Postganglionic Input

There is considerable divergence of preganglionic input to postganglionic neurons (ratio of pre-to-postganglionic neurons is approximately 1:10) (reviewed in Janig and McLachlan, 1992a). Moreover, any given postganglionic neuron also receives convergent innervation from several different preganglionic neurons. Similarly, targets of sympathetic postganglionic neurons receive convergent innervation from many different neurons. For instance, a 1 mm^2 area of skin is innervated by ~75 sympathetic postganglionic neurons (Gibbins et al., 1998). Also, similar to preganglionic neurons, postganglionic neurons diverge to innervate large areas of vasculature. For instance, a single neuron can innervate a wide region of skin as much as 7 mm in length, which must contain many diverging blood vessels (Gibbins et al., 1998). What is still unknown is whether this divergence is specific to single organs or extends to multiple organs.

Intraganglionic Organization

Dendrites of sympathetic postganglionic neurons can envelop other neurons, forming pericellular dendritic nests (Cajal, 1995). Moreover, dendrites of nearby neurons often clump together to form dense glomeruli. Since synaptic terminals are found at both dendrites and soma

of sympathetic postganglionic neurons, dendritic glomeruli may be a target of dense preganglionic input. In addition to axodendritic and axosomatic synapses formed by preganglionic neurons on postganglionic neurons, dendrodendritic and dendrosomatic synapses are also formed between different postganglionic neurons (reviewed in Gibbins and Morris, 2006). Such synapses are observed between dendrites of one neuron that surround a neighboring neuron and also between dendrites of neighboring neurons. These synapses are thought to participate in inhibitory norepinephrinergic communication (Kawai and Senba, 1997). An interesting possibility from this intraganglionic organization pattern is that neuronal populations may form distinct neural networks within sympathetic ganglia. This would make it easier for a group of neurons projecting to a given target to interact with each other.

SYMPATHETIC GANLGIA: GENERALIZED RELAYS OR SPECIALIZED INTEGRATORS?

The concept of mass activation of the sympathetic ganglia can be traced back to Walter Canon (reviewed in Janig and McLachlan, 1992b). He described the mass activation of sympathetic ganglia in response to an acute stressor. This 'fight-or-flight' response is reported in most Physiology textbooks and implies that sympathetic ganglia functions as a generalized relay between the central nervous system and innervated end organs. However, sympathetic ganglia respond by mass activation only to this type of physiological scenario, i.e., one demanding an urgent and immediate response. It is not at all clear whether sympathetic ganglia generally respond this way to all physiological stimuli.

Integration of Signals in Sympathetic Ganglia

Early evidence that the sympathetic nervous system actually integrates signals from many sources comes from intracellular recordings of sympathetic postganglionic neurons showing the presence of subthreshold postsynaptic potentials (Eccles, 1955, Crowcroft and Szurszewski, 1971). This indicates that summation of subthreshold postsynaptic potentials occurs as input from several sources is combined into a single output (reviewed in Kreulen, 1984). The concept of integration is also supported anatomically since prevertebral ganglia receive input from many different sources including: preganglionic neurons in the intermediolateral nucleus of the spinal cord (Langley, 1893), sensory neurons in dorsal root ganglia (Crowcroft and Szurszewski, 1971), intestinofugal neurons in the gut (Kreulen and Szurszewski, 1979b, a), and from the celiac branch of the vagus nerve (Rosas-Ballina et al., 2008). More recently, intracellular recordings were made *in vivo* in anesthetized rats from lumbar sympathetic postganglionic neurons projecting to vasculature (Bratton et al., 2010). This study showed that 'strong' inputs, which originate from one presynaptic fiber accounted for 32% of action potentials observed whereas the remainder were driven by integration of several 'weak' synaptic inputs. This is one of the first studies to show that *in vivo*, sympathetic ganglia behave not just as a relay for strong inputs but also as integrators of weak inputs.

Distinct Pathways through Sympathetic Ganglia

More detailed analyses of sympathetic ganglia show further evidence of a specialized, rather than generalized, system. For instance, sympathetic neurons classified as phasic and tonic neurons (as discussed above) show general differences in location, input type, and expression of potassium channel subtype (**Table 1.1**) (reviewed in Janig and McLachlan, 1992a). While

general anatomical and functional differences exist between phasic and tonic neurons, none of these properties holds true for all phasic and all tonic neurons. For instance, careful morphological analyses of phasic and tonic neurons indicates that soma area is larger for tonic (1258±508 μm^2; n=17) than phasic (754±273 μm^2; n=18) neurons; however, there is a great deal of overlap between the two populations (Boyd et al., 1996).

Another way to classify different sympathetic postganglionic neurons is by neurochemical makeup as observed via immunohistochemistry (Elfvin et al., 1993). As many as 90% of sympathetic neurons in paravertebral ganglia are NE-and-NPY-positive. In contrast, only about 65% of sympathetic neurons in prevertebral ganglia are NE-and-NPY-positive. The remainders of NE-positive neurons are either SOM-positive (25%) or lack any of these peptide (10%). Since NE-and-NPY-positive nerve terminals are observed around mesenteric arteries and veins, it is thought that NE-and-NPY-positive neurons project to mesenteric vasculature. Similarly, since NE-and-SOM-positive nerve terminals are observed in the submucosal plexus and are no longer present after sectioned the mesenteric nerves (Costa and Furness, 1984), it is thought that NE-and-SOM-positive sympathetic neurons project there.

The above studies suggest a propensity for NE/NPY neurons to project to blood vessels and for NE/SOM neurons to project to the gut. However, they do not necessarily imply that NPY acts as a marker for all neurons projecting to blood vessels and that SOM acts as a marker for all neurons projecting to the gut. Indeed, retrograde tracing experiments of neurons projecting to blood vessels indicate that not all sympathetic neurons innervating blood vessels contain NPY. When retrograde tracers were applied to cutaneous blood vessels, only ~50% of retrogradely-labeled neurons contained NPY, which was similar to the proportion of NPY-positive neurons in

unlabeled neurons (Gibbins and Morris, 1990, Morris, 1995). Moreover, the neurochemical coding of sympathetic neurons does not relate to whether a neuron is tonic or phasic. ~50% of SOM-positive sympathetic neurons in prevertebral ganglia were tonic and the remainder was phasic (Keast et al., 1993).

The concept of sympathetic ganglia as just a generalized relay has clearly been shown to be false. Instead, it acts as specialized unit involved in both the relay and integration of signals. What is still unclear is whether there are different neuronal populations in sympathetic ganglia. Early attempts to correlate neurochemical makeup (NE/NPY, NE/SOM, or only NE), input type (strong or weak), response to depolarization (tonic or phasic), and cell morphology (soma size, number of dendrites, and average length of dendrites) have only been met with limited success. Ultimately, identifying distinct pathways within sympathetic ganglia requires classifying sympathetic neurons based on their innervated target. It was proposed that neurons projecting to blood vessels are NPY-positive, have a phasic discharge, and receive strong inputs compared to neurons projecting to the gut that are SOM-positive, have a tonic discharge, and receive weak inputs (reviewed in Janig and McLachlan, 1992a). However, the retrograde tracing studies discussed above show that these different categories of sympathetic neurons are not as neatly parsed out as hypothesized. Although anatomically distinct pathways in the sympathetic nervous system may not have different functional characteristics, the selective activation of these pathways may have important functional implications in responding to physiological challenges.

Distinct Pathways through Sympathetic Ganglia to Arteries or Veins

There is direct and indirect evidence that the arterial or resistance and venous or capacitance components of splanchnic circulation are separately innervated by sympathetic

ganglia (reviewed in Kreulen, 2003). For instance, stimulation of splanchnic nerves resulted in constriction of veins at much lower frequencies (1-2Hz) than constriction of arteries (10-20Hz) (Kreulen, 1986, Hottenstein and Kreulen, 1987). Correspondingly, capacitance in splanchnic circulation was more sensitive to lower frequencies of stimulation than resistance (Karim and Hainsworth, 1976). These observations can be explained by separate sympathetic innervation of arteries and veins but also by different neurotransmitters or receptor levels at the neuroeffector junctions of arteries and veins (Luo et al., 2003, Park et al., 2010).

Direct evidence that arteries and veins have separate sympathetic innervation was previously shown by our laboratory (Browning et al., 1999, Zheng et al., 1999). Retrograde tracing of the inferior mesenteric artery and vein in *ex vivo* preparations showed that there are distinct arterial and venous sympathetic postganglionic neurons in the inferior mesenteric ganglia of guinea pigs. In support of this, separate sympathetic innervation was also found to arteries and veins supplying the rat hindlimb (Dehal et al., 1992). In contrast, Hsieh *et al.* (2000) found that the CG provided largely overlapping sympathetic innervation to mesenteric arteries and veins (~55% of all labeled neurons). However, in that study, primary branches of the superior mesenteric artery and vein were exposed to retrograde tracers without taking care to remove paravascular nerves, which project to other targets like abdominal organs (Hottenstein and Kreulen, 1987). Additionally, the fluorescent tracers used in that study, fast blue and diamidino yellow, are both known to be taken up by fibers of passage (Bratton et al., 2010, Yoshimoto et al., 2010). Thus, it is possible that the tracers were taken up by surrounding paravascular nerves and this resulted in the overlapping sympathetic innervation seen by the authors.

SYMPATHETIC NERVE ACTIVITY IN HYPERTENSION

Sympathetic nerve activity plays an important role in controlling arterial pressure by influencing vasoconstriction of arteries and veins. In general, whole body sympathetic nerve activity positively correlates with arterial pressure in human patients and in animal models of hypertension as measured via sympathetic nerve activity and norepinephrine spillover rate (Esler, 2000, Malpas, 2010). In addition, there is evidence that increased sympathetic nerve activity is involved early during the development of hypertension as it has been observed in patients with borderline hypertension. Early studies in humans using norepinephrine spillover rate measurements indicate that the contribution of sympathetic nerve activity to arterial pressure regulation occurs in a regional rather than global manner (Esler et al., 1984, Esler et al., 1989). For instance, cardiac and renal norepinephrine spillover rates were higher whereas splanchnic spillover rate was not higher in hypertensive patients. While norepinephrine spillover rates provide valuable information about the regional importance of sympathetic nerve activity, they also present several confounds and sympathetic nerve recordings are considered to be a more accurate measurement of sympathetic nerve activity. Regional sympathetic nerve activities have been examined in animal models of hypertension (Osborn et al., 2011) and indicate that splanchnic nerve activity is elevated in several models, renal nerve activity is elevated only in some models (in Dahl salt-sensitive rats (Foss et al., 2013) but not deoxycorticosterone (DOCA)-salt rats (Kandlikar and Fink, 2011a) nor angiotensin-II-salt rats, whereas cardiac (in DOCA-salt rats; Wehrwein et al., unpublished data) and lumbar (in angiotensin-II-salt rats, (Yoshimoto et al., 2010)) sympathetic nerve activities are both not elevated.

Studies where the CG is surgically removed in animal models of hypertension reinforce the idea that splanchnic nerve activity is involved in the development of hypertension. Celiac

ganglionectomy decreases basal arterial pressure and attenuates hypertension in spontaneously hypertensive rats (Ye et al., 2011), angiotensin II-salt hypertensive rats (King et al., 2007), and DOCA-salt hypertensive rats (Kandlikar and Fink, 2011b). In addition, surgical sectioning of the splanchnic nerves was used to successfully treat hypertension in human patients several decades ago (Hoobler et al., 1951). Increased splanchnic nerve activity in hypertension is likely to decrease splanchnic capacitance and cause redistribution of blood to arteries.

ARTERIAL PRESSURE REGULATION

Sufficient arterial pressure is required to transport volumes of blood to and from tissues and is dependent on resistance and blood flow or cardiac output. Changes in cardiac output are likely instigated by changes in cardiac sympathetic nerve activity, which is elevated in human hypertensive patients. Indirect evidence of increased cardiac output in humans is demonstrated by increased heart rate in many hypertensive patients (Widimsky et al., 1957, Eich et al., 1962, Julius and Esler, 1975) and direct evidence is demonstrated by increased cardiac-specific norepinephrine spillover (Esler et al., 1986).

In contrast, animal studies find that cardiac output is not significantly altered during the development of hypertension. For instance, in both aldosterone-induced (May, 2006) and angiotensin-induced (May, 1996) hypertension in sheep, the increase in arterial pressure is not correlated with cardiac output but instead, highly correlated with peripheral resistance. In addition, sympathetic denervation of the heart is shown to have no effect on the development or maintenance of DOCA-salt hypertension in rats (Wehrwein et al., unpublished data). Hence, under pathophysiological conditions like hypertension, cardiac output may be altered as a result

of the disease, but animal studies indicate that changes in cardiac output are unlikely to lead to the development of hypertension.

Arteries and veins both influence arterial pressure but via different mechanisms. Arteries are resistance vessels that have more smooth muscle and are less elastic, whereas veins are capacitance vessels that have less smooth muscle and are more elastic. Resistance in small arteries and arterioles directly influences arterial pressure. However, arterial pressure can also be indirectly influenced by capacitance in veins via both cardiac output and peripheral resistance (reviewed in Fink, 2009). The large capacity of veins allows this low-pressure reservoir to contain as much as two-thirds of the systemic blood volume (Milner, 1990). Redistribution of this large reservoir due to decreased capacitance can increase venous return to the heart thereby increasing cardiac output and arterial pressure in the short term and also, shift blood volume from the venous to arterial side thereby increasing arterial pressure in the long term. This phenomenon can occur under both physiological conditions like exercise and heat stress as well as pathophysiological conditions like hypertension and hemorrhage.

REDISTRIBUTION OF BLOOD

De Jager's experiments in 1886 modeling a closed circulatory system with elastic and rigid tubes formed the basis for our knowledge of the redistribution of blood from different vascular compartments and from the arterial to venous side and vice versa. He proposed that increased resistance in one section of the circulation would increase volume upstream of that section and decrease volume downstream of that section.

The splanchnic circulation, in particular, contains ~1/3 of our blood volume and is thought to play an important role in the redistribution of blood. During physiological stresses like

exercise and heat stress, vasoconstriction occurs in the splanchnic region (Rowell, 1973). When body temperature is increased from 35 to 40 º Celsius in humans, cardiac output increases by 6.6 L/min and this is mainly directed to the cutaneous vascular bed. Simultaneously, splanchnic blood flow decreases 40% (0.6 L/min), renal blood flow decreases 30% (0.4 L/min), and muscle blood flow decreases 7% (0.2 L/min). Hence, of all major vascular beds, the splanchnic vascular bed contributes the most towards redistribution of blood in this physiological stress condition.

Similarly, during submaximal exercise, splanchnic blood flow is reduced by 40% of the resting value in humans (Perko et al., 1998). While total peripheral resistance is reduced, splanchnic and mesenteric resistances corresponding to the celiac artery and superior mesenteric artery, respectively, are both increased. The celiac artery has the predominant influence on this response with a 50% reduction in blood flow compared to only 25% for the superior mesenteric artery. Implicit from this data is that splanchnic capacitance must also be reduced, thereby increasing venous return. This, via the Frank-Starling mechanism, may at least partly account for the threefold increase in cardiac output observed during exercise (Perko et al., 1998). The above examination of blood flow during exercise illustrates the importance of differential regulation of vascular compartments by the sympathetic nervous system. Clearly, accurate measurements of venous tone in humans would greatly advance what we already know about cardiovascular physiology, but these measurements are currently are currently hindered by the lack of valid and reliable techniques (reviewed in Pang, 2001).

Mean circulatory filling pressure (MCFP) is considered the best technique for measuring whole body venous tone (reviewed in Pang, 2001). It refers to the pressure measured in the vasculature immediately after cardiac arrest and after equilibrating arterial and venous pressures.

In the rat angiotensin II-salt model of hypertension, arterial pressure and MCFP both increased throughout the angiotensin II-salt treatment period (King et al., 2007). The ganglionic blocker hexamethonium completely abolished the increase in both arterial pressure and MCFP. In this model of neurogenic hypertension, decreased capacitance via increased venous tone may actively shift blood to the arterial side and thereby, increase arterial pressure. Reduced MCFP has also been found in other animal models of hypertension including spontaneously hypertensive rats (Samar and Coleman, 1979, Martin et al., 1998), angiotensin II –infused dogs (Young et al., 1980), and one-kidney, one-clip Goldblatt hypertensive rats (but see (Edmunds et al., 1990) and (Yamamoto et al., 1983) for exceptions).

Venous compliance measured in hypertensive patients via less accurate techniques like venous occlusion plethysmography also indicate reduced venous compliance (London et al., 1978). Importantly, there is evidence for reduced venous compliance in patients with borderline hypertension (Takeshita and Mark, 1979) and with a family history of hypertension (Widgren et al., 1992) indicating a role for venous capacitance in the development of hypertension.

In healthy subjects, hemorrhage of 15-20% of total blood volume over 30 min did not alter arterial pressure, heart rate, cardiac output, splanchnic blood flow, splanchnic arterial resistance, or central blood volume (Price et al., 1966). However, splanchnic blood volume and splanchnic capacitance were reduced. This is one of the few documented instances of dissociation between resistance and capacitance. There is good rationale for differential control over resistance and capacitance, especially in pathophysiological circumstances like hemorrhage when venoconstriction is required to counter lost blood volume but when simultaneous arterial constriction may lead to ischemia of critical tissue.

NEURAL TRACERS

Many different types of retrograde tracers are available to anatomically trace neuronal circuits following application of tracers to the terminal field of innervation (reviewed in Kobbert et al., 2000). Each of these classes of tracers has its own advantages and disadvantages.

Fluorescent Tracers

The first successful fluorescent tracer used was Evans Blue dye combined with albumin (reviewed in Kobbert et al., 2000). This led to the discovery of many other fluorescent tracers including diamidinophenylindol (DAPI), diamidino yellow, fast blue, true blue, nuclear yellow, and fluorogold. These tracers are weak bases that can cross cell membranes in their uncharged form and accumulate in lysosomes and endosomes due to a favorable pH gradient (Wessendorf, 1991). Most of these tracers are visible in the cell soma of retrogradely labeled neurons under a fluorescent microscope without any need for histochemical processing. Some fluorescent tracers including DAPI, diamidino yellow, and nuclear yellow are expressed only in nuclei, whereas the other tracers are expressed only in the cell soma and not in nuclei. A general disadvantage of this group of tracers is that they are known to be taken up via fibers of passage (Bratton et al., 2010, Yoshimoto et al., 2010).

Non-Fluorescent Tracers

The earliest tracer used in retrograde tracing experiments was the plant enzyme horseradish peroxidase (HRP), which is transported to the cell soma via active retrograde transport (Weiss and Hiscoe, 1948). HRP can be visualized under light after oxidization with hydrogen peroxide and a chromagen like tetramethylbenzidine or 3, 3'-diaminobenzidine.

Alternatively, HRP can be visualized fluorescently with an antibody specific to HRP and a secondary antibody tagged with a fluorophore.

It is now well known that the disease cholera is caused by the microbial toxin, cholera toxin, secreted by the gram-negative bacterium, *Vibrio cholera* (De, 1959). The structure and molecular actions of cholera toxin are well researched (reviewed in Sanchez and Holmgren, 2011). The toxin is made up of two types of subunits connected by a disulfide bond: subunit B is a 56 kDa oligomer composed of five identical light subunits responsible for receptor binding and subunit A is a single heavy 28 kDa toxic subunit. Initiation of toxic effects occurs after binding of subunit B that forms a five-membered ring that binds to the cell surface receptor, monosialoganglioside GM1. After binding to GM1, cholera toxin is endocytosed by the cell via vesicles. It is then actively transported to the endoplasmic reticulum in the cell soma, where subunit A dissociates from subunit B. The A1 portion of the A subunit binds to ADP-ribosylation factor 6, hence exposing its active site allowing it to permanently ribosylate the Gs alpha subunit of the G protein. This leads to constitutive cAMP production causing water and sodium secretion into the lumen of the small intestine, which leads to rapid dehydration.

Cholera toxin subunit B (CTb), the non-toxic part of cholera toxin, is exploited as a retrograde tracer in both the central and peripheral nervous systems (reviewed in Kobbert et al., 2000). CTb binds to GM1, which is abundant in neurons, especially on synaptic membranes; hence, it likely that CTb is taken up specifically at synaptic terminals. Once it is inside the cell, it is retrogradely transported to the cell soma in vesicles and remains in vesicles until lysosomal degradation. Historically, CTb was used in its unconjugated form and visualized under light microscopy following reaction with DAB substrate. However, with the availability of a specific

antibody for CTb, it is now possible to visualize it fluorescently using a secondary antibody tagged with a fluorophore. Alternatively, CTb conjugated with one of several fluorophores is also commercially available but the efficacy of these tracers has not been directly compared with that of unconjugated CTb (Conte et al., 2009). CTb is visualized in labeled neurons as granular staining in cell soma since it remains within vesicles.

Viral Tracers

More recently, alphaherpes viruses including herpes simplex virus (HSV) and pseudorabies virus (PRV) have been exploited as neural tracers (reviewed in Enquist and Card, 2003, Song et al., 2005). Strains of HSV and PRV that are used as tracers are different from wild-type viral strains as is described below. General advantages of viral tracers vs. non-viral tracers are that: 1) they are transynaptic, i.e., they are able to cross synapses to label entire neural circuits whereas non-viral are all monosynaptic; and 2) they are self-replicating that yields higher labeling signal in infected neurons compared to neurons labeled with non-viral tracers. Varying the survival time of experimental animals following exposure to tracers manipulates the number of synapses crossed by the viral tracer.

Virus entry was initially researched for HSV and is shown to parallel that of PRV (reviewed in Norgren and Lehman, 1998, Pomeranz et al., 2005). Attachment to the host cell occurs via the interaction between viral protein gC, which is encoded by gene UL44, to glycosaminoglycans present on heparin sulphate or chondroitin sulphate. While this step increases HSV infection likelihood, it is not necessary for successful infection. However, the interaction between gD and its receptors is required for HSV infection. One of the receptors for gD is the herpesvirus entry mediator and only recently, another receptor for gD was discovered

to be nectin-1, which is an intercellular adhesion molecule. Following receptor-recognition by gD, fusion with the plasma membrane or endocytic vesicle of the target cell is triggered and aided by gB, gH, and gL.

Then, the virus is retrogradely transported towards the cell soma where viral DNA is released into the nucleus through nuclear pores. Viral DNA replicates in the host nucleus independent of host DNA but borrowing the replicative machinery of the host cell. Viral egress from the nucleus to the rest of the cell has also been well researched and occurs similarly for HSV and PRV (reviewed in Norgren and Lehman, 1998, Pomeranz et al., 2005). The proteins US3, UL31, and UL34 are involved in this process. UL31 and UL34 help form the primary enveloped virion that has the virus capsid enveloped with a part of the inner membrane of the nucleus. US3 contributes to de-envelopment of the primary virion and its entry into the cytoplasm. Then, the primary virion loses its primary envelope and gains its final envelope by associating with tegument and envelope proteins and budding into the trans-Golgi apparatus. Several viral proteins are identified to contribute to this process, including UL36, UL37, VP22, UL11, UL37, UL47, UL48, and UL51. Travel of this mature virus to the cell surface occurs within a vesicle from the envelopment compartment of the trans-Golgi apparatus. From this point onwards, wild-type strains of HSV and PRV can continue traveling in both anterograde and retrograde directions.

Wild-Type PRV

Despite the name PRV, which suggests that it is similar to the rabies virus, it is actually part of the same *Alphaherpesvirinae* subfamily of viruses, as is HSV (reviewed in Pomeranz et al., 2005, Muller et al., 2011) . In its native form, PRV was discovered by Aládar Aujeszky in

1902 to cause Aujeszky's disease in swine and other susceptible mammals. PRV infection and subsequent morbidity and mortality depend on age of animal, strain of PRV, and concentration of PRV. In piglets, mortality is near 100% with symptoms typically appearing 3 to 5 days after infection. Symptoms include neurological disorders like ataxia, nystagmus, seizures, trembling, and incoordination. Mortality typically occurs 1 to 2 days after these symptoms appear. In weaned pigs 3 to 9 weeks of age, symptoms after infection are similar to that in piglets but also include respiratory problems like sneezing, nasal discharge, severe cough, and difficulty breathing. However, most animals with these symptoms recover and mortality in this cohort is only around 10%. PRV-infected adult swine predominantly display respiratory problems and mortality is even lower in this cohort at around 2%. If pregnant sows are infected, the virus can cross the placenta and typically lead to fetal death.

While swine are the host species, PRV can also infect and is fatal in many other mammals like cattle, sheep, goats, cats, dogs, raccoons, and rodents (reviewed in Pomeranz et al., 2005, Muller et al., 2011). However, humans and tailless apes are not susceptible to PRV. The predominant symptom in nonnative species is pruritus causing the animal to scratch part of its body till tissue destruction occurs; hence, the disease was called 'mad-itch' in the past.

The virus is shed in saliva and nasal secretions and is spread through oral or nasal contact (reviewed in Pomeranz et al., 2005, Muller et al., 2011). It is highly contagious and can be economically costly as it is capable of wiping out entire herds. Infection can be successfully prevented by a strict regimen of regular vaccinations. The disease is mostly eradicated in Canada, United States, United Kingdom, New Zealand, and some countries in the European Union but remains a concern in most developing countries.

PRV as a Neural Tracer

Tracing with the wild-type PRV Becker strain is well known and has the following characteristics: 1) wild-type PRV can spread in both anterograde and retrograde directions (Brittle et al., 2004). 2) Tract tracing with PRV produces similar results to other commonly used tracers. For instance, after injection in the ventral stomach musculature, both wild-type PRV and CTb were transported to the dorsal motor nucleus of the vagus (Card et al., 1990). 3) PRV infection is contained within a synaptically connected neural circuit and does not spread to regionally adjacent but synaptically unconnected neural circuits. This was shown by specific labeling of the hypoglossal nucleus after PRV injection into the tongue (Card et al., 1990). No PRV labeled neurons were found in the nearby regions of the dorsal motor nucleus of the vagus or nucleus of the solitary tract. 4) PRV infects a wide variety of cell types besides neurons but after infecting a neuronal circuit, PRV is largely confined within neurons in that circuit since nonneuronal cells do not replicate the virus. For instance, PRV can spread from neurons to surrounding astrocytes but since astrocytes do not replicate PRV, they do not contribute to the spread of PRV within a neuronal circuit (Card et al., 1993, Rinaman et al., 1993). 5) An intact neural circuit is required for the transport of PRV. For instance, when the left but not right vagus nerve is severed, PRV injections to the ventral stomach musculature resulted in labeling in the right but not left dorsal motor nucleus of the vagus (Card et al., 1990).

Attenuated PRV strains were produced as live vaccines and contain mutations to reduce virulence. One vaccine strain in particular, PRV Bartha (McFerran and Dow, 1975), has been well characterized and is now routinely used in neural tracing. A direct comparison of virulence between wild-type and attenuated PRV strains shows that injection of wild-type PRV into mice

flank skin is fatal in 3 days, whereas injection of PRV Bartha is fatal in 9 days (Brittle et al., 2004). However, there is some variability in survival time between species and between injection routes. The mutations responsible for reduced virulence in PRV Bartha are in the following genes with the respective viral proteins they encode in parentheses: UL21, UL44 (gC), US8 (gE), US9, US7 (gI), and US2 (reviewed in Pomeranz et al., 2005). Additionally, the mutations to gE, gI, and US9 prevent PRV Bartha from being transported anterogradely. The retrograde-only spread of PRV Bartha makes it easier to analyze neuronal circuits.

Recombinant versions of the PRV Bartha strain that express either enhanced green fluorescent protein (EGFP) or red fluorescent protein (RFP) were created for the purpose of dual tract tracing with PRVs. The EGFP-expressing PRV is known as PRV152 and the RFP-expressing PRV is known as PRV614. These recombinant viruses were created by inserting the fluorescent protein expression cassette into the middle of the gG gene (Banfield et al., 2003, Cano et al., 2004). Neurons infected with these tracers express fluorescent reporter proteins throughout the cell, filling the cell soma and nucleus completely and often also the dendritic arbor and axon. Due to the replicative ability of PRVs, the fluorescent signal is typically intense and visible under epifluorescence microscopy without any need for further tissue processing.

In order to evaluate the ability of PRV152 and PRV614 to work simultaneously, a mixture of both tracers was injected into the anterior chamber of the eye and labeling patterns were examined in the brain of a single rat 96 hr later (Banfield et al., 2003). All brain regions examined contained a majority of double-labeled neurons (~75%), with ~21% being green labeled only and ~4% being red labeled only. These data indicate that the two tracers can be

successfully used for dual tract tracing in the central nervous system, but that there is a slight infection-preference for PRV152 than PRV614.

Studies done in primary cultures of dorsal root ganglion (DRG) provide further details about how PRV152 and PRV614 interact (Banfield et al., 2003). When DRG cultures were simultaneously injected with both tracers, nearly all neurons were double-labeled 24 hr and 48 hr after tracer application. However, when one tracer is applied 2, 4, and 6 hr prior to the second one, then less double labeling is observed 24 hr after application of the last tracer. With a $\geq$ 4 hr delay between tracer applications, only ~1% of DRG cells were double-labeled. In contrast, substantially more double-labeling (~29% of DRG cells) was observed with a 2 hr delay between tracer applications. This suggests that a significant amount of competitive inhibition occurs when the time delay between application of PRVs is > 2 hr.

Wild-Type HSV

HSV is also a member of the *Alphaherpesvirinae* subfamily of viruses (reviewed in (Turner and Jenkins, 1997, Norgren and Lehman, 1998, Song et al., 2005)). Humans are the host species of HSV but the virus can also infect rats, mice, hamsters, rabbits, guinea pigs, and monkeys (Norgren and Lehman, 1998). HSV-1 causes orofacial infections and encephalitis and is the most common form of herpes (reviewed in Whitley and Roizman, 2001). HSV-2 causes genital infections and can be transmitted to a neonate during birth from the infected mother. In the United States, prevalence of HSV-1 and HSV-2 are approximately 58% and 16% of the population, respectively.

To cause infection, HSV enters the body through a mucosal membrane or a skin cut and establishes itself in epithelial cells (reviewed in Whitley and Roizman, 2001). Active replication at this stage activates the immune system and causes formation of a fever blister. HSV can then travel retrogradely to sensory neurons innervating epithelial cells and thereafter, either establish viral replication or establish a latent infection for the lifetime of the infected individual. HSV latency if characterized by the presence of HSV DNA in nuclei of infected neurons and the absence of any viral proteins, which leaves the host's immune system unaware of the virus' presence. During latency, HSV may periodically activate to cause recurring bouts of herpes.

Due to available diagnostic tools and treatment options, HSV infection is rarely fatal. Diagnosis of HSV occurs via polymerase chain reaction detection of HSV DNA or by virus isolation in cell culture (reviewed in Tang et al., 1999). There are currently no vaccines and no cures for HSV; however, antiviral treatments can reduce the severity, duration, and frequency of HSV reactivation from latent state.

HSV as a Neural Tracer

Neural tracing with HSV is less common than with PRV due to the following reasons: 1) Variability in the degree of HSV infection only yields successful infections approximately 50% of the time (Joshi et al., 1995). 2) HSV is not confined and replicated within just neurons of a neural circuit. It is known that HSV can spread to astrocytes adjacent to infected neurons and infected astrocytes will replicate and spread the virus to other synaptically connected cells (Itoyama et al., 1991). This complicates analysis of neural circuits beyond the 1st synapse because labeled 2nd order neurons may not be synaptically connected to 1st order neurons but to

1st order nonneuronal cells. 3) There are no recombinant strains of HSV that endogenously express fluorescent reporter proteins like PRV152 and PRV614.

A strain of HSV-1 isolated originally from a patient with encephalitis, H129, infects sensory neurons up into the dorsal root ganglion, and then progresses anterogradely to the spinal cord and then the brain (Rinaman and Schwartz, 2004). This strain of HSV presents advantages for neural tracing not found with PRV strains and hence, it has been used extensively to examine neuroanatomy of the central sensory circuitry including of the eye, tooth pulp, adipose, and gut tissues.

Use of Viral With Non-Viral Tracers

Co-application of viral with non-viral tracers has been done to distinguish between 1st order labeled neurons and subsequent order labeled neurons, i.e. between direct and indirect neural input, respectively. However, not all tracer combinations are shown to work well together. For instance, application of Fluorogold with HSV to the cornea interfered with the ability of HSV to infect trigeminal neurons (LaVail et al., 1993). Similarly, application of wheat germ agglutin-conjugated to horseradish peroxidase with PRV interfered with PRV infection (Chen et al., 1999). In contrast, CTb does not interfere with PRV infection when both tracers are simultaneously applied to the olivocerebellar pathway located in the ventrolateral medulla (Chen et al., 1999). However, cell counts for PRV-labeled and CTb-labeled neurons showed a positive correlation between survival time and total number of PRV-labeled neurons ($r = 0.72$) but a negative correlation between survival time and total number of CTb-labeled neurons ($r = -0.18$) (correlations were analyzed from data published in table 2 in (Chen et al., 1999). This indicates that the two tracers have different transport and degradation times, and that a compromise for

survival time needs to be reached that yields a good number of both PRV-and-CTb-labeled neurons.

RESEARCH AIM

The overall goals of this dissertation research are: 1) to further elucidate the role of prevertebral sympathetic ganglia in arterial pressure regulation 2) determine whether there are anatomically separate neuronal populations to arteries and veins in sympathetic ganglia 3) study whether sympathetic neurons project narrowly to adjacent vessels or project widely to distantly located blood vessels. Several different techniques are used to accomplish these goals including: high performance liquid chromatography and real-time quantitative polymerase chain reaction to study 5-HT levels, 5-HT synthesis, and gene expression of 5-HT-related genes in the second chapter; immunohistochemistry for c-fos in the third chapter; and use of viral and non-viral retrograde tracer combinations in the fourth and fifth chapters.

SPECIFIC AIMS AND HYPOTHESES

The following specific aims and hypotheses correspond to the four dissertation data chapters:

Specific Aim 1: Are levels of 5-HT or expression of 5-HT related genes changed in sympathetic ganglia due to hypertension?

Hypothesis: 5-HT levels or 5-HT_3 receptor levels are hypothesized to be higher in hypertensive sympathetic ganglia since 5-HT is shown to activate sympathetic neurons via the 5-HT_3 receptor and increased sympathetic activity is noted in hypertension.

Specific Aim 2: Is the basal or the post-stimulus level of neuronal activation different between normotensive and hypertensive sympathetic ganglia?

Hypothesis: Basal and post-stimulus neuronal activation is hypothesized to be higher in hypertensive sympathetic ganglia since increased sympathetic activity is noted in hypertension.

Specific Aim 3: What is the best method for applying retrograde tracers to arteries and veins?

Hypothesis: A combination of two strains of PRV tracers applied *in vivo* to isolated arteries and veins is hypothesized to be the best method for tract tracing from mesenteric arteries and veins.

Specific Aim 4A: Is there separate or overlapping sympathetic innervation to mesenteric arteries and veins?

Hypothesis: Different populations of sympathetic postganglionic neurons are hypothesized to project to either arteries or veins based on previous *in vitro* studies from our laboratory done in guinea pigs.

Specific Aim 4B: What are the innervation patterns for sympathetic postganglionic neurons projecting to mesenteric vasculature?

Hypothesis: Sympathetic postganglionic neurons are hypothesized to project widely to two distantly located arteries or two veins.

CHAPTER TWO: ROLE OF SEROTONIN IN SYMPATHETIC PREVERTEBRAL GANGLIA OF NORMOTENSIVE AND HYPERTENSIVE RATS

ABSTRACT

Serotonin (5-HT) can modulate firing of sympathetic postganglionic neurons in sympathetic prevertebral ganglia. While sympathetic drive is elevated in human hypertensive patients and in many animal models of hypertension, including the deoxycorticosterone acetate (DOCA)-salt rat model, it is unknown whether the 5-HT system is affected by hypertension. It is hypothesized that the 5-HT system is further activated in hypertensive CGs and that this contributes to increased sympathetic activity. Using HPLC, 5-HT and its metabolite, 5-HIAA, was measured in the celiac ganglia (CG) and 5-HT was found to be synthesized *de novo* in the CG but in a substrate-independent manner. 5-HT and 5-HIAA levels were similar in normotensive and hypertensive CGs. Gene expression of the 5-HT synthesis gene, tryptophan hydroxylase (TPH), and 5-HT reuptake gene, 5-HT reuptake transporter (SERT), and 5-HT_3 receptor were measured. Of these genes, TPH2 and 5-HT_{3A} were both downregulated in hypertensive CGs indicating that synthesis and receptor levels may be lower in hypertensive CGs. Accordingly, when 5-HT levels were measured in the spleen, which is largely innervated by the CG, they were found to be significantly lower in hypertensive spleens. Surprisingly, instead of an overactive 5-HT system, we found an underactive one in hypertensive CGs. This challenges the notion that the whole ganglion is overactive in hypertension and instead indicates that specific pathways may be selectively activated in hypertensive CGs.

INTRODUCTION

The autonomic nervous system has central and peripheral branches; the central branch consists of areas in the brain and spinal cord, whereas the peripheral branch consists of sympathetic and parasympathetic ganglia. Sympathetic postganglionic neurons are innervated by preganglionic neurons located in the intermediolateral cell column (IML) of the spinal cord, and innervate blood vessels and peripheral organs. Postganglionic neurons are mainly noradrenergic but other neurotransmitters including neuropeptide Y, somatostatin, vasoactive intestinal polypeptide, and serotonin [5-hydroxytryptamine (5-HT)] are also found in sympathetic ganglia (reviewed in McLachlan, 1995).

5-HT, originally identified as a potent vasoconstrictor, is primarily synthesized in the enterochromaffin cells of the intestine and in discrete areas of the brain (reviewed in Vanhoutte, 1985). It is also localized in prevertebral sympathetic ganglia like the celiac ganglia (CG) within small intensely fluorescent (SIF) cells, a small number of postganglionic neurons, and nerve fibers distributed throughout the ganglion (Ma et al., 1985, Gale and Cowen, 1988, Happola, 1988, Karhula et al., 1995). SIF cells function as interneurons in sympathetic ganglia and it is possible that they may synthesize 5-HT and release it to synaptically connected postganglionic neurons in sympathetic ganglia (reviewed in Tanaka and Chiba, 1996, Hanani, 2010).

There are several proposed functions of 5-HT in sympathetic ganglia. Firstly, 5-HT causes fast depolarization via the 5-HT_3 receptor in ~80% of cultured sympathetic postganglionic neurons (Meehan and Kreulen, 1991, Knoper et al., 1992). Intracellular recordings of neurons in the CG show that 5-HT also causes slow excitatory postsynaptic potentials that are resistant to cholinergic antagonists (Kiraly et al., 1983, Dun et al., 1984). Secondly, 5-HT decreases the

sensitivity of nicotinic acetylcholine (ACh) receptors in sympathetic ganglia by interfering with ACh binding with receptors (Akasu et al., 1981, Akasu and Koketsu, 1986). Lastly, 5-HT also enhances the magnitude of long-term potentiation in sympathetic ganglia via 5-HT_3 receptors (Alkadhi et al., 1996).

The contributions of circulating 5-HT in the blood and neuronal 5-HT in the central nervous system to arterial pressure regulation are well known. For instance, systemic 5-HT levels are positively correlated with arterial pressure and SERT inhibitors like fluoxetine can cause an increase in arterial pressure (Amsterdam et al., 1999, Lazartigues et al., 2000). Also, 5-HT locally administered to the brain via intracerebroventricular injections increases arterial pressure in a dose-dependent manner in rats (Kuhn et al., 1980). Since these findings point to an important role of 5-HT in the pathophysiology of hypertension, it is surprising that the 5-HT system (as shown in **Fig. 2.1**) in sympathetic ganglia has not been further examined in an animal model of hypertension.

The goals of this study are twofold: to further characterize the 5-HT system within sympathetic ganglia and to determine if the 5-HT system locally present in sympathetic ganglia is changed in hypertension. To further characterize the 5-HT system, concentrations of 5-HT and its metabolite, 5-hydroxyindoleacetic acid (5-HIAA), will be measured in the CG. Also, 5-HT synthesis will be examined in the CG and compared to that of serotonergic areas of the brain. To compare the 5-HT system between normotensive and hypertensive rats, 5-HT and 5-HIAA levels will be measured in both groups. Also, genes related to 5-HT synthesis and re-uptake, and genes for the 5-HT_3 receptor subtypes will be quantified and compared between normotensive and hypertensive rats. It is predicted that increased 5-HT levels, increased 5-HT receptor levels,

Figure 2.1. Synthesis and metabolism pathway for 5-HT. The substrate tryptophan is converted into the intermediary product, 5-HTP, via the enzyme tryptophan hydroxylase. 5-HT is then synthesized from 5-HTP via the amino acid decarboxylase (AAD) enzyme and can be further metabolized into 5-HIAA by monoamine oxidase (MAO) enzyme. 5-HT can also be taken up into neurons by 5-HT reuptake transporter (SERT).

increased 5-HT synthesis, decreased 5-HT re-uptake, increased activity of 5-HT neurons, or a combination of these variables will be present in hypertensive CG. In turn, this may contribute to increased excitability of sympathetic postganglionic neurons and more vasoconstriction in hypertensive rats.

METHODS AND MATERIALS

Animals

All of the protocols were approved by the Michigan State University All University Committee on Animal Use and Care. Adult male Sprague-Dawley rats (300-350 g) from Charles River Laboratories (Portage, MI) were used in all studies. Animals were housed two per cage with *ad libitum* access to food and water while being kept on a 12:12 hr light-dark cycle in a room with regulated temperature (22-24°C).

Normotensive sham and hypertensive DOCA-salt rats were prepared as previously described (Luo et al., 2003). Briefly, DOCA-salt rats underwent uninephrectomy, subcutaneous DOCA (200mg/kg) implantation, and had access to drinking water containing 1% NaCl and 0.2% KCl (hypertensive group). Normotensive shams were also uninephrectomized but did not receive an implant of DOCA and had access to normal drinking water (normotensive group). After 4 weeks of this regimen, systolic BP was measured by tail cuff plethysmography [systolic BP=134.4±2.0 mmHg for normotensive rats (n=16) and 186.0±3.6 mmHg for hypertensive rats (n=15)].

Perfusion

The effect of perfusion on 5-HT and 5-HIAA levels in the CG was tested by comparing 5-HT and 5-HIAA levels in CGs of perfused (n=3) and non-perfused (n=3) rats. All rats were euthanized with sodium pentobarbital (80 mg kg^{-1} i.p.) and were either perfused intra-aortically with ice-cold 0.9% sterile saline after making an incision in the right atria or not perfused. CGs

were then dissected from all animals and placed into ice cold 0.1 M phosphate-citrate buffer with 15% methanol and stored at -80°C until further analysis.

Tryptophan and NSD-1015 Treatments

3-Hydroxybenzylhydrazine dihydrochloride or NSD-1015 (#54880, Sigma, St. Louis, MO), an amino acid decarboxylase inhibitor that prevents 5-HT synthesis leading to a buildup of 5-HTP levels, was administered as previously described (Lookingland et al., 1986) to test whether 5-HT synthesis occurs in the CG. NSD-1015 was dissolved in 0.9% sterile saline and rats were treated with either NSD-1015 (100 mg/kg i.p.; n=8) or an equivalent volume of vehicle (n=8). L-tryptophan (#T8941, Sigma, St. Louis, MO) is the precursor of 5-HT and it was used as previously described (Lookingland et al., 1986) to determine whether it could drive increased synthesis of 5-HT. L-tryptophan was dissolved in 0.9% sterile saline, and NSD-1015-and-vehicle-treated rats were treated with either L-tryptophan (100 mg/kg i.p.; n=4) or an equivalent volume of vehicle (n=4). L-tryptophan was administered 1 hr prior to sacrifice and NSD-1015 was administered 30 min prior to sacrifice.

All rats were euthanized with sodium pentobarbital (80 mg kg^{-1} i.p.) and then, CGs and brains were dissected from all animals. CGs were immediately placed into ice cold 0.1 M phosphate-citrate buffer with 15% methanol and stored at -80°C until further analysis. Brains were quickly frozen over dry ice and stored at − 80 °C. Coronal brain sections (500 μm) were prepared on a cryostat (− 10°C) and the paraventricular nucleus (PVN) and frontal cortex (FC) were microdissected using a modification of the Palkovits technique (Palkovits, 1973). Tissue punches were placed into ice cold 0.1 M phosphate-citrate buffer with 15% methanol and stored

at -80°C until further analysis. 5-HT, 5-HIAA, and 5-HTP were measured in all tissues as described below.

Comparisons between Normotensive and Hypertensive Rats

In order to test whether 5-HT and 5-HIAA levels in sympathetic ganglia are affected by hypertension, these levels were compared between normotensive (n=7) and hypertensive rats (n=6). All rats were euthanized with sodium pentobarbital (80 mg kg^{-1} i.p.). CGs were dissected, placed into ice cold 0.1 M phosphate-citrate buffer with 15% methanol, and stored at -80°C until further analysis. In a separate experiment, 5-HT and 5-HIAA levels were compared between normotensive (n=8) and hypertensive (n=8) rats in an innervated target of the CG, the spleen. After euthanizing rats, part of the spleen capsule was dissected from all rats and placed into ice cold 0.1 M phosphate-citrate buffer with 15% methanol, and stored at -80°C until further analysis. Gene expression of 5-HT synthesis (TPH1 and TPH2) and re-uptake genes (SERT) were also compared in CGs from normotensive (n=7) and hypertensive (n=7) rats. After euthanizing rats, CGs were dissected from all rats and placed in Trizol (Invitrogen) and kept on ice until further processing.

High Performance Liquid Chromatography (HPLC)

All samples will be prepared for HPLC as previously described by sonication to release the neurotransmitters into the supernatant. The protein pellet will be assayed for protein concentration using a Bradford assay. The supernatant will be assayed for 5-HT and 5-HIAA, or 5-HTP, using HPLC with electrochemical detection as previously described (Lookingland et al., 1986).

Real Time Reverse Transcription-Polymerase Chain Reaction (RT-PCR)

Total RNA in the CG will be isolated using a standard Trizol protocol as previously described (Cao et al., 2007). Briefly, tissues will be homogenized in Trizol (Invitrogen) soon after dissections, chloroform (J. T. Baker) will be added, samples will be centrifuged (12000 *g*, 15 min, and 4°C), propanol (J. T. Baker) will be added to the supernatants, and samples will be kept at -20°C for 48 hr. Then, 75% ethanol will be added to the RNA pellets after centrifugation (12000 *g*, 15min, and 4°C) and samples will be kept at -20°C for 24 hr. RNA pellets will be washed once again with 75% ethanol after centrifugation (7500 *g*, 10 min, and 4°C) and immediately afterwards, RNA pellets will be resuspended in Tris-EDTA buffer (Qiagen). Samples will be stored at -80°C until further analysis. The concentration, purity, and integrity of RNA will be ascertained spectrophotometrically using a Nanodrop ND-100 Spectrophotometer. Subsequently, RNA will be DNase (Roche)-treated to reduce genomic DNA contamination.

A two-step RT-PCR will be performed. DNAse-treated RNA will be reverse transcribed using a mix of Oligo dT primers (Invitrogen), random hexamer primers (Promega), and Superscript III (Invitrogen). The cDNA synthesized from 700 ng of total RNA will be used in subsequent real time RT-PCR (Stratagene Mx3000P). Forward and reverse primers for TPH1, TPH2, SERT, 5-HT_{3A}, 5-HT_{3B}, and the housekeeping gene Cyclophilin A (Ppia) (**Table 2.1**) have been designed based on the *Rattus Norvegicus* gene sequences (NCBI GenBank) using PrimerQuest (Integrated DNA technologies) software. The relative expression ratio of the target gene was calculated, based on Ct difference (Δ) of sample versus control after each sample was normalized to gene expression of the Ppia.

Gene	Sequence	Amplicon Length (bp)	NCBI Accession Number
TPH1	FWD:5'TTTGGACTGTGCAAGCAAGATGGG 3' RWS:5'GTTTGCAGGCAACCTTGGGATCAA 3'	133	NM_001100634.2
TPH2	FWD:5'TTCACAATCGAGTTCGGCCTTTGC 3' RWS:5'GCATTCCTGCAAGCAGGTTGTCTT 3'	153	NM_173839.2
SERT	FWD:5'AGATGTGTCAGAGGTGGCCAAAGA 3' RWS:5'AAGAACGTGGATGCTGGCATGTTG 3'	93	NM_013034.4
5-HT$_{3A}$	FWD:5'GCAGCTGGTGCATAAGCAGGATTT 3' RWS:5'TGGCTGAGCAGTCATCAGTCTTGT 3'	161	NM_024394.2
5-HT$_{3B}$	FWD:5'TGGCCTATGTTGTGAGCCTCTTGA 3' RWS:5'TATAGCCCACCAGCACATTGGTCT 3'	126	NM_022189.1
Ppia	FWD:5'AGCATACAGGTCCTGGCATCTTGT 3' RWS:5'CAAAGACCACATGCTTGCCATCCA 3'	117	NM_017101.1

Table 2.1. Primer sequences for genes related to 5-HT synthesis, tryptophan hydroxylase (TPH1 and TPH2), 5-HT reuptake, 5-HT reuptake transporter (SERT), 5-HT$_3$ receptor (5-HT$_{3A}$ and 5-HT$_{3B}$), and the housekeeping gene, cyclophilin A (Ppia).

Statistics

Student's *t* test was used to analyze all comparisons. All tests were performed using SPSS 17.0. Statistical significance was set at $p \leq 0.05$. Results are presented as mean ± standard error of the mean.

RESULTS

Effect of Perfusion

Perfusion was done in some rats to determine whether the 5-HT and 5-HIAA measured in sympathetic ganglia was present in the blood contained in the ganglia. A comparison of 5-HT and 5-HIAA concentrations between perfused and non-perfused rats shows that there was no significant effect of perfusion on 5-HT (**Fig. 2.2A**) or 5-HIAA (**Fig. 2.2B**) levels. Moreover, the 5-HIAA/5-HT ratio that is indicative of activity in serotonergic neurons is not significantly different between perfused and non-perfused rats (**Fig. 2.2C**). Notably, the 5-HIAA/5-HT ratio is very low.

Tryptophan and NSD-1015 Treatments

NSD-1015 treatment was used to determine whether *de novo* 5-HT synthesis occurs in the CG and compare that synthesis to that of the well characterized serotonergic brain regions, the FC and PVN. NSD-1015 treatment will prevent the conversion of 5-HTP to 5-HT and lead to a buildup of 5-HTP if the tissue is capable of 5-HT synthesis. As expected, no 5-HTP was measured in CG, PVN, or FC in the absence of NSD-1015 treatment. Following NSD-1015, detectable levels of 5-HTP were measured in the CG and both brain regions (**Fig. 2.3**). Tryptophan treatment prior to NSD-1015 should increase 5-HT synthesis if synthesis is substrate-dependent. However, tryptophan treatment did not significantly increase 5-HTP levels in CG although it did significantly increase 5-HTP concentration in the FC and PVN (**Fig. 2.3**).

5-HT and 5-HIAA were detected only in tissue from rats not treated with NSD-1015. Surprisingly, although 5-HT synthesis in the CG did not increase following tryptophan treatment,

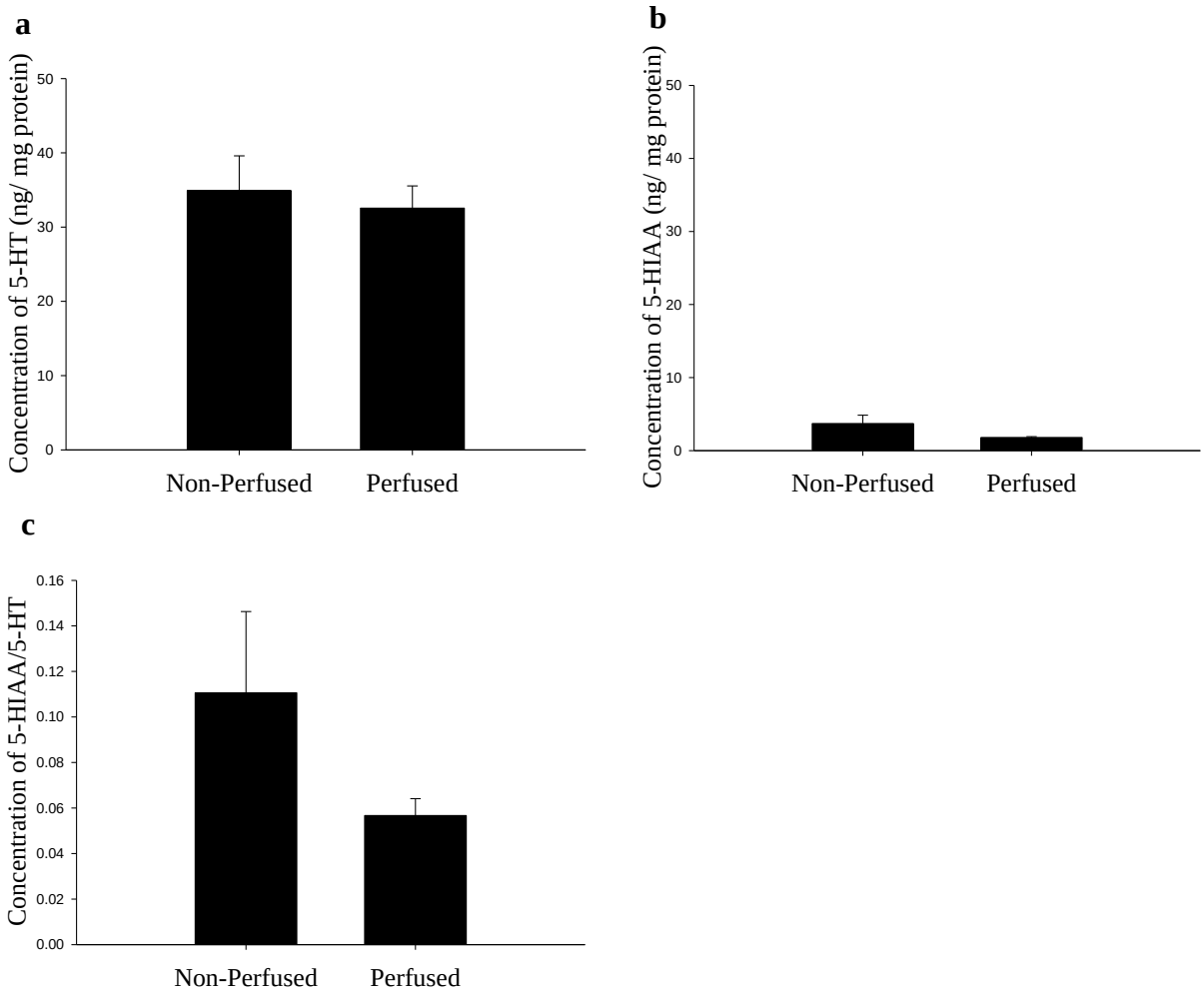

Figure 2.2. Perfusion did not influence concentrations of 5-HT, 5-HIAA, or the 5-HIAA/5-HT ratio in the CG. Concentrations of 5-HT (A) and 5-HIAA (B), measured via HPLC, and the 5-HIAA/5-HT ratio (C) were not different between CGs dissected from saline perfused (n=3) and non-perfused (n=3) rats.

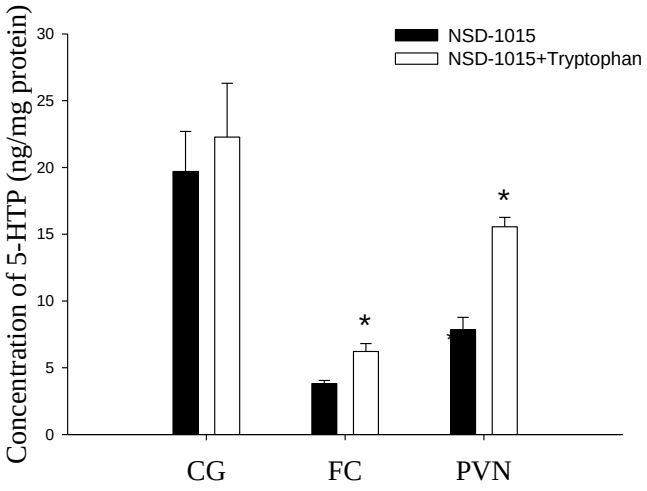

Figure 2.3. 5-HT synthesis occurs in the CG but unlike in the FC and PVN, synthesis is not substrate dependent. 5-HTP was measured in the CG after NSD-1015 treatment (n=4) indicating that 5-HT occurs in the CG. Following tryptophan treatment prior to NSD-1015 treatment (n=4), 5-HTP concentration in the CG did not increase as it does in serotonergic regions of the brain, the FC and PVN, suggesting that 5-HT synthesis in the CG is not substrate dependent. * indicates a significant difference between NSD-1015 treated and NSD-1015 and tryptophan treated rats.

5-HT (**Fig. 2.4A**) but not 5-HIAA (**Fig. 2.4B**) nor 5-HIAA/5-HT ratio (**Fig. 2.4C**) was significantly higher in the CG. In contrast, in both brain regions, tryptophan significantly increased 5-HIAA concentration but not 5-HT concentration nor 5-HIAA/5-HT ratio.

Comparisons between Normotensive and Hypertensive Rats

5-HT and 5-HIAA levels were compared in CGs between normotensive and hypertensive rats. Neither 5-HT (**Fig. 2.5A**) nor 5-HIAA (**Fig. 2.5B**) concentrations were significantly different between normotensive and hypertensive CGs. Moreover, 5-HIAA/5-HT ratios were also similar between normotensive and hypertensive CGs (**Fig. 2.5C**).

Gene expression of genes related to 5-HT synthesis (TPH1 and TPH2), 5-HT re-uptake (SERT), and 5-HT_3 receptor (5-HT_{3A} and 5-HT_{3B}) were measured in CGs from normotensive and hypertensive rats. There was no difference in TPH1 and SERT gene expression between normotensive and hypertensive CGs (**Fig. 2.6A**). However, TPH2 gene expression was significantly lower in hypertensive than normotensive CGs (**Fig. 2.6A**). Also, 5-HT_{3A} gene expression was significantly lower in hypertensive than normotensive CGs but 5-HT_{3B} gene expression was not significantly different between the two groups (**Fig. 2.6B**).

5-HT and 5-HIAA levels were also assayed in an innervated target of the CG, the spleen, collected from normotensive and hypertensive rats. 5-HIAA levels were not detectable in most spleen samples and not shown. Significantly lower 5-HT levels were measured in spleens from hypertensive than normotensive rats (**Fig. 2.7**).

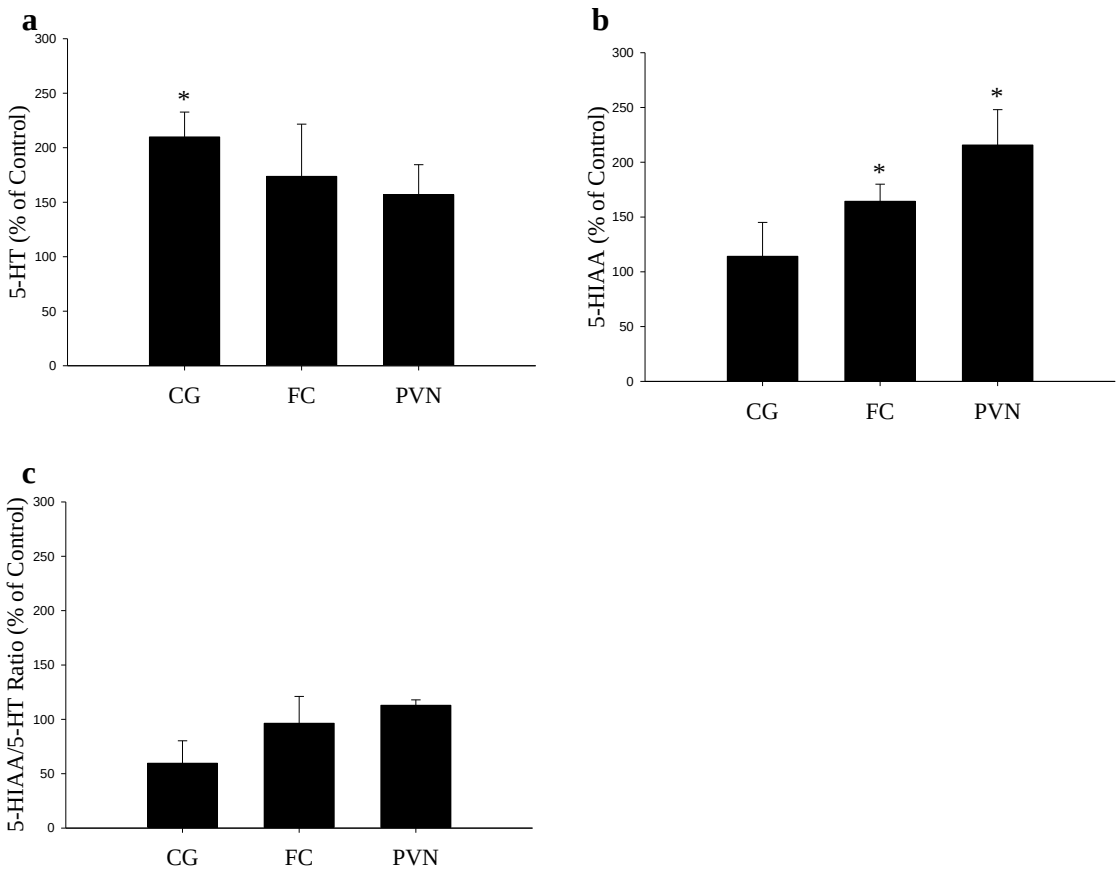

Figure 2.4. Tryptophan treatment significantly increases 5-HT but not 5-HIAA concentrations in the CG. Concentrations of 5-HT and 5-HIAA were compared in the CG and the serotonergic brain regions, FC and PVN, with (n=4) or without (n=4) tryptophan treatment. Data for tryptophan treated rats are shown as percentage of data from vehicle treated rats. * indicates a significant difference between tryptophan treated and vehicle treated groups for a given tissue.

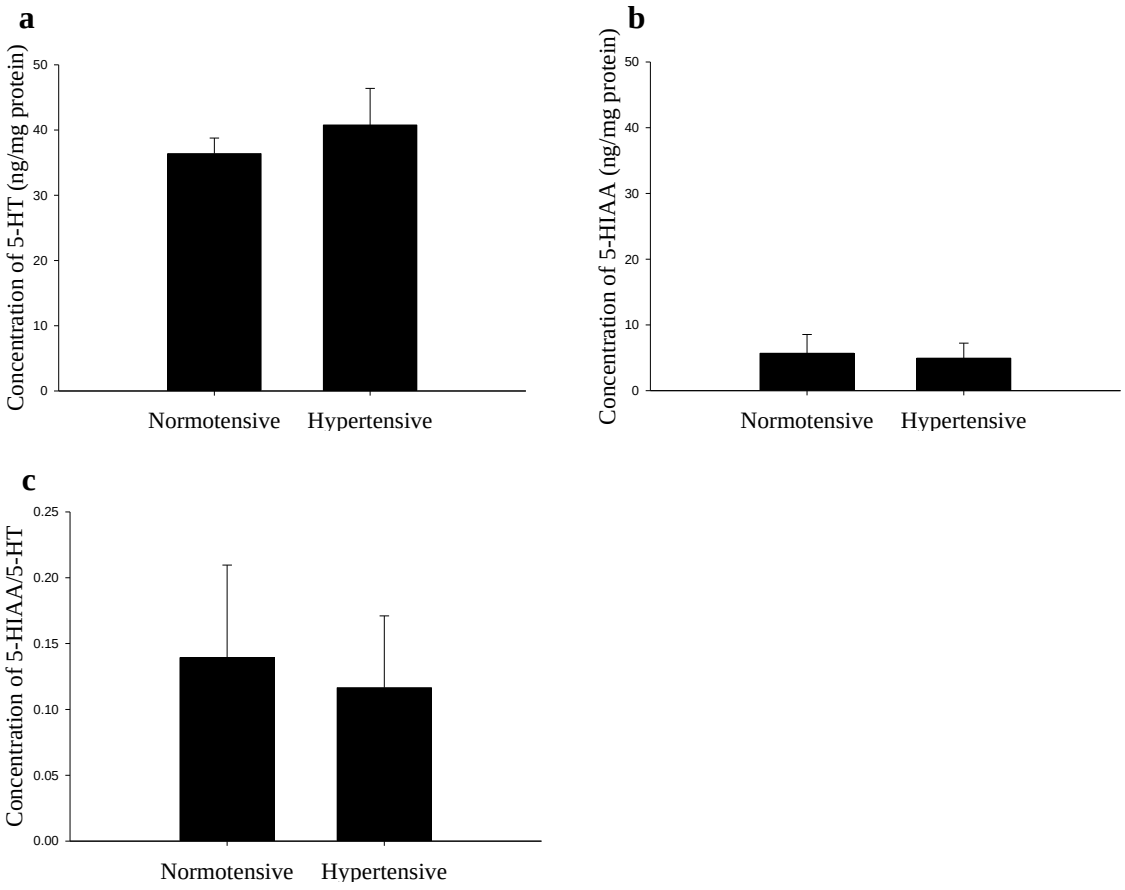

Figure 2.5. There is no difference in 5-HT or 5-HIAA concentrations between normotensive and hypertensive CGs. Concentrations of 5-HT (A) and 5-HIAA (B), measured via HPLC, and the ratio of 5-HIAA/5-HT (C) were compared between normotensive (n=7) and hypertensive (n=6) rats.

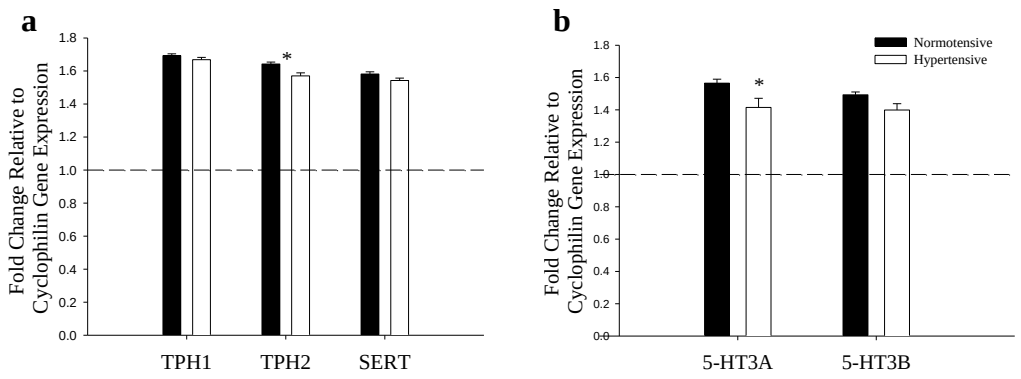

Figure 2.6. There is significantly less gene expression of TPH2 and 5-HT3A but not of TPH1, SERT, or 5-HT3B in hypertensive than normotensive rats. Gene expression of TPH1, TPH2, SERT, 5-HT3A, and 5-HT3B were measured with real time RT-PCR. Data were normalized as fold change relative to gene expression of the housekeeping gene, cyclophilin. * indicates a significant difference between normotensive and hypertensive groups for a given gene.

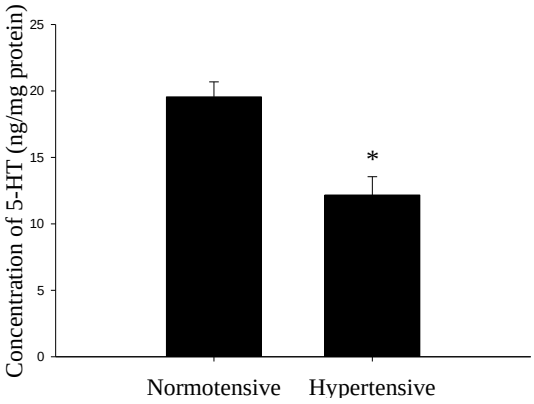

Figure 2.7. Significantly less 5-HT is present in spleens, a target innervated by the CG, from hypertensive relative to normotensive rats. Concentration of 5-HT was measured in spleens dissected from normotensive (n=8) and hypertensive (n=8) rats. * indicates a significant difference between normotensive and hypertensive groups.

DISCUSSION

This is the first study to compare the serotonergic system within sympathetic ganglia of normotensive and hypertensive animals. Key findings from our studies are: 1) 5-HT is present in the CG; 2) 5-HIAA levels and the 5-HIAA/5-HT ratio is low in the CG; 3) 5-HT can be synthesized *de novo* in the CG; 4) 5-HT synthesis in the CG is not substrate-dependent as it is in the FC and PVN; 5) 5-HT and 5-HIAA levels were not different in CGs of normotensive and hypertensive rats; 6) TPH2 gene expression is lower in CGs of hypertensive than normotensive rats; 7) 5-HT_{3A} gene expression is also lower in CGs of hypertensive than normotensive rats; and 8) 5-HT levels are lower in the spleen of hypertensive than normotensive rats.

5-HT and 5-HIAA Levels in the CG

The presence of 5-HT in sympathetic ganglia replicates previous findings. Immunohistochemical studies of sympathetic ganglia shows that 5-HT is mainly localized within SIF cells, some sympathetic neurons, and in nerve fibers distributed evenly throughout the ganglia (Ma et al., 1985, Gale and Cowen, 1988, Happola, 1988, Karhula et al., 1995). 5-HT was also measured via HPLC in the guinea pig CG and found to be ~2pmol/ganglion or ~0.4ng/ganglion (Ma et al., 1985). This low level of 5-HT detected may be due to a lower level of sensitivity in 5-HT measurements or due to inter-species differences.

Levels of 5-HIAA, a metabolite of 5-HT, were measured for the first time in sympathetic ganglia and were detectable but low. Consequently, the 5-HIAA/5-HT ratio, which has been previously used as an indicator of neuronal activity (Lookingland et al., 1986), was also low in the CG. 5-HT is either packaged in vesicles for synaptic release or is metabolized into 5-HIAA by mitochondrial monoamine oxidase (reviewed in Lovenberg and Kuhn, 1982, Fernstrom,

1983). Hence, low levels of 5-HIAA relative to 5-HT indicate that 5-HT must be stored rather than metabolized in sympathetic ganglia. It is possible that 5-HT is stored in neuronal vesicles for synaptic release to targets innervated by sympathetic ganglia or that it is stored in SIF cells.

Saline perfusion prior to dissecting CGs had no effect on 5-HT levels, 5-HIAA levels, or 5-HIAA/5-HT ratio. Thus, 5-HT and 5-HIAA levels in the CG are not a reflection of 5-HT and 5-HIAA levels in blood circulating within the ganglia.

5-HT Synthesis in the CG

Detectable levels of 5-HTP after NSD-1015 treatment in the CG and both brain regions indicate that *de novo* 5-HT synthesis occurs in the CG as in the FC and PVN. This is in accordance with previous findings showing that 5-HT immunoreactive neurons were present in the superior cervical ganglia after treating rats with tryptophan, a monoamine oxidase inhibitor (nialamide), and a SERT blocker (fluoxetine) (Happola, 1988). Also, in CG isolated from guinea pigs, treatment with tryptophan, or a monoamine oxidase inhibitor (paragyline) increased 5-HT concentration as measured by HPLC (Ma et al., 1985). In contrast to the FC and PVN, 5-HTP concentrations in the CG did not increase following treatment with tryptophan. Typically, the activity of tryptophan hydroxylase is limited by availability of the substrate, tryptophan, since the K_m for tryptophan hydroxylase is higher than available tryptophan concentrations (Friedman et al., 1972, Carlsson and Lindqvist, 1978). However, 5-HT synthesis in the CG is not substrate-dependent, which suggests that tryptophan levels are sufficient under physiological conditions.

Interestingly, although 5-HT synthesis in the CG did not significantly increase after tryptophan treatment as measured by 5-HTP concentrations, 5-HT concentrations did

significantly increase. This may be due to increased 5-HT re-uptake from surrounding tissue and circulation. Notably, sympathetic ganglia do not have a blood brain barrier to prevent entry of excess circulating 5-HT (Ten Tusscher et al., 1989). The increased 5-HT concentration did not result in increased 5-HIAA concentrations in the CG, but did in the FC and PVN. Accordingly, tryptophan treatment slightly decreased the ratio of 5-HIAA/5-HT in the CG but not in the FC or PVN. Hence, the excess 5-HT in the CG must be stored within neuronal vesicles or in SIF cells rather than being metabolized or released in the ganglia.

Comparisons between CGs from Normotensive and Hypertensive Rats

This is the first study to closely investigate how the local 5-HT system in sympathetic ganglia is changed by hypertension. We hypothesized that the 5-HT system would be overactive in hypertensive CGs since 5-HT can activate sympathetic postganglionic neurons and a higher sympathetic drive is found in hypertensive animals. In contrast, we found no difference in basal 5-HT or 5-HIAA concentrations or in the 5-HIAA/5-HT ratio between normotensive and hypertensive rats.

Next, we examined 5-HT synthesis, re-uptake, and 5-HT_3 receptor expression by looking at gene levels of TPH1, TPH2, SERT, 5-HT_{3A}, and 5-HT_{3B}. Both isoforms of TPH, TPH1 and TPH2, were examined since gene expression of these isoforms has not been studied in sympathetic ganglia. Elsewhere, TPH1 is predominantly expressed in the periphery and TPH2 is predominantly expressed in the central nervous system (reviewed in Veenstra-VanderWeele and Cook, 2003). We found that both TPH1 and TPH2 genes are present in the CG but that there is significantly less TPH2 expression in CGs from hypertensive than normotensive rats. This suggests that there is less 5-HT synthesis in hypertensive CGs. Moreover, since there is no

difference in 5-HT concentration in cell bodies of sympathetic postganglionic neurons, less 5-HT synthesis may correspond to less 5-HT at sympathetic nerve terminals. Indeed, we found a significantly lower 5-HT concentration in spleens from hypertensive than normotensive rats. It was previously shown that most sympathetic innervation to the spleen originates from the CG (King et al., 2008). Hence, it is possible that less 5-HT synthesis within sympathetic postganglionic neurons leads to less 5-HT at innervated targets.

It is unlikely that the difference in spleen 5-HT concentration between normotensive and hypertensive groups is due to a difference in circulating levels of 5-HT because circulating 5-HT was found to be significantly higher in this animal model of hypertension (Diaz et al., 2008). The functional significance of this is less clear in the spleen but at sympathetic neuroeffector junctions with mesenteric blood vessels, another target innervated by the CG, 5-HT inhibits NE release (Gothert et al., 1986, Meehan and Kreulen, 1991). Less 5-HT present at sympathetic neuroeffector junctions may lead to more NE release and contribute to increased vasoconstriction in hypertension.

No difference in gene expression of SERT was found between normotensive and hypertensive CGs indicative of a similar level of 5-HT re-uptake in both groups. However, 5-HT_{3A}, but not 5-HT_{3B}, gene expression was significantly lower in hypertensive than normotensive CGs. The 5-HT_3 receptor is a ligand-gated ion channel that has two known subunits in rodents (5-HT_{3A} and 5-HT_{3B}) (reviewed in Barnes et al., 2009). The 5-HT_{3A} subunit alone is necessary for the formation of functional 5-HT_3 receptors but incorporation of 5-HT_{3B} subunits causes at least a 16-fold increase in single channel conductance and influences ionic selectivity. Gene expression of both subunits were expressed is the CG, confirming previous

findings (Doucet et al., 2007). Since the 5-HT_3 receptor is implicated in excitatory effects in sympathetic ganglia (Kiraly et al., 1983, Dun et al., 1984, Meehan and Kreulen, 1991, Knoper et al., 1992), less gene expression of 5-HT_{3A} may indicate lowered levels of 5-HT-induced excitatory signaling within sympathetic ganglia in hypertension. While this is contrary to previous findings of increased splanchnic nerve activity in hypertension (Magee and Schofield, 1992), it is possible that only selective pathways within sympathetic ganglia are activated during hypertension.

CONCLUSIONS

In this study, we find that 5-HT is present and can be synthesized *de novo* in a substrate-independent manner in sympathetic prevertebral ganglia. This is different from the synthesis we observed in other serotonergic brain regions like the frontal cortex and paraventricular nucleus, which occurs in a substrate-dependent manner. While 5-HT and 5-HIAA levels were not different between CGs from normotensive and DOCA-salt hypertensive rats, we found other differences in the 5-HT system. Gene expression of both TPH2 and 5-HT_{3A} was lower in hypertensive than normotensive CGs. This suggested that there is less 5-HT-mediated activation of sympathetic postganglionic neurons in hypertensive CGs. We also found lower 5-HT levels in spleens of hypertensive than normotensive rats indicating that innervated targets of sympathetic ganglia may not receive as much 5-HT in hypertension. Instead of an overactive 5-HT system contributing to a higher sympathetic drive in hypertension, we observed a less active 5-HT system. 5-HT released at neuroeffector junctions is shown to inhibit NE release but less 5-HT released to mesenteric blood vessels may lead to more NE release, as is seen in hypertension. Alternatively, whole ganglia levels of neurotransmitters may not accurately reflect local exposure to specific vascular-projecting neuronal pathways that are especially relevant in hypertension.

CHAPTER THREE: NEURONAL ACTIVATION IN PREVERTEBRAL SYMPATHETIC GANGLIA OF NORMOTENSIVE AND HYPERTENSIVE RATS FOLLOWING DIRECT AND INDIRECT STIMULATION

ABSTRACT

Sympathetic nerve activity is chronically elevated in human hypertensive patients and in many animal models of hypertension, including the deoxycorticosterone acetate (DOCA)-salt rat model. Neuronal activation is not well understood in sympathetic ganglia, which provide sympathetic innervation of vasculature. Using c-fos as a marker of neuronal activation, we examined basal c-fos expression in prevertebral sympathetic ganglia of normotensive and DOCA-salt hypertensive rats. No basal c-fos expression was observed in sympathetic ganglia from normotensive or hypertensive rats. However, more c-fos expression was observed after 6 Hz than 2 Hz preganglionic nerve stimulation, indicating that the c-fos antibody used was a valid marker of neuronal activation. Continuous or burst modes of nerve stimulation did not result in different levels of c-fos expression. Stimuli that directly activate sympathetic ganglia, including preganglionic nerve stimulation and systemic nicotine treatment (2 mg/kg sc), induced a smaller increase in c-fos expression in hypertensive compared to normotensive sympathetic ganglia. In contrast, 2-deoxy-D-glucose treatment (800 mg/kg i.p.), a metabolic stimulus that indirectly activates sympathetic ganglia, induced a similar increase in c-fos expression in normotensive and hypertensive sympathetic ganglia. Based on these results, it is likely that in hypertension, nicotinic receptors in sympathetic ganglia are desensitized due to increased preganglionic nerve activity and hence, are less responsive to direct ganglionic activators.

INTRODUCTION

Hypertension, or high blood pressure, is of neurogenic origin in an estimated 50% of clinically diagnosed patients and in many rodent models (Esler et al., 2010). Neurogenic hypertension is characterized by increased sympathetic activity that contributes to the development and maintenance of hypertension. Sympathetic ganglia are especially important contributors since they are the last neuronal link between the central nervous system and vasculature. For instance, surgical removal of a prevertebral sympathetic ganglion, the celiac ganglion (CG), markedly attenuates development of hypertension in animal models of hypertension including spontaneously hypertensive rats (Ye et al., 2011), angiotensin II-salt-treated rats (King et al., 2007), and deoxycorticosterone acetate (DOCA)-salt-treated rats (Kandlikar and Fink, 2011b). The CG innervates abdominal organs and mesenteric vasculature, which collectively holds approximately one-third of total blood volume (Rothe, 1983). Celiac ganglionectomy studies suggest that increased splanchnic nerve activity contributes to hypertension. However, neuronal activation in sympathetic ganglia remains to be examined in hypertension.

Sympathetic nerve activity in both pre-and-post-ganglionic nerves occurs in irregular bursts from large numbers of fibers firing synchronously. Burst stimulation via field stimulation to isolated rat mesenteric blood vessels (Nilsson et al., 1985) and via nerve stimulation to the cervical paravertebral ganglia (Lacroix et al., 1988) both resulted in greater vasoconstriction of arteries relative to continuous stimulation. However, the two modes of stimulation had a similar effect on vasoconstriction of veins. A lingering question of importance is whether the pattern of stimulation also affects neuronal activation in sympathetic ganglia.

A widely used and accepted index of measuring neuronal activation in the central nervous system is the expression of Fos, an immediate early gene (Curran and Morgan, 1995). In addition, Fos expression as a marker of neuronal activation in sympathetic ganglia has been validated by several studies. For instance, Fos immunoreactivity is observed in sympathetic ganglia in response to preganglionic nerve stimulation (Mei et al., 2001), nicotine treatment (Koistinaho, 1991), and 2-deoxy-D-glucose (2-DG) treatment (Mei et al., 2001). The present study will validate the use of a specific c-fos antibody that does not cross-react with other Fos proteins by measuring c-fos expression after 2 Hz and 6 Hz of preganglionic nerve stimulation.

The main goals of this study are to 1) determine if basal neuronal activation is elevated in sympathetic ganglia from hypertensive rats; 2) determine whether the pattern of nerve stimulation affects neuronal activation in sympathetic ganglia; and 3) determine if neuronal activation in response to direct activators like preganglionic nerve stimulation and systemic nicotine treatment as well as indirect activators like 2-DG is different in sympathetic ganglia from normotensive and hypertensive rats. We predict that basal c-fos expression will be higher in hypertensive compared to normotensive CGs. Since the threshold of activation is expected to be higher in hypertensive CGs, we predict that stimulation of CGs will lead to less c-fos expression in hypertensive compared to normotensive CGs.

METHODS AND MATERIALS

Animals

Adult male Sprague-Dawley rats (250-300 g; Charles River Laboratories, Inc., Portage, MI) were used for all experiments. Normotensive sham and hypertensive DOCA-salt rats were prepared as previously described (Luo et al., 2003). Briefly, DOCA-salt rats underwent uninephrectomy, subcutaneous DOCA (200 mg/kg) implantation, and had access to drinking water containing 1% NaCl and 0.2% KCl (hypertensive group). Normotensive shams were also uninephrectomized but did not receive an implant of DOCA and had access to normal drinking water (normotensive group). After 4 weeks of this regimen, systolic BP was measured by tail cuff plethysmography (systolic BP=133.3±2.8 mmHg for normotensive rats and 191.1±3.6 mmHg for hypertensive rats, n=20)

All experimental protocols were approved by the Michigan State University All University Committee on Animal Use and Care. Animals were housed two per cage with *ad libitum* access to food and water while being kept on a 12:12hr light-dark cycle in a room with regulated temperature (22-24°C).

Nerve Stimulation

Prevertebral sympathetic ganglia include the CG and the much smaller inferior mesenteric ganglion (IMG) that provide much of the innervation to abdomino-pelvic tissue. The IMG was used in all nerve stimulation studies as it is easy to access and isolate for *in vitro* preparations. In order to isolate it, the distal 5 cm of the colon along with the abdominal aorta were dissected and transferred to a petri dish coated with Sylgard (Dow Inc.) and filled with

Krebs' solution (containing in mM: NaCl 118.5, KCl 4.7, KH_2PO_4 1.2, $NaHCO_3$ 23.8, dextrose 5.5, and aerated with 95%O_2/5%CO_2). Extraneous tissue including the colon, paraspinal musculature, lymph nodes, and lymph ducts were all carefully dissected away until the IMG and both intermesenteric nerves leading to the IMG were clearly visible. A 5 mm section of the intermesenteric nerves was isolated, cleaned of fat and connective tissue, and placed onto a bipolar platinum-iridium hook electrode. The nerve-stimulation electrode was connected to a stimulus isolation unit (Grass SIU5).

c-fos expression after preganglionic nerve stimulation at either 2 Hz or 6 Hz continuously was used to validate whether c-fos is a good marker of neuronal activation in sympathetic ganglia (n=5). Also, c-fos expression after 'continuous' and 'burst' modes of 6Hz preganglionic nerve stimulation was measured to determine whether different stimulation modes result influence neuronal activation (n=5). For continuous stimulation, preganglionic nerves were stimulated at the set frequency (2 Hz or 6 Hz for 1 sec stimulus duration). For 6 Hz burst stimulation, preganglionic nerves were stimulated at 30 Hz for 200 msec (ie. 6 pulses) and 0 Hz for 800 msecs as previously described (Andersson, 1983). Hence, the total number of pulses were equivalent between continuous and burst stimulation modes. 0 Hz controls were used to examine whether manipulation of the ganglion or preganglionic nerves resulted in any c-fos expression (n=2). c-fos expression after 6 Hz continuous nerve stimulation was measured in normotensive and hypertensive rats (n=5).

Nerve stimulation occurred for 60 min followed by 45 min of no stimulation, after which the ganglion was fixed in 4% paraformaldehyde overnight, cryoprotected in 30% sucrose overnight, embedded, and stored at -80°C until analysis.

Baseline and Treatment Conditions

Basal and post-treatment c-fos expression was examined in CGs since previous studies show the CG to be an important contributor to neurogenic hypertension. c-fos expression was measured in untreated normotensive and hypertensive CGs to determine basal neuronal activation (n=5). In addition, c-fos expression was observed in normotensive and hypertensive IMGs following preganglionic nerve stimulation (6 Hz continuous) and in normotensive and hypertensive CGs treated with nicotine (2 mg/kg sc; n=5) and 2-DG (800 mg/kg i.p.; n=5). Preganglionic nerve stimulation and nicotine will directly activate sympathetic ganglia via nicotinic receptors on postganglionic neurons. 2-DG is a glucose analog that does not undergo further glycolysis causing hypoglycemia (Brown, 1962, Smith and Epstein, 1969) and subsequently, will cause indirect activation of sympathetic ganglia leading to glucagon and adrenaline release to counter hypoglycemia (Vollmer et al., 1997, Taborsky et al., 1998). The doses for nicotine and 2-DG are similar to those used in previous studies where these doses led to maximal c-fos expression in sympathetic ganglia (Koistinaho, 1991, Mei et al., 2001). All rats were euthanized with sodium pentobarbital 90 min after treatment with nicotine, or 2-DG, or no treatment. Then, CGs were dissected, cleaned of fat and connective tissue, drop fixed in 4% paraformaldehyde overnight, cryoprotected in 30% sucrose overnight, embedded, and stored at -80°C until analysis.

Immunohistochemistry

Serial sections (15 μm) of frozen tissue were collected in five series and only one series was processed for histology and cell counts. Immunohistochemistry was done as previously described (Cao et al., 2007). Briefly, sections were washed for 3X5 min in tris buffered saline

supplemented with tween 20, blocked for 30 min with normal goat serum, incubated with a monoclonal rabbit anti-c-fos (Cell Signaling, #2250) for 48 hr, and incubated with biotinylated goat anti-rabbit (Vector Labs, #BA1000) for 1 hr. Immunoreactivity was visualized with the chromagen Nova Red (Vector Laboratories). c-fos immunoreactivity (ir) was localized only to nuclei of sympathetic neurons. Images were collected using standard bright-field microscopy. c-fos ir neurons were counted in all images after blinding the observer to treatment conditions. Number of c-fos ir neurons were normalized to areas of ganglion in m^2 as measured in Image J (National Institutes of Health).

Statistics

Student's *t* test was used to analyze all comparisons. All tests were performed using SPSS 21 (IBM). Statistical significance was set at $p \leq 0.05$. Results are presented as means ± standard error of means.

RESULTS

Induced c-fos expression after preganglionic nerve stimulation in IMGs

Preganglionic nerves were directly stimulated using either continuous stimulation burst stimulation and c-fos expression was measured in the IMG to determine whether modes of stimulation influenced the patterns of neuronal activation. No significant difference was observed in c-fos expression between the two stimulation protocols (**Fig. 3.1**).

Since no difference was found between continuous and burst modes of stimulation, data from both groups were collapsed when comparing c-fos expression between 2 Hz and 6 Hz of preganglionic nerve stimulation (**Fig. 3.2**). c-fos expression was significantly higher after 6 Hz compared to 2 Hz of preganglionic nerve stimulation (**Fig. 3.2**). Unstimulated controls (0 Hz) did not show any c-fos expression (data not shown). Hence, c-fos expression reflected more neuronal activation after a higher frequency of preganglionic nerve stimulation as predicted, indicating that c-fos expression is a valid marker of neuronal activation in sympathetic ganglia.

Since there was no difference in continuous and burst modes of stimulation, only continuous stimulation was used to compare c-fos expression between normotensive and hypertensive IMGs. The increase in c-fos expression was significantly less after 6 Hz preganglionic nerve stimulation in hypertensive compared to normotensive IMGs. (**Fig. 3.3**).

Basal and induced c-fos expression after nicotine and 2-DG treatment in CGs

We hypothesized that c-fos expression would be higher in hypertensive CGs relative to normotensive CGs since there is a higher sympathetic drive in hypertension. Surprisingly, no c-fos expression was observed in CGs of either normotensive or hypertensive rats (**Fig. 3.4**).

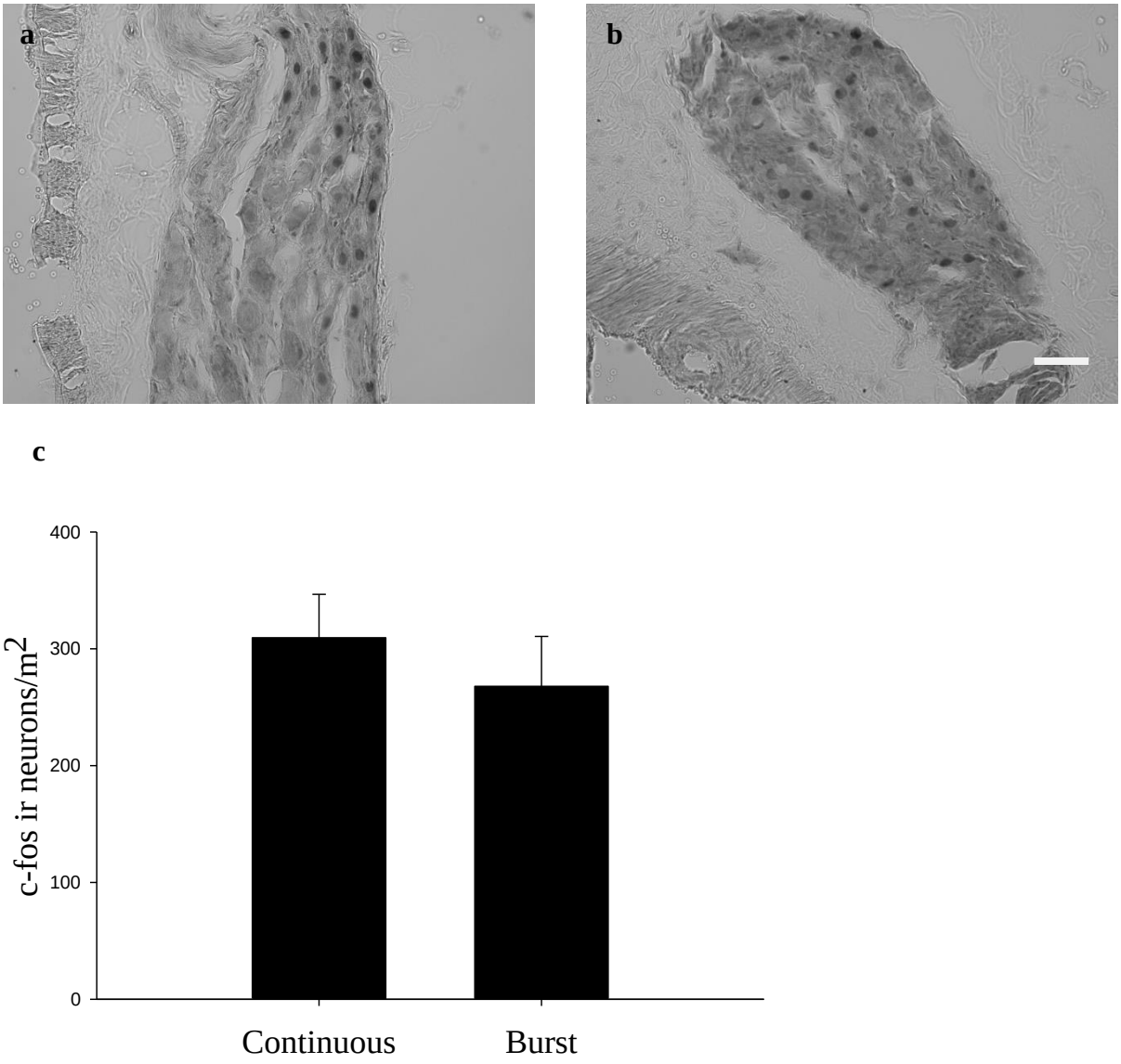

Figure 3.1. Continuous and burst modes of preganglionic nerve stimulation produced similar c-fos expression in the IMG. Representative images are shown for c-fos expression after 6 Hz of (a) continuous and (b) burst preganglionic nerve stimulation. (c) Quantification of c-fos ir neurons per unit area of ganglion is shown (n=5). Scale is 100μm.

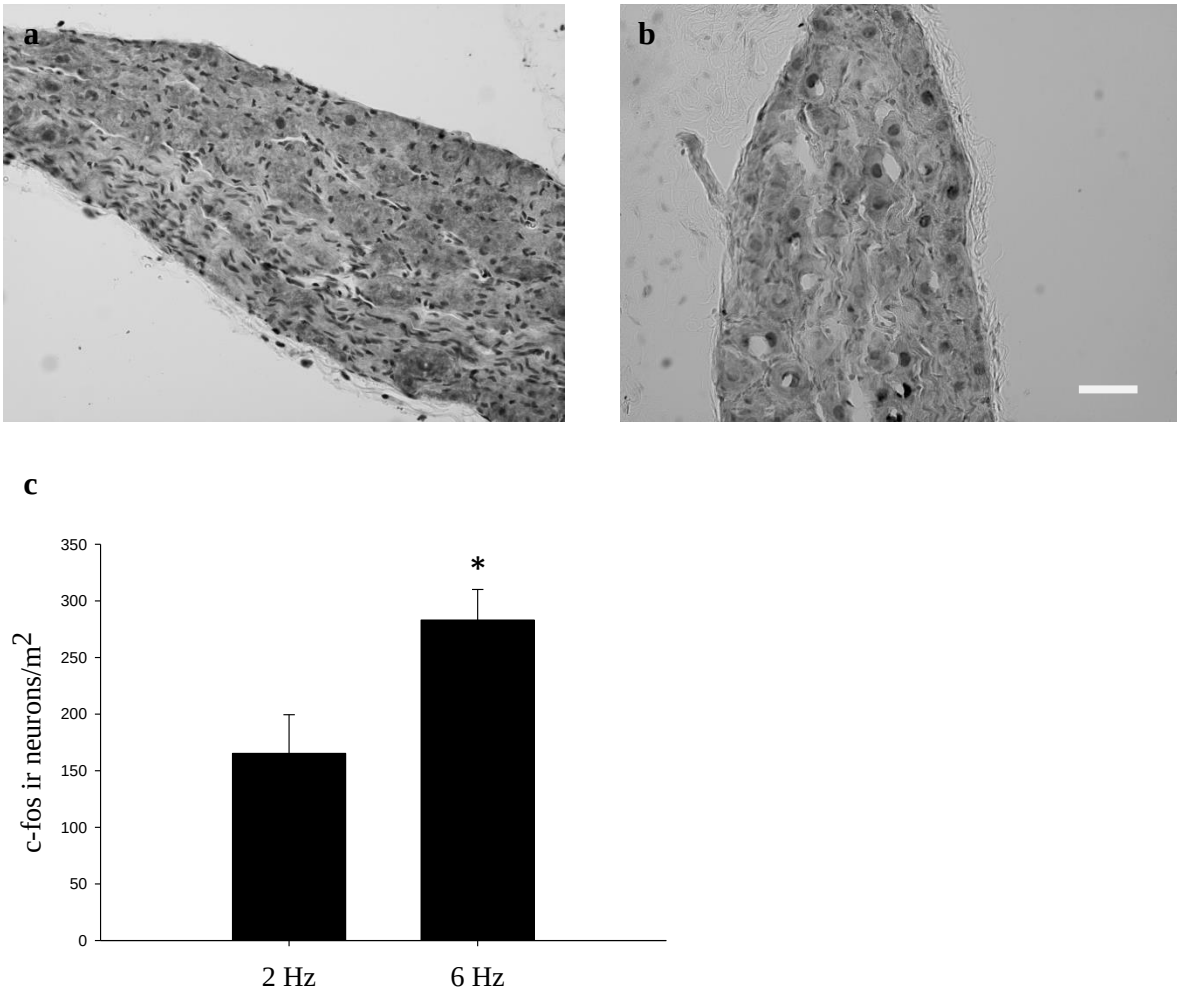

Figure 3.2. Neuronal activation in the IMG depends upon intensity of preganglionic nerve stimulation. Representative images are shown for c-fos expression after (a) 2 Hz (n=5) and (b) 6 Hz (n=10) of preganglionic nerve stimulation. (c) Quantification of c-fos ir neurons per unit area of ganglion is shown. * indicates a significant difference between 2 Hz and 6 Hz of nerve stimulation. Scale is 100μm.

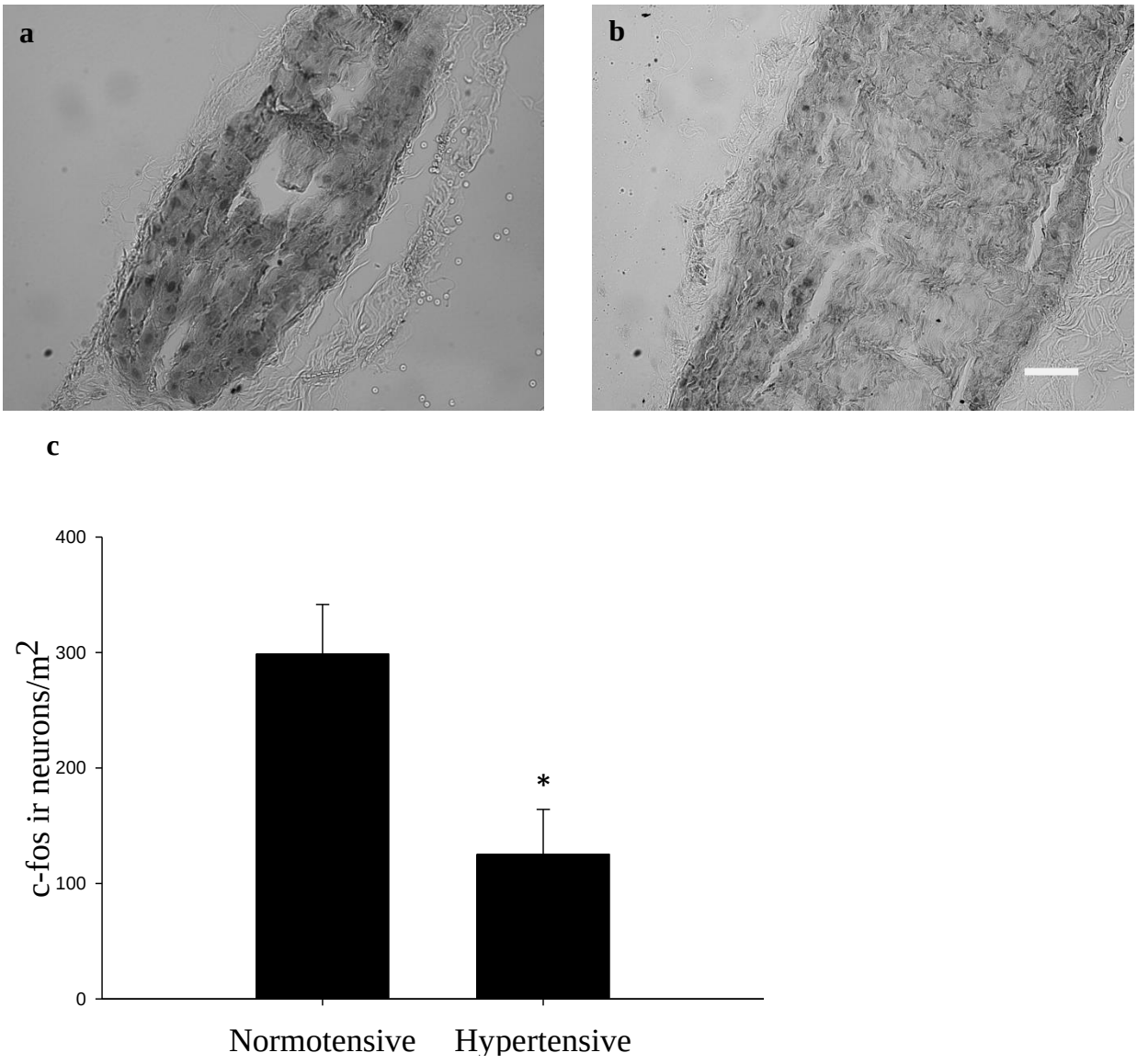

Figure 3.3. Preganglionic nerve stimulation leads to a smaller increase in neuronal activation in hypertensive compared to normotensive IMGs. Representative images are shown for c-fos expression in IMGs after 6 Hz of continuous preganglionic nerve stimulation in (a) normotensive and (b) hypertensive rats. (c) Quantification of c-fos ir neurons per unit area of ganglion is shown (n=5). * indicates a significant difference between normotensive and hypertensive IMGs. Scale is 100μm.

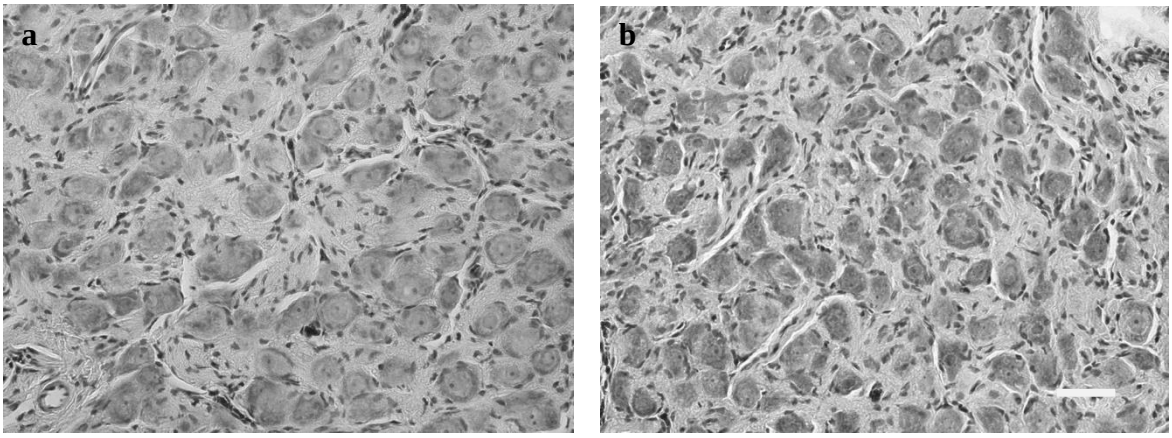

Figure 3.4. Basal c-fos expression is similar between normotensive and hypertensive CGs. Representative images are shown for basal c-fos expression in CGs of (a) normotensive and (b) hypertensive rats. No c-fos ir neurons are observed in normotensive or hypertensive CGs under basal conditions (n=3). Scale is 100μm.

After a single injection of nicotine (2mg/kg sc), there was significant expression of c-fos, roughly equivalent to the effect of 6 Hz nerve stimulation. Interestingly, the level of expression was 2.5 times greater in ganglia of normotensive animals compared to ganglia of hypertensive animals (**Fig. 3.5**). A single injection of 2-DG (800mg/kg i.p.) evoked a more modest amount of c-fos expression compared to nicotine (17 vs. 40 c-fos ir neurons/m^2) (**Fig. 3.6**). In contrast to nicotine effects, there was no difference in c-fos expression between CGs from normotensive and hypertensive animals. Hence, c-fos expression differs between normotensive and hypertensive sympathetic ganglia based on the acute activator used.

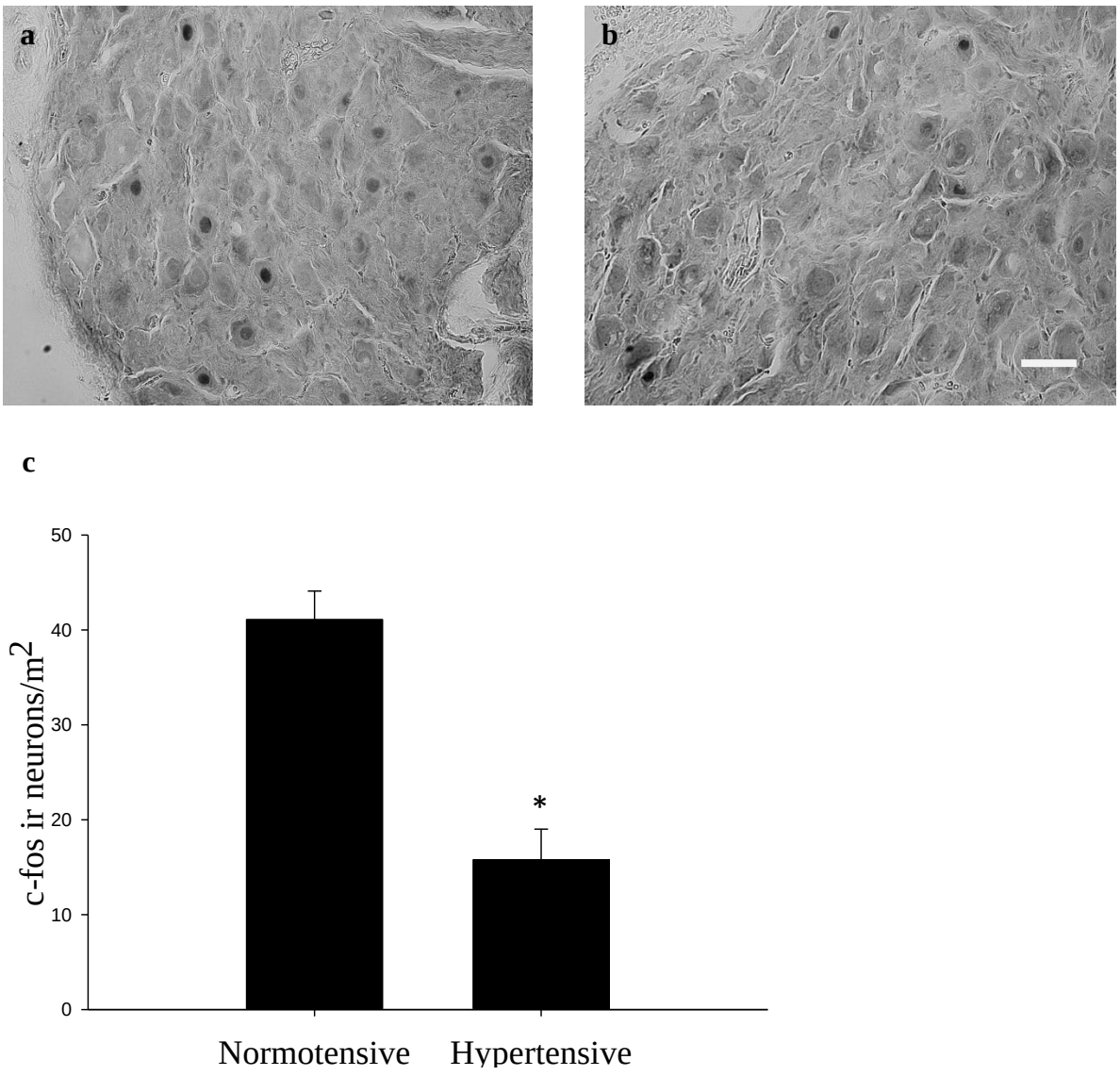

Figure 3.5. Nicotine treatment induces a smaller increase in neuronal activation in hypertensive compared to normotensive CGs. Representative images are shown for c-fos expression after nicotine treatment (2mg/kg sc) in (a) normotensive and (b) hypertensive rats. (c) Quantification of c-fos ir neurons per unit area of ganglion is shown (n=5). Scale is 100μm.

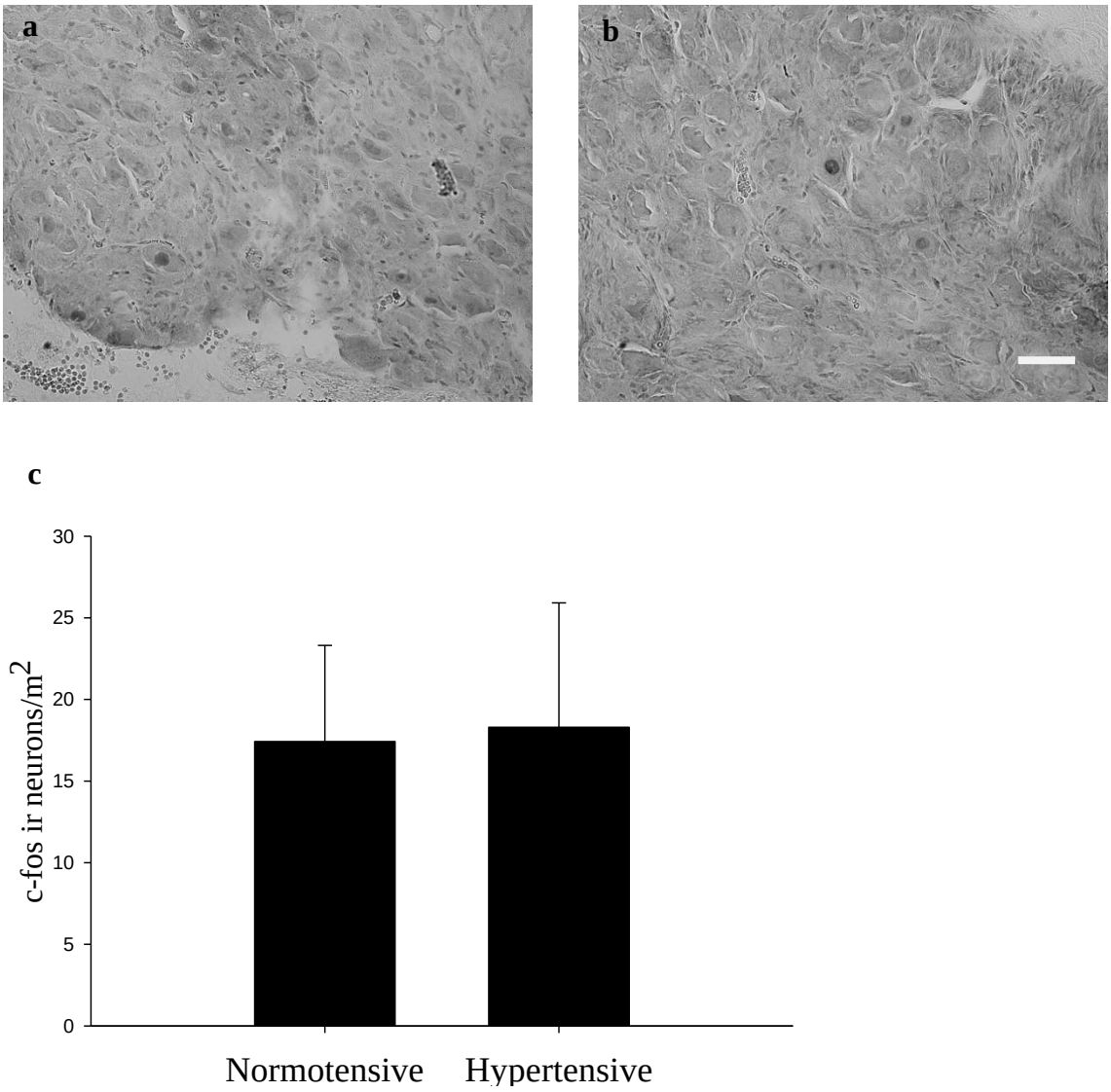

Figure 3.6. Neuronal activation is similar between normotensive and hypertensive CGs after 2-DG treatment. Representative images are shown for c-fos expression after 2-DG treatment (800mg/kg ip) in (a) normotensive and (b) hypertensive rats. (c) Quantification of c-fos ir neurons per unit area of ganglion is shown (n=5). Scale is 100μm.

DISCUSSION

This is the first study to examine patterns of neuronal activation in prevertebral sympathetic ganglia of normotensive and hypertensive rats. Key findings from our studies are: 1) electrical stimulation of preganglionic nerve fibers *in vitro* produced a frequency-dependent increase in c-fos expression in the IMG; 2) c-fos expression between continuous and burst modes of preganglionic nerve stimulation was not different; 3) basal c-fos expression in CGs of normotensive and hypertensive rats was not different; 4) administration of nicotine *in vivo* produced an increase in c-fos positive neurons; 5) direct sympathetic stimulation by preganglionic nerve stimulation or nicotine treatment showed a smaller increase in c-fos expression of hypertensive compared to normotensive sympathetic ganglia; and 6) indirect sympathetic stimulation by 2-DG treatment showed no difference in c-fos expression between normotensive and hypertensive CGs.

Preganglionic nerve stimulation

The c-fos monoclonal antibody used in the current study was validated as a marker of neuronal activation in sympathetic ganglia. The prediction that preganglionic nerve stimulation would produce a frequency-dependent increase in neuronal activation in sympathetic ganglia was reflected in significantly more c-fos expression after 6 Hz than 2 Hz of preganglionic nerve stimulation. Additionally, unstimulated controls (0 Hz) showed no c-fos expression indicating that manipulation of the ganglion or preganglionic nerves was not sufficient to result in detectable c-fos expression.

A previous study using a different c-fos antibody also showed a high number of c-fos ir neurons in the CG after preganglionic nerve stimulation (Mei et al., 2001). However, the

previous study found that isolation of the preganglionic nerve itself without stimulation resulted in some fos expression, although it was significantly less than after nerve stimulation. This may be due to a difference in antibodies or in handling of the *in vitro* preparation.

Neuronal activation level did not differ following continuous and burst modes of preganglionic nerve stimulation, suggesting that sympathetic postganglionic neurons are not influenced by the firing synchrony of preganglionic nerves. Instead, greater arterial vasoconstriction observed after burst, relative to continuous, stimulation (Nilsson et al., 1985, Lacroix et al., 1988) may be due to differences at the post-synaptic neuroeffector junction.

Basal neuronal activation

Contrary to our hypothesis, basal c-fos expression was similar between normotensive and hypertensive CGs. In contrast, previous findings showed higher basal c-fos expression in the rostral ventral medulla neurons and preganglionic sympathetic neurons of spontaneously hypertensive rats relative to Wistar Kyoto controls (Minson et al., 1996). One technical explanation for differences between studies is that different antibodies were used. In the current study, a specific c-fos antibody was used that binds only to the c-fos protein and not to other Fos proteins such as FosB, FRA1, and FRA2. Previous studies may have used less specific antibodies that show baseline 'Fos-like' expression.

It is unlikely that there is no basal neuronal activation in sympathetic ganglia since splanchnic postganglionic nerve recordings measure a basal sympathetic tone (Fluckiger et al., 1989), indicative of basal neuronal activation in prevertebral sympathetic ganglia. It is more likely that the level of activation of ganglionic neurons in both normotensive and hypertensive

rats is less than that evoked by synchronous preganglionic nerve stimulation at 2 Hz as was done *in vitro* in the present study.

Neuronal activation after direct sympathetic stimulation

Both continuous preganglionic nerve stimulation and nicotine treatment cause neuronal activation in sympathetic ganglia. There was a smaller increase in neuronal activation for hypertensive than normotensive sympathetic ganglia following both nerve stimulation and nicotine treatment. A commonality between these two methods of stimulation is that both act directly on sympathetic postganglionic neurons via activation of nicotinic receptors (Skok, 2002). Hence, desensitization of nicotinic receptors on sympathetic postganglionic neurons of hypertensive rats due to higher preganglionic nerve activity may explain a smaller increase in neuronal activation in hypertensive compared to normotensive sympathetic ganglia. A similar desensitization to prolonged nicotine exposure is shown to occur in the central nervous system (Fenster et al., 1999).

In hypertensive rats, the same stimulus intensity yields less neuronal activation relative to normotensive rats. This is supported by a previous study showing a trend for less c-fos expression in the rostral ventral medulla neurons of spontaneously hypertensive rats (SHR; 269±33) compared to Wistar Kyoto rats (WKY; 474±56) after sodium nitroprusside infusion, which decreased mean arterial pressure by 60% of resting pressure (Minson et al., 1996). However, important differences with the current study are that sodium nitroprusside is an indirect stimulator of the sympathetic nervous system via baroreceptor activation and that this effect was observed in central nervous system.

Although the increase in neuronal activation is smaller in sympathetic ganglia of hypertensive rats, it may be that fewer activated neurons contribute to higher postganglionic nerve activity in hypertension. This may be possible through altered synaptic efficiency in hypertensive compared to normotensive sympathetic ganglia. Previous studies support this by showing that postganglionic nerve activity is enhanced to a greater extent in SHRs relative to WKYs after a wide range of preganglionic nerve stimulation (Magee and Schofield, 1992).

Neuronal activation after indirect sympathetic stimulation

In contrast to preganglionic nerve stimulation and nicotine treatment, 2-DG treatment increased neuronal activation similarly in normotensive and hypertensive systemic ganglia. An explanation for why 2-DG may not have a similar effect on neuronal activation in normotensive and hypertensive sympathetic ganglia as preganglionic nerve stimulation and nicotine treatment is that unlike these other stimuli, 2-DG indirectly activates sympathetic ganglia. Since 2-DG is a glucose analog that does not undergo glycolysis, it causes hypoglycemia. This drop in blood glucose levels is detected by glucose sensing neurons in the brain (Anand et al., 1964, Oomura et al., 1964) and leads to regional activation of the sympathetic nervous system (Niijima, 1989). Hypoglycemia increases sympathetic activation of the pancreatic (Bloom et al., 1978), hepatic (Pascoe et al., 1989), and adrenal branches (Niijima, 1975, Karlsson and Ahren, 1991) but not the renal branch (Niijima, 1975) of the splanchnic nerve, which leads to the release of glucagon, glucose, and adrenaline, respectively. Hence, the involvement of central integration in indirect activation may attenuate neuronal activation in sympathetic ganglia.

Alternatively, our results may indicate that as a metabolic stimulus, 2-DG triggers a pathway in the CG that is independent of the one involved in arterial pressure regulation. As a

result, we observed a similar response in normotensive and hypertensive sympathetic ganglia to 2-DG. In contrast, direct sympathetic stimulation via preganglionic nerve stimulation and nicotine is likely to activate all pathways in sympathetic ganglia including the one involved in arterial pressure regulation. The existence of different functional pathways in sympathetic ganglia projecting to vascular and non-vascular targets has been previously substantiated (Gibbins, 1992, Janig and McLachlan, 1992a, Browning et al., 1999, Kreulen, 2003).

CONCLUSIONS

In this study, we used c-fos expression as a marker of neuronal activation in sympathetic postganglionic neurons. More c-fos expression was measured after 6 Hz of preganglionic nerve stimulation than 2 Hz, which indicated that c-fos expression was a valid marker of neuronal activation. Surprisingly, basal c-fos expression was similar in normotensive and DOCA-salt hypertensive CGs contrary to previous findings of a higher sympathetic drive in hypertensive rats. However, after direct stimulation of the ganglia via preganglionic nerve stimulation or nicotine treatment, c-fos expression increased less in hypertensive than normotensive sympathetic ganglia. This may be due to desensitization of nicotinic receptors due to higher preganglionic nerve activity. However, indirect stimulation via 2-DG treatment led to a similar increase in both normotensive and hypertensive CGs. Indirect stimulation involves central integration, which may attenuate neuronal activation in the CG. Alternatively, 2-DG may stimulate a metabolic pathway in sympathetic ganglia that is unaffected by hypertension.

CHAPTER FOUR: DISTINCT ANATOMICAL CHARACTERISTICS OF ARTERY-PROJECTING AND VEIN-PROJECTING SYMPATHETIC NEURONS

ABSTRACT

Arteries and veins both contribute to arterial pressure regulation but through different mechanisms; arteries influence arterial pressure directly through vasoconstriction whereas veins influence arterial pressure indirectly through blood volume distribution. Previous studies looking at innervation of arteries and veins show conflicting results, perhaps due to uptake of retrograde tracers by fibers of passage. In the present study, we developed a novel surgical preparation for isolating small segments (5-10 mm) of adjacent secondary branches of the superior mesenteric artery and vein from which paravascular nerves had been separated and perivascular nerves remained intact. Pseudorabies viral (PRV) tracers (PRV152 expressed green fluorescent protein and PRV614 expressed red fluorescent protein) were exposed onto blood vessel segments for 30 min and then washed away. Fluorogold was injected i.p. 1wk prior to PRV exposure to identify all neurons in abdominal sympathetic ganglia. Paravertebral ganglia from only 1 of 5 rats showed PRV labeling of only 3 neurons. Analysis of CGs showed that of 7768 sympathetic postganglionic neurons labeled with fluorogold (n=5), 26.3±2.1% projected to veins, 13.7±1.6% projected to arteries, 0.9±0.1% projected to both arteries and veins, and 59.1±1.6% were unlabeled. Vein-projecting neurons had significantly larger cross-sectional areas than artery-projecting neurons and unlabeled neurons. Neuropeptide Y (NPY) immunofluorescence showed that a similar proportion of vascular-projecting neurons expressed NPY (44%) as unlabeled neurons (50%). In conclusion, artery-projecting and vein-projecting sympathetic postganglionic neurons in the CG are anatomically distinct and show differences in soma size.

INTRODUCTION

Mesenteric blood vessels of the splanchnic circulation are the largest reservoir of blood (~60% of total blood volume) that can be rapidly redistributed (Lundgren, 1983). Redistribution of blood can occur during physiological conditions like exercise and postural changes and during pathophysiological conditions like hypertension and hemorrhage. In hypertension, constriction of arteries directly increases arterial pressure but constriction of veins is hypothesized to increase arterial pressure by redistributing blood from the venous to arterial side of the circulation (Fink, 2009). Support for this comes from several reports of increased venous tone in animal models of hypertension (Samar and Coleman, 1979, Young et al., 1980, Martin et al., 1998, Fink et al., 2000, King et al., 2007) and in human hypertensive patients (London et al., 1978). Hence, both arteries and veins are important regulators of arterial pressure and sympathetic innervation of each blood vessel type needs to be studied.

Arteries and veins respond differently to sympathetic stimulation (reviewed in Kreulen, 2003). Stimulation of splanchnic nerves resulted in constriction of mesenteric veins at much lower frequencies (1-2Hz) than constriction of mesenteric arteries (10-20Hz) (Kreulen, 1986, Hottenstein and Kreulen, 1987). These observations can be explained by distinct sympathetic innervation of arteries and veins and also by different neurotransmitters or post-synaptic receptor levels at the neuroeffector junctions of arteries and veins (Luo et al., 2003; Park et al., 2010).

In our laboratory, it was previously shown using retrograde tracing of the inferior mesenteric artery and vein in *ex vivo* preparations that arteries and veins are separately innervated (Browning et al., 1999, Zheng et al., 1999). Furthermore, there is also separate sympathetic innervation of arteries and veins supplying the rat hindlimb (Dehal et al., 1992).

However, Hsieh *et al.* (2000) found that the celiac ganglion (CG) provides largely overlapping sympathetic innervation to mesenteric arteries and veins (~55% of all labeled neurons). In that study, primary branches of the superior mesenteric artery and vein were exposed to retrograde tracers without verifying that paravascular nerves were dissected, which project to other targets like abdominal organs (Hottenstein and Kreulen, 1987). Additionally, it is known that fibers of passage take up both the fluorescent tracers used in that study, fast blue and diamidino yellow (Bratton et al., 2010, Yoshimoto et al., 2010). Thus, it is possible that the tracers were taken up by surrounding paravascular nerves and this resulted in the overlapping sympathetic innervation seen by the authors.

In the current set of experiments, we describe a novel *in vivo* preparation developed to expose segments of rat mesenteric arteries and veins to retrograde, pseudorabies viral (PRV) tracers. This preparation allows for careful dissection of connective tissue, fat, and paravascular nerves as well as separation of adjacent artery and vein pairs. The advantages of using PRV tracers is that they are not taken up by fibers of passage and they self-replicate to produce a strong signal in labeled neurons (Enquist and Card, 2003, Cano et al., 2004). Other purported markers of vascular-projecting sympathetic neurons include presence of neuropeptide Y (NPY) (Elfvin et al., 1993) and smaller soma area (Gibbins et al., 2003) compared to neurons projecting to other targets. These markers will be examined in the current study in sympathetic neurons retrogradely labeled from blood vessels. We hypothesize that following dissection of paravascular nerve fibers, we will observe distinct populations of artery-projecting and vein-projecting neurons.

METHODS AND MATERIALS

Animals

Adult male Sprague-Dawley rats (Zivic-Miller Laboratories, Zelienople, PA) weighing 275–350g were used in this study. Rats were housed with *ad libitum* access to food and water while being kept on a 12:12hr light-dark cycle in a room with regulated temperature (22-24°C). During viral exposure and postinoculation intervals, rats were housed in a Biosafety Level 2 laboratory and their health was closely monitored throughout the experimental period. All procedures conformed to the regulations detailed in the NIH *Guide for the Care and Use of Laboratory Animals* and were approved by the University of Pittsburgh Institutional Animal Care and Use Committee. All surgeries and subsequent dissections and tissue sectioning were done at University of Pittsburg and confocal microscopy was done at Michigan State University.

In Vitro Preparation

As previously described (Browning et al., 1999), *in vitro* preparations in which the intact CG was dissected along with the celiac artery and hepatic vein were incubated for several days. Dissections were done by eviscerating the abdominal organs of the rat between the diaphragm and kidneys. This preparation was placed in a large petri dish coated with Sylgard (Dow Corning Corp.) and constantly bathed with DPBS (Gibco). Organs were carefully dissected away leaving only a part of them for orientation purposes. The CG was accessed by dissecting away surrounding fat and connective tissue. Blood and blood clots were flushed out from the celiac artery and hepatic portal vein. Only the CG, part of the abdominal aorta, the celiac artery, part of the liver, and the hepatic portal vein were left and these tissues were pinned out onto a smaller petri dish, covered with organ culture media, and incubated at 37°C in a 95%O_2/5%CO_2

humidified incubator. Preparations were incubated for 0, 3, or 5 days and drop-fixed with 4% paraformaldehyde for 24 hr afterwards. Samples were cryoprotected with 30% sucrose overnight and then sectioned and stained with hematoxylin and eosin (H&E).

Organ culture media was minimal essential medium supplemented with 2.5mL rat serum, 2 mM glutamine, 0.3% glucose, 1000 U/mL penicillin-streptomycin, 10 mg/mL ascorbic acid, 0.25 mg/mL glutathione, 0.05 mg/mL $DMPH_4$, 50 ng/mL nerve growth factor (Millipore), and 10 M each of cytosine arabinoside, fluorodeoxyuridine, and uridine. All reagents were purchased from Invitrogen unless specified otherwise. Feeding media was replaced approximately every 12 hr.

Surgeries

Rats were anesthetized with isoflurane and the mesenteric vasculature was accessed following an abdominal incision. Adjacently located secondary branches of the superior mesenteric artery and vein, 5-10 mm in length were pinned onto a glass petri dish with a Sylgard (Dow Corning Corp.) base, cleared of surrounding fat, separated from each other, and encased in polyethylene tubing. All the exposed tissue on the petri dish was constantly bathed with Hanks' balanced salt solution (HBSS; Gibco). After placing the blood vessel segments in individual polyethylene chambers, both ends of the tubing were sealed with Silicone sealant (Dow Corning Corp.), retrograde tracers were pipetted onto the blood vessels (~5-10 µL). Fluorogold (Fluorochrome LLC) and fast blue (Polysciences) were pipetted onto absorptive gelfoam (Pharmacia and Upjohn Co.) and the chamber was then sealed with silicone glue (Kwik-Cast sealant, World Precision Instrument) for the duration of the survival time. PRVs were pipetted onto blood vessels for 30 min, pipetted off, and vessels were washed 3X with HBSS. All

exposed tissue was returned inside the abdominal cavity, the abdominal incision sutured, and the rat left to recover for 4-5 days.

Retrograde Tracers

Initially, fluorogold (Fluorochrome LLC) and fast blue (Polysciences) were applied to blood vessels and labeling patterns in the CG were observed. However, we found PRV tracers to be more effective and used them in all subsequent preparations. Prior to using PRV tracers, fluorogold was injected (1mL of 0.5%, intraperitoneally) 1wk before surgeries to label all sympathetic postganglionic neurons as previously demonstrated (Tang et al., 1999). Two isogenic strains of the PRV Bartha vaccine strain were used as retrograde tracers (further described in (Banfield et al., 2003)): one that expressed the enhanced green fluorescent protein (EGFP; PRV152) and another that expressed the red fluorescent protein (RFP; PRV614). Both PRV152 and PRV614 had similar concentrations ($8.6X10^8$ pfu/mL and $8.1X10^8$ pfu/mL, respectively). These tracers were a kind gift of Dr. Lynn Enquist at Princeton University. Use of these tracers was counterbalanced on arteries and veins and no significant difference was observed in labeled neurons obtained with PRV152 or PRV614.

Immunohistochemistry

Following appropriate survival times, rats were deeply anesthetized, perfused with 0.9% saline, and then with paraformaldehyde-lysine-periodate fixative (PFA-LP) (McLean and Nakane, 1974). Then, both paravertebral chain ganglia and CGs were dissected, cryoprotected overnight in 30% sucrose, and serial sectioned (30μm) into five series. One of the five series of CG sections was washed with 3X5 min in tris-buffered saline supplemented with tween 20,

blocked for 30 min with normal donkey serum, incubated with rabbit anti-NPY (Immunostar, #22940) for 48 hr, and incubated with donkey anti-rabbit AF647 (Jackson Immunoresearch Laboratories, #711-605-152) for 2 hr.

Controls used to examine paravascular nerve fibers had blood vessels that were either prepared as described above for exposure to tracers or underwent a sham procedure in which the blood vessels were pinned out for 30 min but neither cleared of fat and paravascular nerves nor separated from each other. Then, blood vessels were dissected, drop-fixed overnight in 4% PFA, paraffin embedded, cross-sectioned (5 μm), and stained with H&E.

Controls used to examine perivascular nerves had blood vessels prepared as described above for exposure to tracers. Then, blood vessels were cleared of blood by injecting them with HBSS, drop-fixed overnight in 4% PFA, and processed as whole-mount samples. Samples were washed 3X5 min in tris-buffered saline supplemented with tween 20, blocked for 30 min with normal goat serum, incubated with rabbit anti-tyrosine hydroxylase (Enzo Life Sciences, #TZ1010-0050) overnight, and incubated with goat anti-rabbit Cy5 (Jackson Immunoresearch Laboratories, #111-175-144) for 1 hr.

Image Analysis

Retrogradely-labeled neurons in the CG were imaged at a confocal microscope (Olympus Fluoview-F1000 Spectral confocal microscope). PMT voltage and gain settings were optimized for each channel prior to collection of sequential Z-stack images. Cell counts and cross-sectional area measurements were obtained from maximum intensity projections of Z-stacks. Cell counts were made for fluorogold-positive, GFP-positive, RFP-positive, NPY-positive, GFP-and-RFP-

positive, GFP-positive and NPY-positive, and RFP-positive and NPY-positive neuronal populations. Cell counts were only made from one of five series of sections. Each section on the series was 150 µm apart from the next thus ensuring that neurons (~30-50 µm in diameter) were not double counted in subsequent sections. The observer was blind to surgical details on what tracer was applied to what blood vessel type. For cross-sectional area measurements, analysis software (Olympus Fluoview) was used to trace the outline of GFP-positive, RFP-positive, and GFP-and-RFP-negative neuronal populations. Area measurements obtained from traced neurons were then compiled and analyzed. Only neurons with visible nuclei were included in cell counts and cross-sectional area measurements.

Intensity-based co-localization analysis was conducted on Fluoview software (Olympus) to quantify amount of co-localization of two signals. This was done with a small sample of randomly selected neurons counted as green (GFP-expressing), red (RFP-expressing), yellow (GFP-and-RFP-expressing), blue (NPY-expressing), blue-green (GFP-and-NPY-expressing), and purple (RFP-and-NPY-expressing) neurons taken from all samples. Intensity thresholds were individually set for each channel of each neuron to distinguish autofluorescence from signal. For each neuron, the distribution of pixels was plotted at various pixel intensities for each selected fluorescence channel. Data was reported as number of pixels overlapping and as % of pixels overlapping of total pixels for artery-projecting, vein-projecting, and artery and vein-projecting neurons. Data was also reported for artery-projecting NPY+ and NPY- neurons and for vein-projecting NPY+ and NPY- neurons.

Statistics

Student's *t* tests were used to analyze all comparisons. Also, Pearson's correlation was used to test if survival time or length of blood vessel exposed to tracers correlated with number of labeled neurons observed. All tests were performed using SPSS 21 (IBM). Statistical significance was set at $p \leq 0.05$. Results are presented as means ± standard error of means.

RESULTS

In Vitro Preparations

Initially, *in vitro* preparations were tested to see if they would be a viable method of labeling artery-projecting and vein-projecting sympathetic neurons. However, we found that tissue integrity became progressively worse as the CG preparations were incubated *ex vivo* for 3 (**Fig. 4.1B**) and 5 (**Fig. 4.1C**) days, relative to 0 days (**Fig. 4.1A**). Since organ culture times of at least 3 days were necessary to allow retrograde tracers to travel back to neuronal somata, this suggests that *in vivo* preparations may be more suitable for looking at sympathetic innervation of blood vessels than *ex vivo* preparations.

Presence of Perivascular and Paravascular Nerves

Blood vessels from *in vivo* surgical preparations were examined after being stripped of fat and paravascular nerves. They were verified to have an absence of paravascular nerves, relative to a sham blood vessel preparation (**Fig. 4.3A and B**). In addition, after such a preparation, the perivascular nerves were intact in both the artery (**Fig. 4.3C**) and the vein (**Fig. 4.3D**). Hence, retrograde tracers exposed to isolated mesenteric blood vessels are selectively taken up via perivascular nerves innervating the blood vessels.

Artery-and-Vein-Projecting Neuronal Populations in Paravertebral and Prevertebral Ganglia

Initially, fluorogold and fast blue were tested as retrograde tracers and applied to small segments of mesenteric blood vessels. However, little labeling was observed in the CG for both fluorogold (**Fig. 4.4A**) and fast blue (**Fig. 4.4B**). With both tracers, only ~10 neurons were

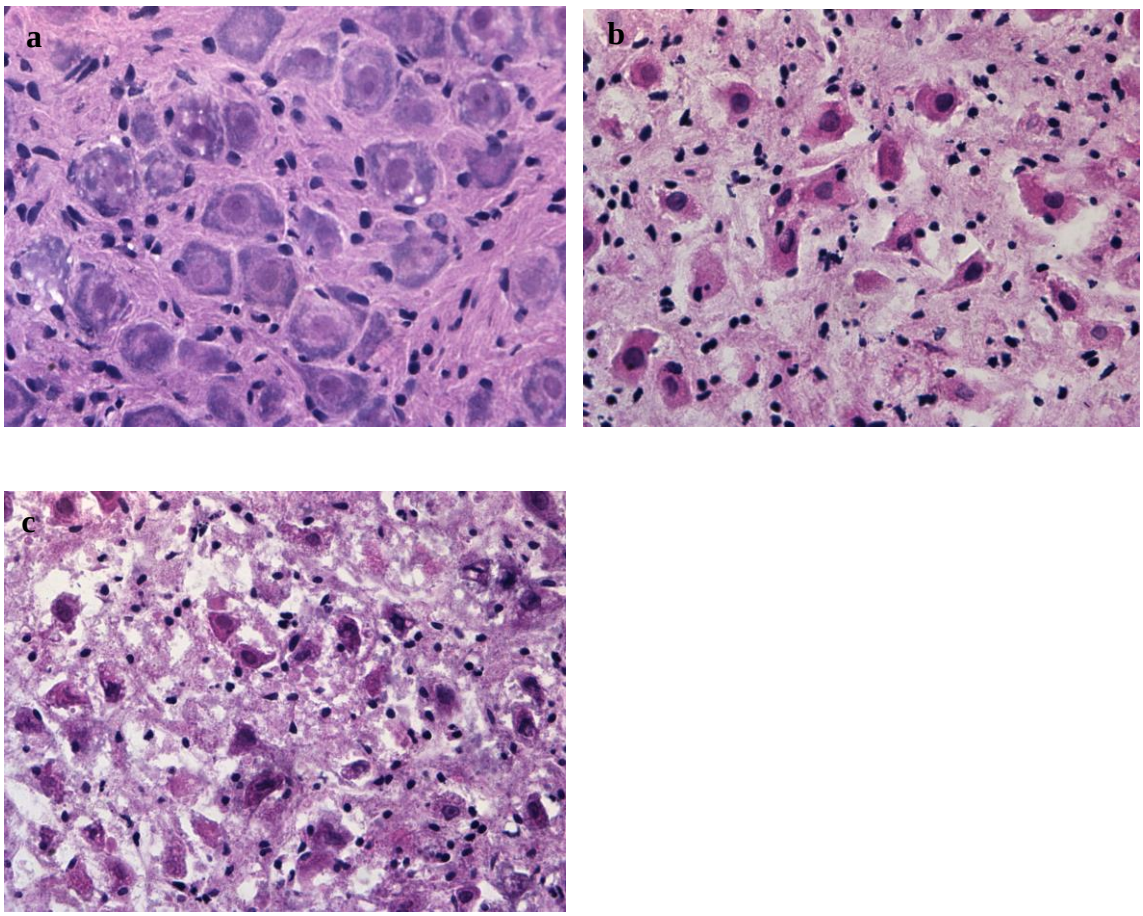

Figure 4.1. Progressive deterioration of tissue quality with increasing ex vivo incubation. H&E stain on frozen sections of CGs obtained immediately after harvesting (a), 1 day after ex vivo incubation (b), and 3 days after ex vivo incubation (c).

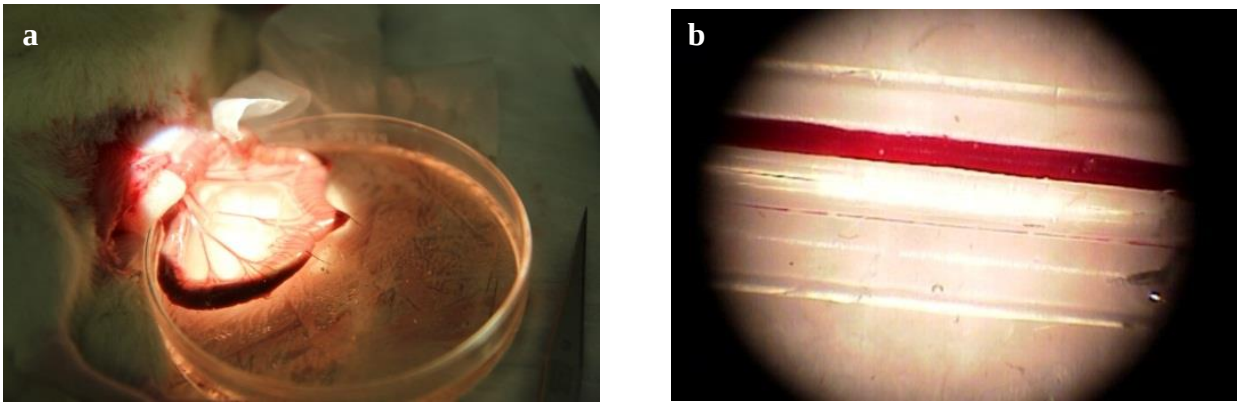

Figure 4.2. Photo of in vivo surgical preparation used for exposing PRV retrograde tracers onto isolated segments of adjacent mesenteric arteries and veins. (a) Part of the small intestine pinned out on a Sylgard-coated petri dish and bathed with HBSS. (b) Image from a dissecting microscope showing segments of adjacent pair of mesenteric artery (bottom) and vein (top) encased in individual chambers made of polyethylene tubing and sealed at ends with silicone sealant; segments in view are 3 mm in length.

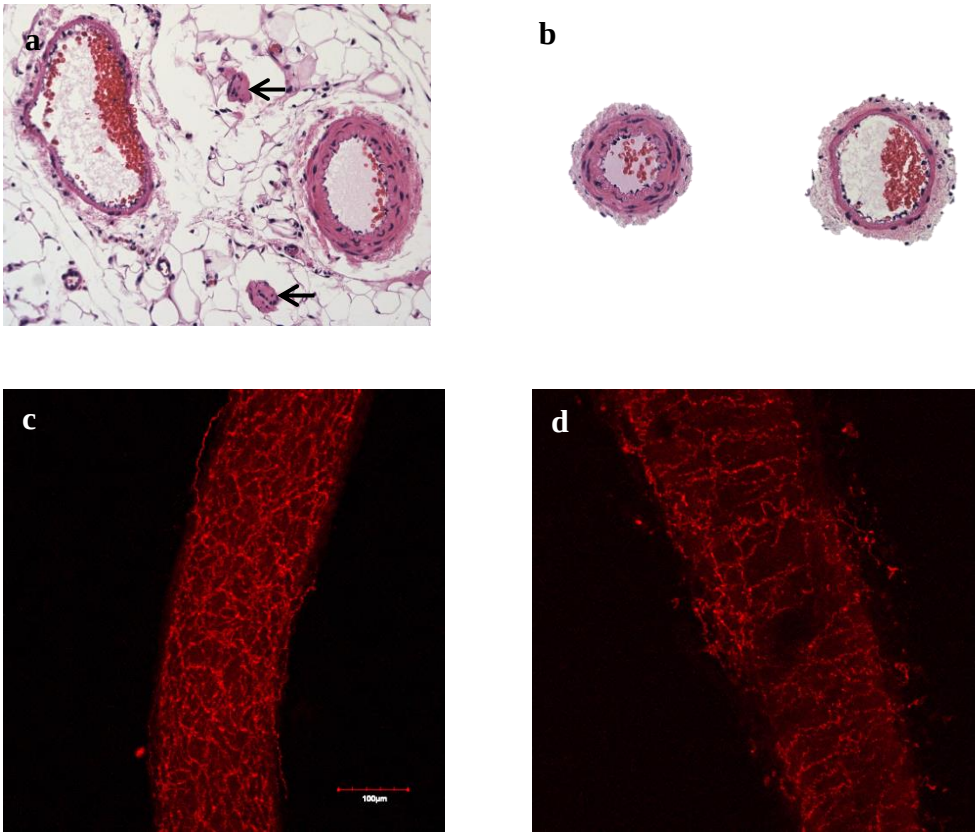

Figure 4.3. Control preparations show that paravascular nerves were dissected but that perivascular nerves were still on operated blood vessels. (a) H&E stain of a sham mesenteric artery and vein preparation in which fat, connective tissue and paravascular nerves were not dissected away; arrows point to intact paravascular nerves. (b) H&E stain of a mesenteric artery and vein preparation in which blood vessels were separated from each other and fat, connective tissue, and paravascular nerves were dissected away. Tyrosine hydroxylase staining indicative of intact perivascular nerves for adjacent (c) artery and (d) vein from a preparation in which blood vessels were separated from each other and fat, connective tissue, and paravascular nerves were dissected away.

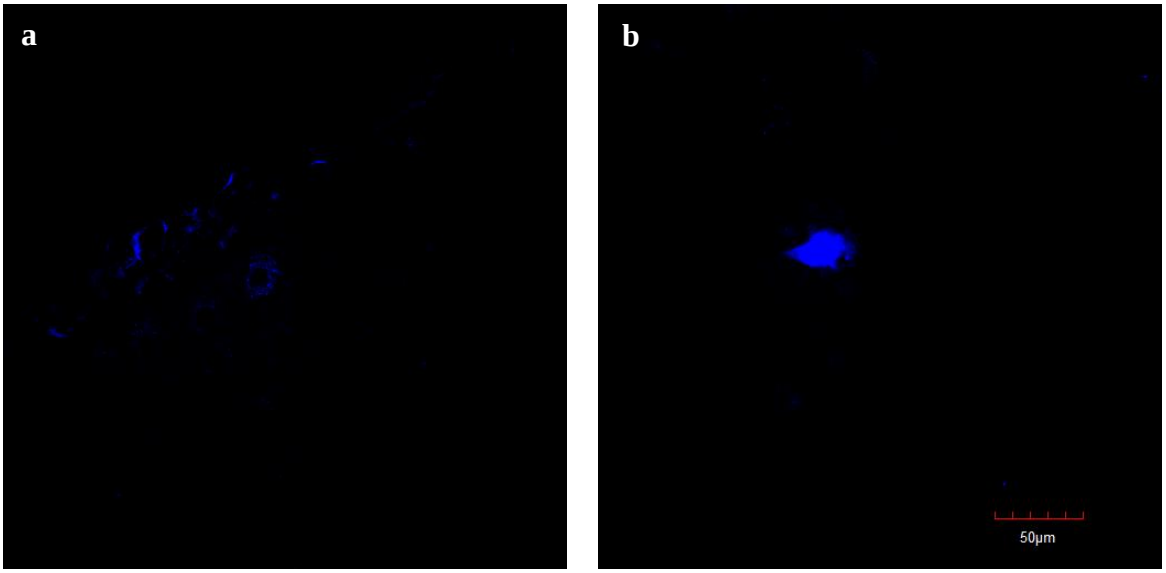

Figure 4.4. Fluorogold and fast blue retrograde tracers applied to mesenteric blood vessels yields few labeled neurons in the CG. Application of fluorogold (a) and fast blue (b) to small ~6 mm segments of mesenteric blood vessels results in few labeled neurons in the CG (~10/CG).

labeled in the whole CG. Subsequently, tracers with a receptor-mediated mechanism of reuptake like PRV were tested to see if they would be more efficient.

An initial pilot experiment indicated that fluorogold injected shortly after exposure of PRV tracers to blood vessels yielded no PRV-labeled neurons, possibly due to reuptake competition of PRVs with the fluorogold tracer. However, fluorogold injections 1 wk prior to exposure of PRV tracers did not visibly affect PRV labeling of sympathetic neurons and successfully led to labeling of all sympathetic postganglionic neurons in the CG (**Fig. 4.5**).

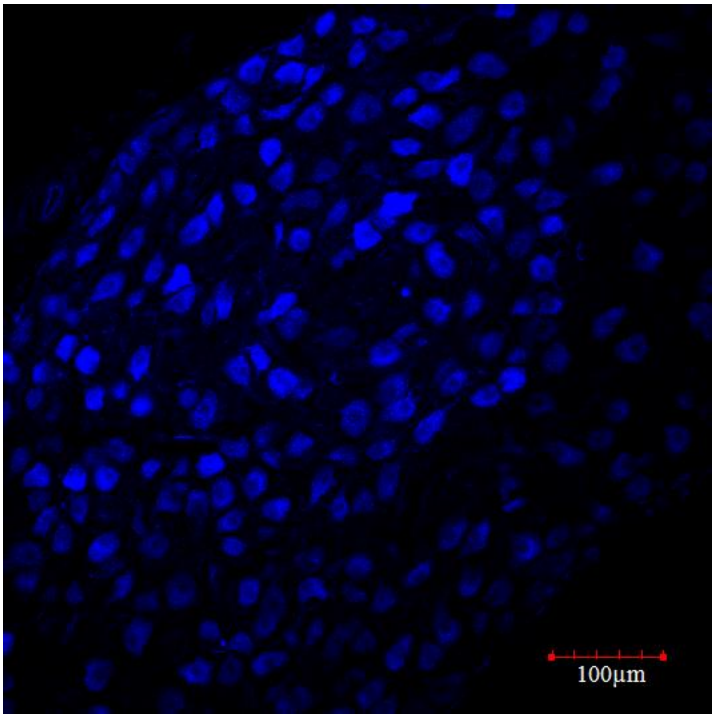

Figure 4.5. All sympathetic postganglionic neurons in the CG are labeled with fluorogold. Fluorogold was injected i.p. (0.5%, 1mL) 1wk prior to surgeries and fluorogold-labeled neurons are shown in blue.

Eight CGs were examined for retrogradely labeled neurons. All CGs showed PRV-labeled neurons (**Fig. 4.6A-H**). Analysis of cell counts indicated that of 7768 sympathetic postganglionic neurons (labeled with fluorogold), 26.3±2.1% were vein-projecting, 13.7±1.6% were artery-projecting, 0.9±0.1% were artery and vein-projecting, and 59.1±1.6% were unlabeled (**Fig. 4.6I**). No topographical organization of artery-projecting and vein-projecting neurons was observed. Instead, these separate populations of neurons appeared to be randomly scattered throughout the whole CG. Only one of five paravertebral chain ganglia had retrogradely labeled neurons (**Fig. 4.7**). This preparation only had three visible labeled neurons in the left chain at the level of T11. Thus, there is little innervation to mesenteric blood vessels from paravertebral chain ganglia.

Co-localization analysis was conducted to verify that single-labeled neurons (green-or-red-labeled) were visually different from double-labeled neurons (green-and-red-labeled). Representative images of a PRV614-labeled neuron (**Fig. 4.8A**), a PRV152-labeled neuron (**Fig. 4.8B**), and a neuron labeled with both PRV152 and PRV614 (**Fig. 4.8C**) shows that there are differences between each of these neurons in the number of pixels at various levels of intensity in channel 1 (red/PRV614) and 2 (green/PRV152). Moreover, there is a significant difference in number of green and red pixels overlapping (**Fig. 4.8D**) and in percent of green and red pixels overlapping of total pixels (**Fig. 4.8E**) between artery-projecting or vein-projecting (ie. single-labeled) and artery and vein-projecting (ie. double-labeled) neurons.

The number of total PRV-labeled neurons did not correlate with survival time of rats (r=0.39, **Fig. 4.9A**) or with the length of blood vessels exposed to PRV tracers (r=0.33, **Fig. 4.9B**).

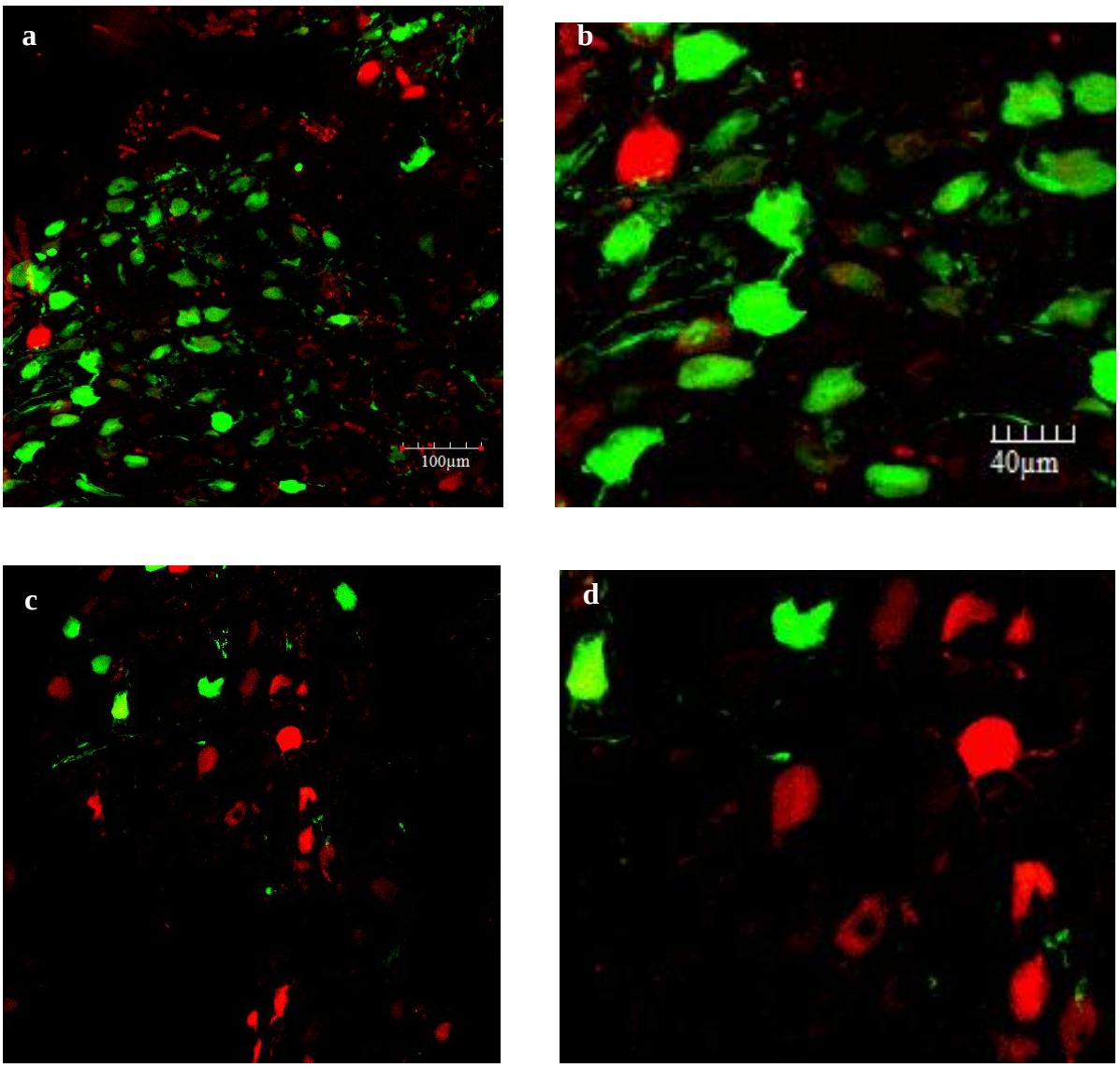

Figure 4.6. Separate sympathetic innervation to mesenteric arteries and veins from sympathetic postganglionic neurons in the CG. Several images of labeled neurons (A,C,G,E) are shown with a magnified view of these images on the right (B,D,F,H). Many single-labeled (red or green) neurons and few double-labeled (artery and vein-projecting) neurons are visible indicating distinct artery-projecting and vein-projecting sympathetic postganglionic neurons. In A, B, C, D green indicates vein-projecting neurons and red indicates artery-projecting neurons whereas in E,F,G,H green indicates artery-projecting neurons and red indicates vein-projecting neurons. (I) Proportions of artery-projecting, vein-projecting, artery and vein-projecting, and unlabeled neuronal populations from 7768 sympathetic postganglionic neurons examined from 8 CGs.

Figure 4.6 (cont'd)

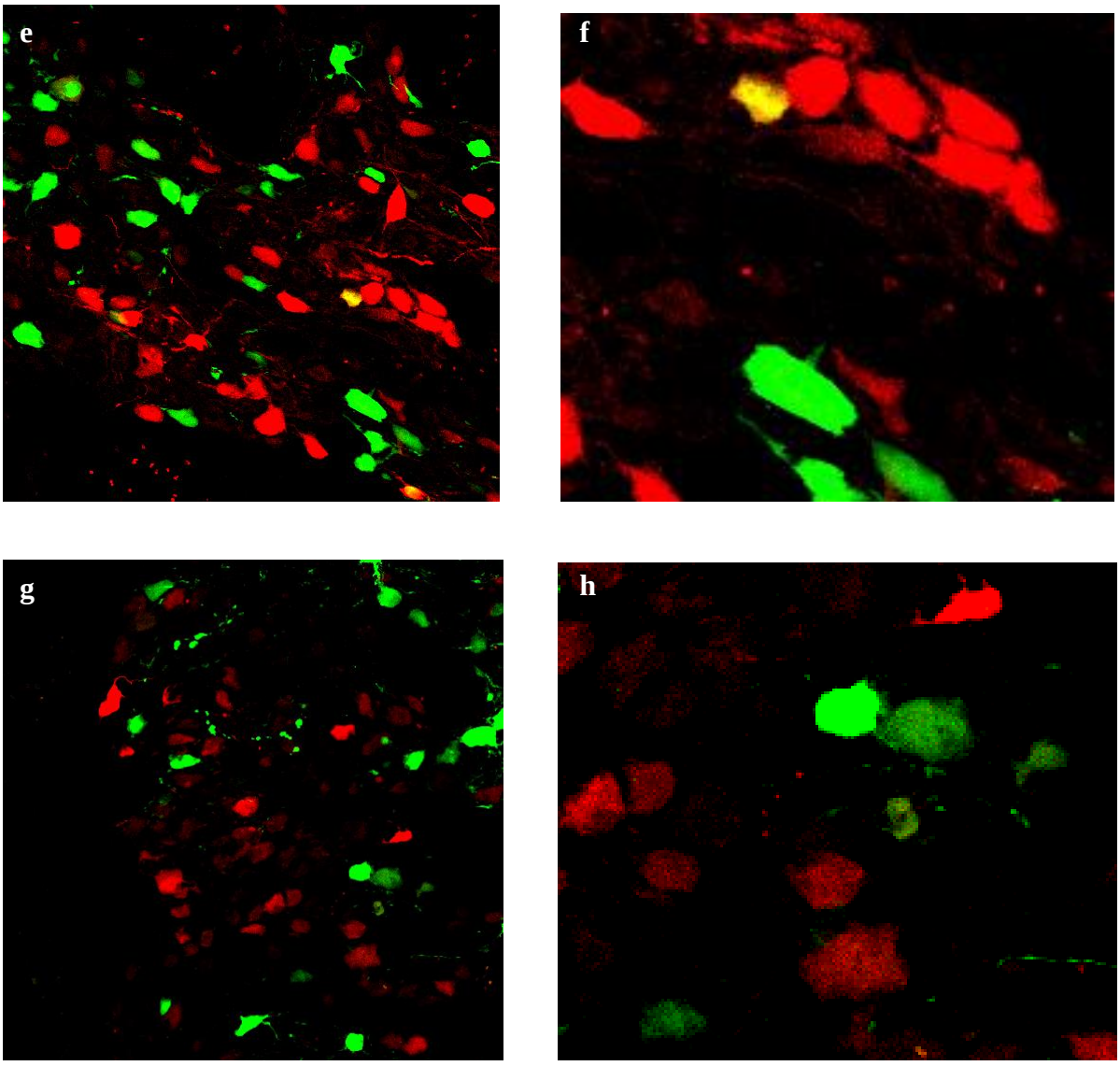

Figure 4.6 (cont'd)

i

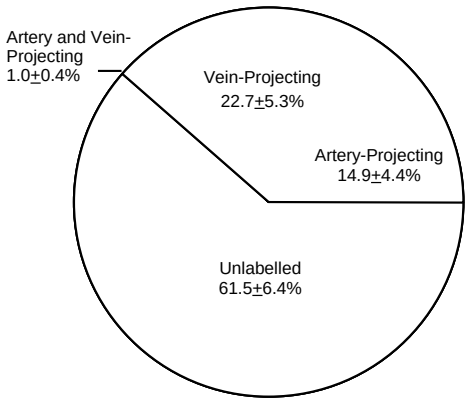

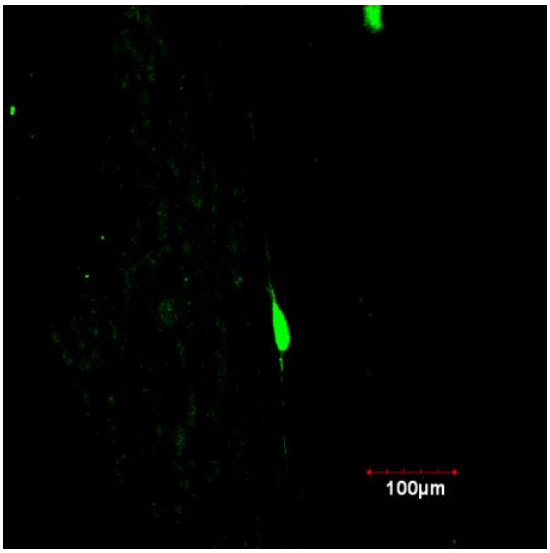

Figure 4.7. Vein-projecting neurons retrogradely labeled with PRV in paravertebral ganglia. These neurons were visualized in the left chain at level T11. This was the only preparation from 5 examined that had any PRV labeling after applying PRV tracers around adjacent arteries and veins and only 3 labeled neurons were observed in this preparation, all vein-projecting.

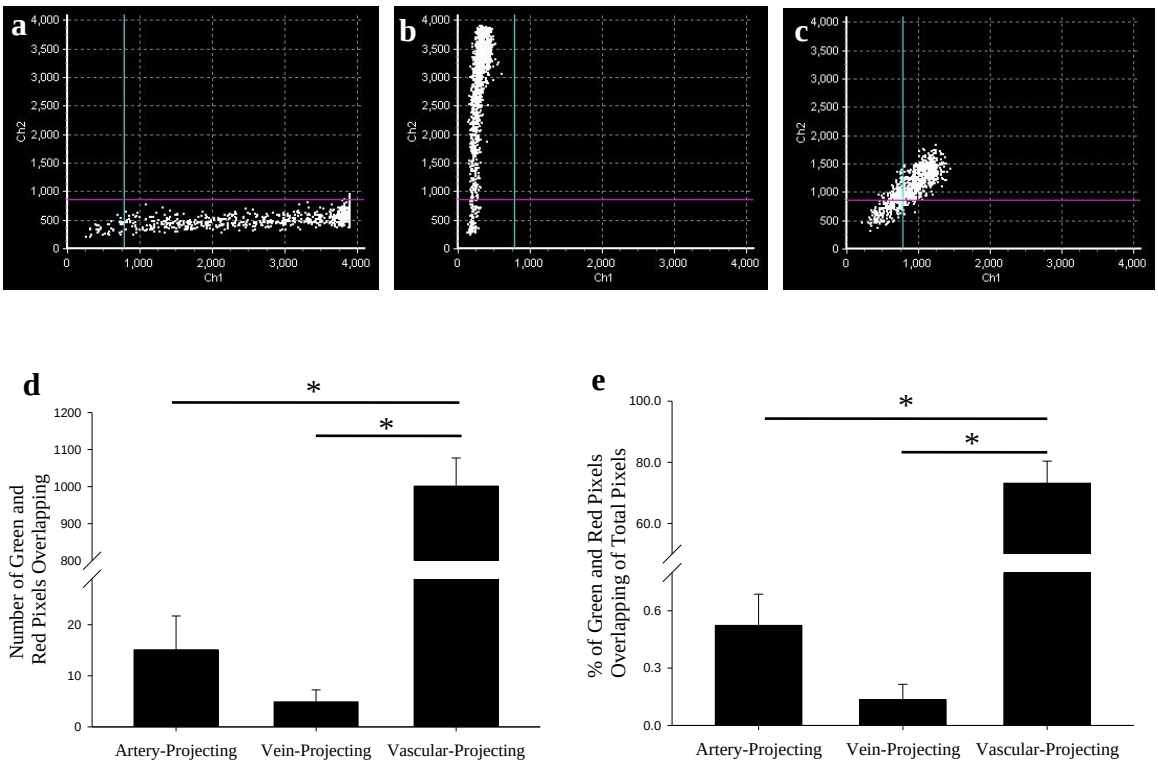

Figure 4.8. Co-localization analysis confirms that artery and vein-projecting neurons are visually different from artery-projecting and vein-projecting neurons. Number of pixels at various levels of intensity is shown for channel 1 (corresponding to RFP) and channel 2 (corresponding to GFP) for a PRV614-labeled neuron (a), a PRV152-labeled neuron (b), and a double-labeled neuron (c). There is a significant difference in number of green and red pixels overlapping (d) and in % of green and red pixels overlapping of total pixels (e) between artery-projecting (n=12 neurons from 8 rats) or vein-projecting (n=10 neurons from 8 rats) and artery and vein-projecting neurons (n=9 neurons from 8 rats).

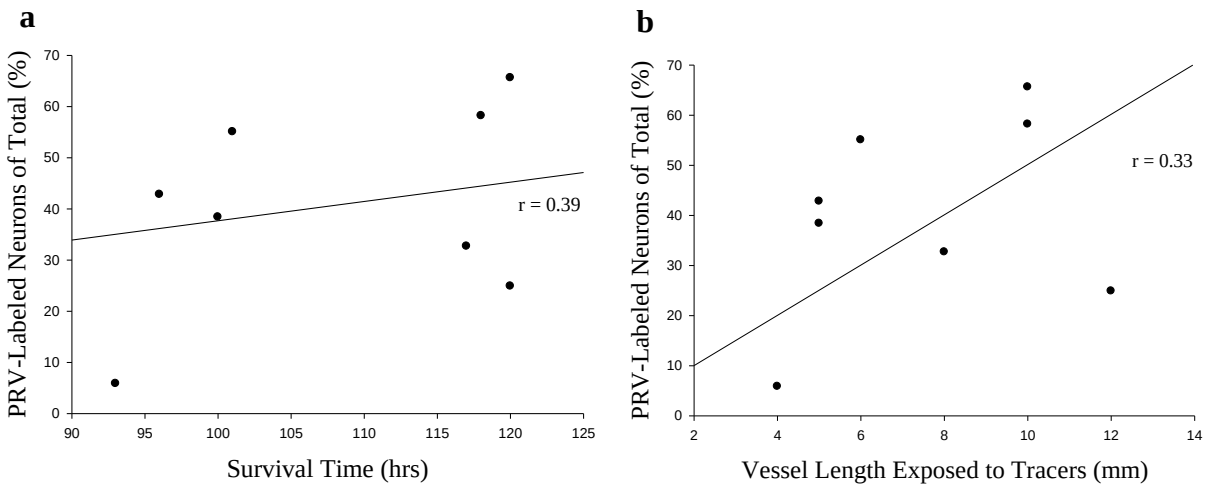

Figure 4.9. There are positive correlations between survival time and vessel length exposed to tracers and number of neurons labeled with PRV. Number of PRV152 and PRV614 labeled neurons are added together and normalized to total number of neurons and plotted against survival time of the rat and vessel length exposed to tracers. Positive correlations that are not significant are found for these variables with a best-fit regression line drawn through the data points and the Pearson's coefficient reported.

Vein-Projecting Neurons have Larger Cross-Sectional Areas than Artery-Projecting Neurons

Analysis of cross-sectional areas of all neuronal populations indicated that vein-projecting sympathetic postganglionic neurons were larger than artery-projecting and unlabeled neurons (**Fig. 4.10A**). There was no difference between artery-projecting and unlabeled neurons. In order to analyze the frequency distributions of all neuronal populations, histograms were plotted for frequency (%) of different cross-sectional areas (**Fig. 4.10B**). Frequency distribution histograms of cross-sectional areas represent bell curves with a right skew for artery-projecting (**Fig. 4.10C**), vein-projecting (**Fig. 4.10D**), and unlabeled (**Fig. 4.10E**) neurons.

Vascular-Projecting Neurons are not Selectively NPY-Positive

NPY immunofluorescence was measured in artery-projecting, vein-projecting, and unlabeled neuronal populations (**Fig. 4.11A**). No difference was observed in percent of NPY immunofluorescent neurons between artery-projecting neurons (43.3±3.4%), vein-projecting neurons (45.1±3.2%), and unlabeled neurons (49.9±1.8%) (**Fig. 4.11B**). Moreover, NPY immunofluorescence was not significantly different in CGs from rats not exposed to PRV tracers (51.5±2.8%, n=3).

Co-localization analysis was conducted to verify that NPY-immunofluorescent positive (NPY+) neurons were visually different from NPY-immunofluorescent negative (NPY-) neurons. Representative images of a PRV614-labeled, NPY- neuron (**Fig. 4.12A**), a PRV152-labeled, NPY- neuron (**Fig. 4.12B**), a PRV614-labeled, NPY+ neuron (**Fig. 4.12C**), and a PRV152-labeled, NPY+ neuron (**Fig. 4.12D**) shows that there are differences between each of these neurons in the number of pixels at various levels of intensity in channels 1 (red/PRV614), 2

a

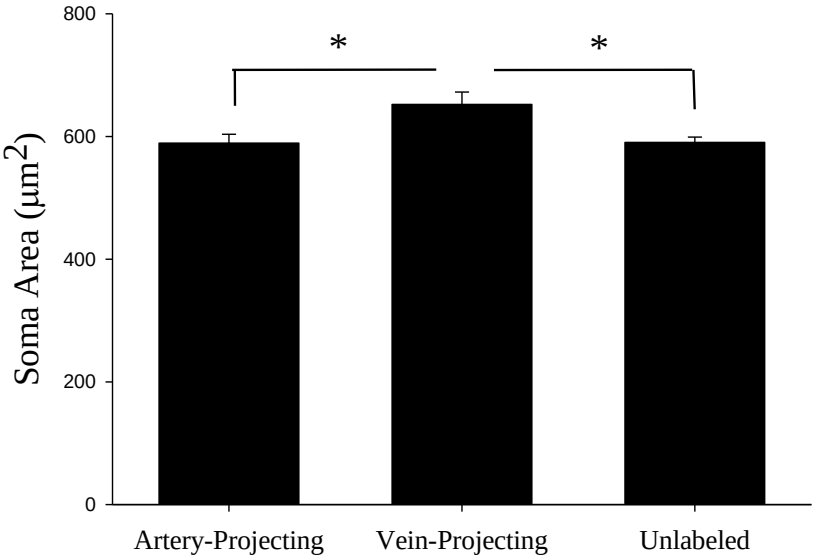

b

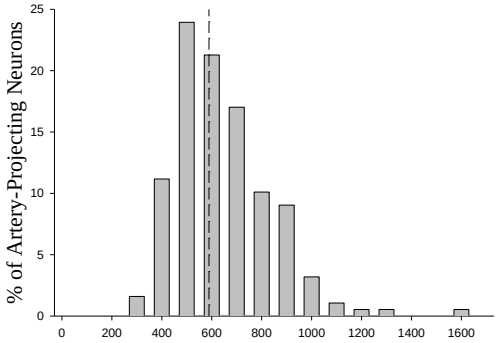

Figure 4.10. Vein-projecting neurons have larger cross-sectional areas but a similar frequency-size histogram as artery-projecting and unlabeled neurons. (a) Cross-sectional areas of artery-projecting (n=188 neurons from 8 rats), vein-projecting (n=142 neurons from 8 rats), and unlabeled neuronal populations (n=401 neurons from 8 rats) in the CG. Frequency-size histograms for artery-projecting (b), vein-projecting (c), and unlabeled (d) sympathetic postganglionic neurons; mean soma size for each population is represented by vertical dotted reference lines.

Figure 4.10 (cont'd)

c

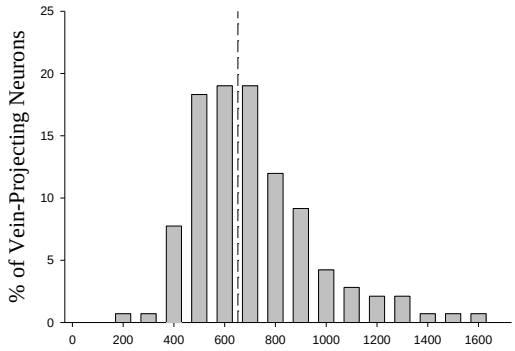

d

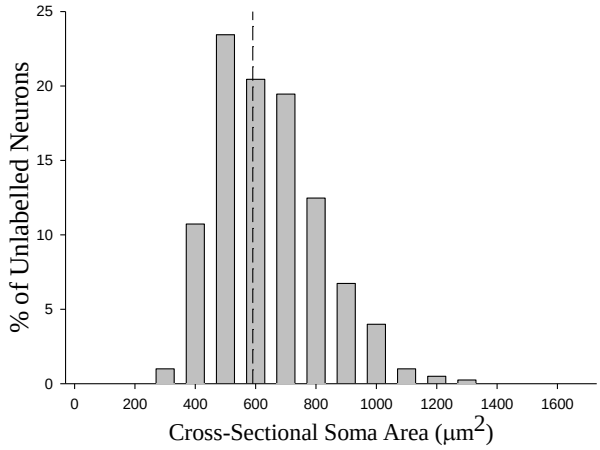

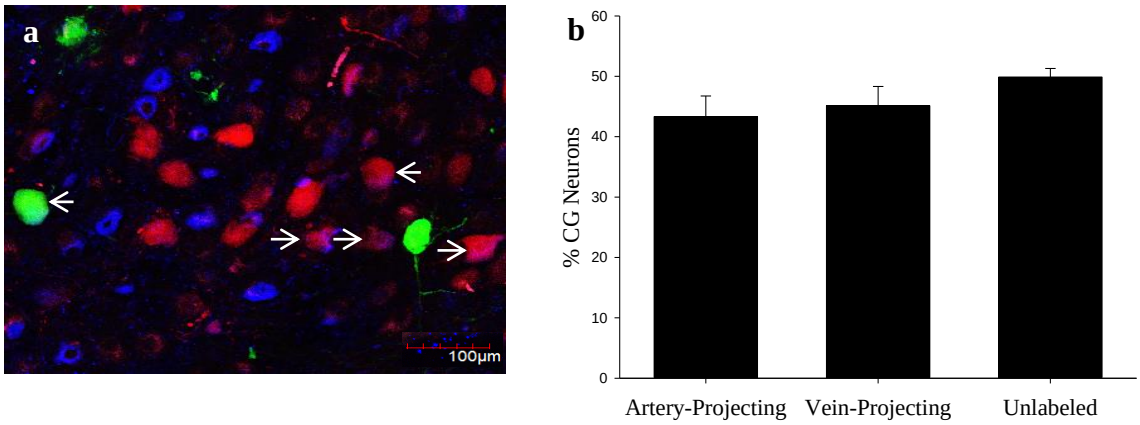

Figure 4.11. NPY is not a selective marker of vascular-projecting neurons. (a) Overlap of NPY immunofluorescence (labeled blue) with artery-projecting (labeled red or magenta when co-localized with NPY) and vein-projecting (labeled green or blue-green when co-localized with NPY) retrogradely labeled neurons in the CG; co-localizations between artery-projecting or vein-projecting neurons and NPY are shown by white arrows. (b) Proportions of NPY immunofluorescent neurons within artery-projecting (n=817), vein-projecting (n=1263), and unlabeled neuronal populations (n=3253) examined in 8 CGs.

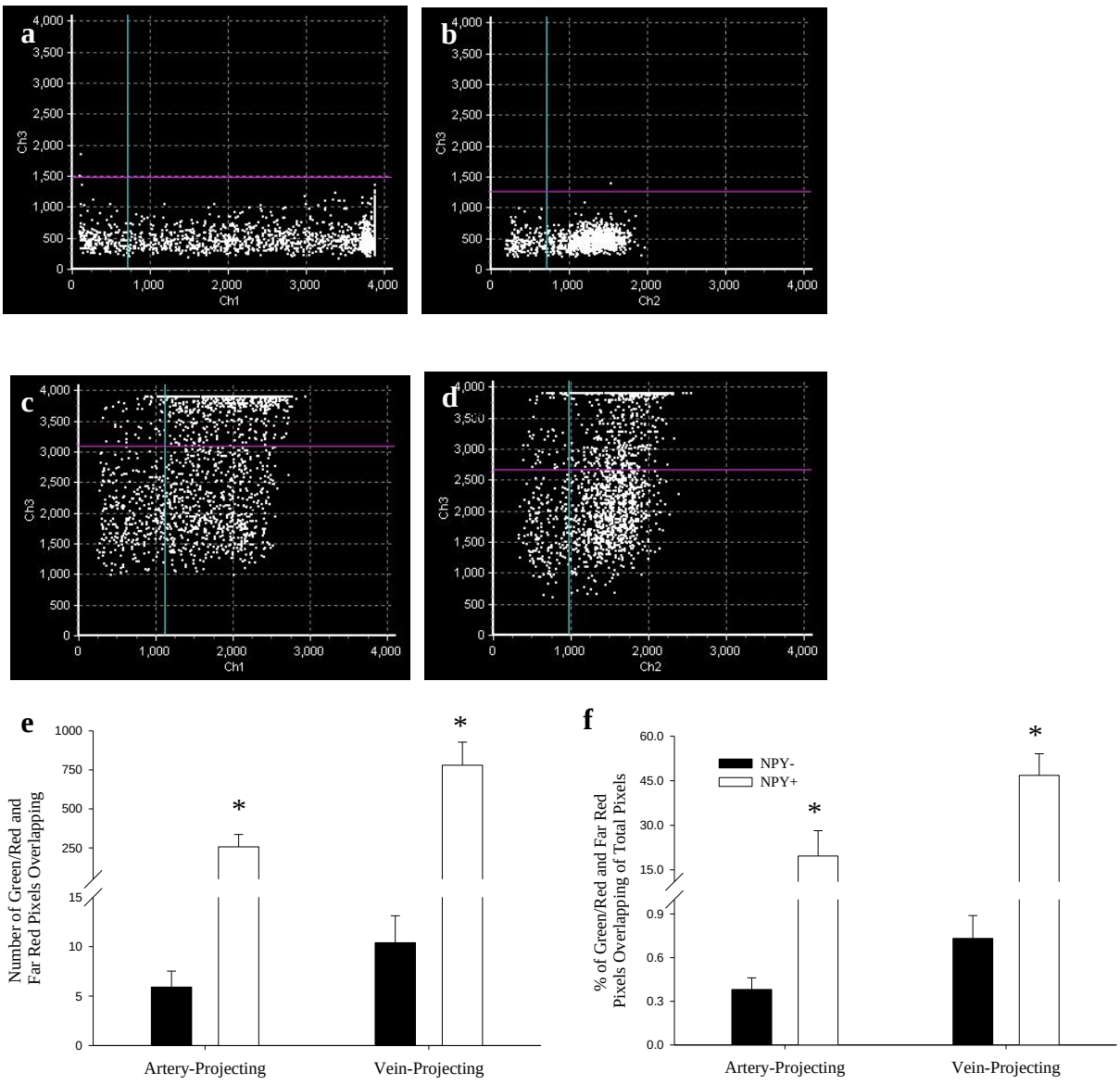

Figure 4.12. Co-localization analysis confirms that NPY-immunofluorescent positive (NPY+) neurons are visually different from NPY immunofluorescent negative (NPY-) neurons. Number of pixels at various levels of intensity is shown for channel 1 (corresponding to RFP), channel 2 (corresponding to GFP), and channel 3 (corresponding to NPY) for a PRV614-labeled neuron (a), a PRV152-labeled neuron (b), a PRV614-and-NPY-labeled neuron (c) and a PRV152-and-NPY-labeled neuron (d). There is a significant difference in number of green or red and blue pixels overlapping (e) and in % of green and red pixels overlapping of total pixels (f) between NPY+ and NPY- neurons for both artery-projecting (n=11 neurons from 8 rats) and vein-projecting (n=10 neurons from 8 rats) neurons.

(green/PRV152), and 3 (far red/NPY). Moreover, there is a significant difference in number of green or red and far red pixels overlapping (**Fig. 4.12E**) and in percent of green or red and far red pixels overlapping of total pixels (**Fig. 4.12F**) between NPY+ and NPY- neurons of both artery-projecting and vein-projecting neurons.

DISCUSSION

Key findings of the study are: 1. PRV tracers are taken up via perivascular not paravascular nerves; 2. The mesenteric blood vessels receive their sympathetic innervation primarily from the prevertebral ganglia; there was very little innervation from the paravertebral chain ganglia; 3. The neurons that innervate mesenteric arteries are for the most part separate from the neurons that innervate mesenteric veins; 4. There are many labeled artery-projecting and vein-projecting neurons in the CG (~40% of all CG neurons) from exposing a relatively small segment of mesenteric blood vessels; 5. Vein-projecting neurons have larger cross-sectional areas than artery-projecting or unlabeled neurons but the distribution frequency histograms are similarly shaped for populations; 6. NPY is not a good marker for vascular-projecting neurons.

PRV Tracers are taken up via Perivascular Nerves

The current study develops a novel *in vivo* method to target isolated segments of mesenteric blood vessels after ensuring that paravascular nerves directly adjacent to those blood vessels have been dissected away. The absence of paravascular nerves but presence of perivascular nerves for both mesenteric arteries and veins was verified for this preparation. In addition, perivascular nerves appear not to be damaged in the process of isolating the blood vessels from each other and surrounding tissue since tyrosine hydroxylase staining in isolated arteries and veins resembles that previously observed (Langley and Anderson, 1895, Costa and Furness, 1984).

Innervation to Mesenteric Blood Vessels is Mainly from Prevertebral Ganglia

A previous study using retrograde tracers around the gut and mesenteric artery found a relatively large number of labeled neurons in paravertebral ganglia projecting to the artery but not the gut (Hill et al., 1987). The authors concluded that sympathetic innervation of mesenteric blood vessels originates mainly from paravertebral ganglia whereas innervation of the gut itself arises mainly from prevertebral ganglia. However, with that study, tracers were not applied in a specific manner to the targets but rather, diffusely injected or left in a gelatin chip to passively diffuse in near vicinity of the target. Again, it is unclear whether paravascular nerves adjacent to the targets could have taken up the tracers. A more recent study by Hsieh et al. (2000) found only a minority of sympathetic innervation to mesenteric blood vessels originating from paravertebral relative to prevertebral ganglia. In accordance with these findings, the present study found little to no innervation to mesenteric blood vessels from paravertebral chain ganglia (<0.01% of all labeled neurons).

Separate Innervation to Mesenteric Arteries and Veins from the CG

Using two isogenic strains of PRVs expressing different fluorescent reporter proteins, we find that the majority of sympathetic innervation to arteries and veins is distinct from each other in the CG. We found that the vast majority of labeled neurons in the CG were single-labeled after applying one PRV to a small segment of artery and the other PRV to a similar length of an adjacent vein. This visual difference between single and double-labeled neurons was confirmed using co-localization analysis, which quantified the number of overlapping green and red pixels in a given neuron. A previous study also showed separate innervation to colonic arteries and veins from the inferior mesenteric ganglion using *ex vivo* preparations (Browning et al., 1999).

Another study found separate sympathetic innervation to arteries and veins in the rat hindlimb (Dehal et al., 1992). However, Hsieh *et al.* (2000) found that the CG provides largely overlapping sympathetic innervation to mesenteric arteries and veins (~55% of all labeled neurons). This may be due to exposure of tracers to paravascular nerves that project to targets in addition to mesenteric blood vessels.

Separate innervation of arteries and veins indicates that there is functional separation between resistance and capacitance, respectively. This is supported by different activation thresholds for arteries and veins; veins activated at stimulation frequency that were approximately one-fold lower than those for arteries (Hottenstein and Kreulen, 1987). Such functional differences between artery-projecting and vein-projecting neurons need to be further examined. Also, there is some evidence for differential control of resistance and capacitance during hemorrhage. In healthy subjects, hemorrhage of 15-20% of total blood volume over 30 min did not alter arterial pressure, heart rate, cardiac output, splanchnic blood flow, splanchnic arterial resistance, or central blood volume (Price et al., 1966). However, splanchnic blood volume and splanchnic capacitance were reduced. Presumably, severe vasoconstriction of veins is important since it would attenuate the volume of blood lost but a similar vasoconstriction of arteries may cause tissue ischemia.

Convergent Innervation of Small Segments of Mesenteric Blood Vessels

Surprisingly, a large number of sympathetic neurons were PRV-labeled (~40% of all sympathetic neurons) after exposing tracers to small segments of blood vessels (~5-10 mm). In contrast, a previous study by Hsieh *et al.* (2000) found that exposing tracers to 15 mm segments of the primary superior mesenteric artery and vein resulted in retrograde labeling in ~7.4% of all

sympathetic neurons. This stark difference in results may be due to the different retrograde tracers used in the two studies. Fast blue and diamidino yellow were used in the previous study and PRV tracers were used in the current study. Interestingly, when we used fluorogold and fast blue in preliminary studies, there were approximately 100-fold fewer labeled neurons with these retrograde tracers than with PRV tracers.

Fluorogold is a weak base that crosses cell membranes in its uncharged form and is trapped in lysosomes and endosomes by a favorable pH gradient whereas fast blue is a hydrophilic tracer that crosses cell membranes via endosomal transport (Wessendorf, 1991, Kobbert et al., 2000). PRV uptake, on the other hand, is mediated via strong interaction between virally expressed glycoprotein gD with cell-surface receptors. Fusion between viral and cellular membranes is then mediated by other virally expressed proteins (gB and gH/gL) (Whitley and Roizman, 2001). The receptor-mediated reuptake mechanism may be more efficacious than that of fluorogold and fast blue. In support of this idea, cholera toxin subunit b, which also has a receptor-mediated mechanism via binding of choleragenoid in the larger B subunit to the GM1 receptor of the cell membrane (Turner and Jenkins, 1997, Fink et al., 2000, Song et al., 2005), exposure to similarly small segments of mesenteric blood vessels yields a similar number of labeled neurons in the CG as PRV tracers (see Chapter 5).

Since viral tracers are able to cross synapses, it is possible that if postganglionic neurons are synaptically connected to each other within sympathetic ganglia then PRVs may label the entire network of synaptically connected neurons. Several reports show that dendrodendritic synapses may be present between sympathetic postganglionic neurons in the rat superior cervical ganglion (Kondo et al., 1980, Kawai, 1996, Zaidi and Matthews, 1997). If PRVs were crossing

dendrodendritic synapses, it is expected that the number of labeled neurons would positively correlate with rat survival time. However, no correlation (-0.01) was observed in the current study between number of labeled neurons and rat survival time.

We are not the first to suggest that there is a great deal of converging input to vasculature from many different sympathetic postganglionic neurons. Gibbins and colleagues (1998) found that in cutaneous blood vessels of guinea pig ear tips, there were 50-100 sympathetic neurons projecting on average to 1 mm^2 of vasculature. It is difficult to make direct comparisons to this previous study since in the present study, only one of five sequential series was stained and analyzed. However, multiplying number of labeled neurons by five, ~102±34 neurons are labeled per 1 mm^2 of mesenteric artery and ~163±47 neurons are labeled per 1 mm^2 of mesenteric vein. But, the surface area of a given segment of vein is considerably larger than of an artery, which may account for more neurons labeled for veins than arteries. The functional significance of this type of organization may be to allow the sympathetic nervous system to apply graded control of the resistance or capacitance of the entire mesenteric circulation by affecting the firing rate or recruitment of artery-projecting or vein-projecting neurons, respectively. This is supported by a difference in activation patterns observed between arteries and veins (Hottenstein and Kreulen, 1987). As mentioned above, veins had a much lower activation threshold than arteries. In addition, the proportional constriction was greater in veins than arteries suggesting that veins are more likely to be activated by additional recruitment of neurons than arteries.

Vein-Projecting Neurons are larger than Artery-Projecting Neurons

Cross-sectional areas of vein-projecting neurons were larger than artery-projecting and unlabeled neurons. However, the frequency distribution histograms of all neuronal populations

were similar. Similar to these results, Browning et al. (1999) also found that vein-projecting neurons in the guinea pig IMG were larger than artery-projecting neurons but that both populations were smaller than unlabeled neurons. A size difference between artery-projecting and vein-projecting neurons provides further evidence that there are different populations of neurons in the CG. Previously, it was postulated that vascular-projecting neurons are smaller than pilomotor or secretomotor neurons (Gibbins et al., 2003), which was thought to correspond to their slower action potential conduction velocities. However, these studies were based on cranial targets and on the cutaneous vascular bed.

Larger soma sizes in sympathetic postganglionic neurons are correlated with larger target size (Voyvodic, 1989). Hence, it is possible that vein-projecting neurons innervate a broader area or more densely innervate their target than artery-projecting neurons. Indeed, for a given segment length, there are typically more sympathetic neurons innervating the vein than artery. However, the surface area of veins is also considerably larger than of arteries and it is possible that after normalizing to surface area of the vessel, there may be no difference in the number of sympathetic neurons innervating the blood vessel.

NPY is not a Selective Marker for Vascular-Projecting Neurons

The 'chemical coding' hypothesis suggests that since NPY is so predominant in perivascular sympathetic nerves innervating blood vessels, NPY must be present only in vascular-projecting sympathetic neurons (Elfvin et al., 1993). However, retrograde tracing studies show that only a subset of between ~40-80% of vascular-projecting neurons express NPY depending on the vascular bed being examined (Gibbins and Morris, 1990, Browning et al., 1999). In addition, this hypothesis has not been well studied in the mesenteric vascular bed. After

labeling artery-and-vein-projecting neurons, the current study identified that NPY is not preferentially expressed in these neurons and is just as prevalent in unlabeled neurons. It is noteworthy that past studies found that short to medium survival times after PRV infection do not alter neurotransmitter levels (Yang et al., 1999). Our results supported these findings as we found no difference in NPY immunofluorescence between CGs after a medium-length PRV infection time (4 days) CGs not exposed to PRV.

CONCLUSIONS

In this study, we developed a novel *in vivo* surgical preparation to study sympathetic innervation from the CG to mesenteric arteries and veins. Small segments of mesenteric arteries and veins were isolated from each other and from other tissue into individual polyethylene chambers. Paravascular nerves surrounding the blood vessel segments were separated but perivascular nerves were intact in operated preparations. Two isogenic strains of PRVs expressing different fluorescent proteins were used for retrograde tracing. A vast majority of single-labeled neurons (40% of all CG neurons) and few double-labeled neurons (1% of all CG neurons) were observed indicating that there is largely separate sympathetic innervation of mesenteric arteries and veins. Several neurons were labeled after applying tracers to small segments of blood vessels indicating that there is a great deal of convergent input to mesenteric vasculature. Vein-projecting neurons had larger soma sizes than artery-projecting and unlabeled neurons. Also, vascular-projecting neurons did not selectively express NPY; other potential markers of this neuronal population need to be investigated.

CHAPTER FIVE: USE OF TWO RETROGRADE TRACERS TO STUDY INNERVATION PATTERNS OF VASCULAR-PROJECING SYMPATHETIC POSTGANGLIONIC NEURONS

ABSTRACT

Our previous work with two PRVs indicates that mesenteric arteries and veins are separately innervated by sympathetic postganglionic neurons. This study examined mixtures of different tracer combinations including two PRVs and a combination of PRV and CTb. When applied to mesenteric blood vessels (adjacent pair of artery and vein), significantly more double-labeled neurons were obtained with the PRV and CTb mixture. This indicates that competition between two PRVs may occur in sympathetic postganglionic neurons and that the PRV and CTb combination is better suited to study separate vs. overlapping sympathetic innervation of arteries and veins. When this combination of tracers was applied to arteries and veins (one tracer on the artery and the second one on the vein), 39.2±3.2% of neurons labeled with PRV were double-labeled and the remaining labeled neurons were single-labeled. Hence, a large proportion of neurons projects to either arteries or veins. Vascular-projecting neurons had larger soma areas than unlabeled neurons and did not selectively express NPY. Also, 23% of all CG neurons were labeled after exposure of retrograde tracers to 6 mm segments of blood vessels suggesting that many vascular-projecting neurons converge to segments of mesenteric blood vessels. A majority of neurons also projected to two adjacent (45.1±8.0% of PRV614-labeled neurons) or two widely separated blood vessels (48.3±3.0% of PRV614-labeled neurons) of the same type suggesting that most sympathetic neurons diverge widely whereas some of them project to very narrow targets.

INTRODUCTION

Sympathetic ganglia form the last neuronal link between sympathetic pathways originating in the brainstem and projecting to peripheral targets. They were simplified as mass action units involved mainly in the 'fight-or-flight' response (reviewed in Janig and McLachlan, 1992b). However, more recently they are shown to be involved in both the integration and relay of signals in a physiologically specific manner (Bratton et al., 2010). Moreover, there is considerable evidence of specificity in sympathetic outflow to different targets. For instance, there is distinct sympathetic innervation to arteries and veins and there are functional differences between isolated artery-projecting and vein-projecting neurons (Browning et al., 1999). Vein-projecting neurons were located in the periphery of sympathetic ganglia and had larger soma areas than artery-projecting neurons. Also, both artery-and-vein-projecting neurons were tonic firing compared to only 40% of unlabeled neurons.

The innervation patterns of vascular-projecting is unknown; however, projection patterns of sympathetic postganglionic neurons projecting to cutaneous vasculature of the ear has been studied. A 1 mm^2 area of skin is innervated by ~75 sympathetic postganglionic neurons indicating that there is convergent sympathetic innervation to sympathetic targets (Gibbins et al., 1998). Also, postganglionic neurons diverge to innervate large areas of vasculature. For instance, a single neuron can innervate a wide region of skin as far apart as 7 mm, which must contain many diverging blood vessels (Gibbins et al., 1998). However, it is unknown whether artery-projecting and vein-projecting sympathetic postganglionic neurons innervate mesenteric arteries and veins that are directly adjacent or widely separated.

The discovery of retrograde tracers has made it possible to isolate populations of sympathetic neurons. The earliest tracer used in retrograde tracing experiments was the plant enzyme horseradish peroxidase (HRP), which is transported to the cell soma via active retrograde transport (Weiss and Hiscoe, 1948). Even before that, it was known that viruses like pseudorabies virus (PRV) of the alphaherpes virus family could travel from the peripheral to central nervous system suggesting that they may be effective neural tracers (reviewed in Norgren and Lehman, 1998, Pomeranz et al., 2005). After decades of research, the molecular mechanism of virus entry, transport, and egress have been well documented for PRVs. In addition, different strains of PRVs have been engineered that only travel retrogradely and express the fluorescent reporter, green fluorescent protein (GFP; PRV152), or red fluorescent protein (RFP; PRV614) (Banfield et al., 2003). These have been extensively used for dual labeling within the nervous system. Combinations of viral and non-viral tracers have also been tested and while certain tracers interfere with viral tract tracing, other tracers like cholera toxin subunit b (CTb) work well with PRV (Chen et al., 1999).

The aims of this study are: 1) determine how much co-localization of tracers occurs in sympathetic ganglia after a mixture of PRV152/PRV614 or PRV614/CTb; 2) study innervation of mesenteric arteries and veins with a PRV614/CTb combination and compare these results with previously obtained ones using a PRV152/PRV614 combination; 3) look at innervation patterns of proximal and distal segments of the same branch of artery or vein, and of adjacent branches of two arteries or two veins, and of distant branches of two arteries or veins. We hypothesize that there are separate neuronal population in the CG projecting selectively to arteries or veins. Also, vascular-projecting neurons are predicted to diverge to widely separated blood vessels.

METHODS AND MATERIALS

Animals

Adult male Sprague-Dawley rats (Charles River Laboratories, Portage, MI) weighing 275–350 g were used in this study. Rats were housed with *ad libitum* access to food and water while being kept on a 12:12 hr light-dark cycle in a room with regulated temperature (22-24°C). During viral exposure and postinoculation intervals, rats were housed in a Biosafety Level 2 laboratory and their health was closely monitored throughout the experimental period. All procedures conformed to the regulations detailed in the NIH *Guide for the Care and Use of Laboratory Animals* and were approved by the Michigan State University Institutional Animal Care and Use Committee.

Retrograde Tracers

Fluorogold (Fluorochrome) was injected (1mL of 0.5%, i.p.) 1 wk prior to surgeries to label all sympathetic postganglionic neurons as previously demonstrated (Tang et al., 1999). Two isogenic strains of the PRV Bartha vaccine strain were used as retrograde tracers (further described in (Banfield et al., 2003)): one that expressed the enhanced green fluorescent protein (EGFP; PRV152) and another that expressed the red fluorescent protein (RFP; PRV614). Both PRV152 and PRV614 had similar concentrations ($1.2X10^9$ pfu/mL and $3.0X10^8$ pfu/mL, respectively). These tracers were a kind gift of Dr. Lynn Enquist at Princeton University. PRV614 was also used in combination with unconjugated CTb (List Biological Laboratories, 2% in HBSS) to study whether this combination gave results different from a PRV152/PRV614 combination. Use of these tracers was counterbalanced between experimental preparations.

Surgeries

The general surgical procedure was similar for all the different preparation types and is briefly described as follows. Rats were anesthetized with isoflurane and the mesenteric vasculature was accessed following an abdominal incision. Secondary branches of the superior mesenteric artery and vein ~6 mm in length were pinned onto a glass petri dish with a Sylgard (Dow Corning Corp.) base, cleared of surrounding fat, separated from each other, and encased in polyethylene tubing. All the exposed tissue on the petri dish was constantly bathed with Hanks' balanced salt solution (HBSS). After placing the blood vessel segments in individual polyethylene chambers, both ends of the tubing were sealed with Silicone sealant (Dow Corning Corp.), retrograde tracers were pipetted onto the blood vessels (~8 µL), and left for 30 min. Then, the tracers were pipetted off the blood vessels, and the vessels were washed 3X with HBSS. All exposed tissue was returned inside the abdominal cavity, the abdominal incision sutured, and the rat left to recover for 4-5 days.

When PRV614 was used in combination with CTb, the tracers were pipetted onto a piece of gelfoam (Pharmacia and Upjohn Co.) placed within the isolated polyethylene chamber. The vessels within their individual chambers were sealed with fast-curing silicone glue (Kwik-Cast, World Precision Instruments). After allowing time for the glue to cure (~5 min), the whole preparation was returned inside the abdominal cavity, the abdominal incision was sutured, and the rat was left to recover for 3 days prior to dissection.

A survival time of 4-5 days was used with PRV152/PRV614 combination but only 3 days was used with PRV614/CTb combination. This was due to pilot experiments with 2 and 4 day survival times. No PRV-or-CTb-labeled neurons were observed in the CG after a 2 day survival

time, indicating that this was not sufficient time for retrograde transport of either of these two tracers (n=2). With a 4 day survival time, 2 of 3 CGs showed no CTb-labeled neurons. The remaining preparation showed a few weakly CTb-labeled neurons (**Fig. 5.1**). We concluded based on these observations that a 2 day survival time was too short but that a 4 day survival time was too long and that CTb may be getting phagocytosed by this timepoint. Hence, a 3 day survival time was selected since it was likely optimal for CTb-labeling. However, it is likely that 3 days was less than optimal for PRV614 and indeed, we found that a 3 day survival time yielded fewer PRV614-labeled neurons on average (but not significantly less) than 4-5 day survival time (**Fig. 5.2**).

In addition to preparation where tracers were applied to adjacent secondary branches of mesenteric artery and vein, three other preparation types were done to determine whether vascular-projecting sympathetic neurons project both to directly adjacent or widely separated blood vessels: 1. PRV614 and CTb were applied to proximal and distal 6 mm segments of the same blood vessel with a 2 mm gap in between these segments; 2. These tracers were applied to two adjacent blood vessel segments (8 mm) of the same type (either arteries or veins) supplying the ileum segment of the small intestine; 3. These tracers were applied to two widely separated blood vessel segments (8 mm) of the same type (either arteries or veins) supplying the ileum and jejunum segments of the small intestine.

A mixture of PRV152 and PRV614 was also injected into the left kidney as previously described (Cano et al., 2004). Briefly, a total 2 µL of the PRV mixture was injected into four different locations in the left renal parenchyma (0.5 µL/location) with a 10 µL Hamilton syringe. Following injections, any visible leakage was absorbed with a cotton tip applicator.

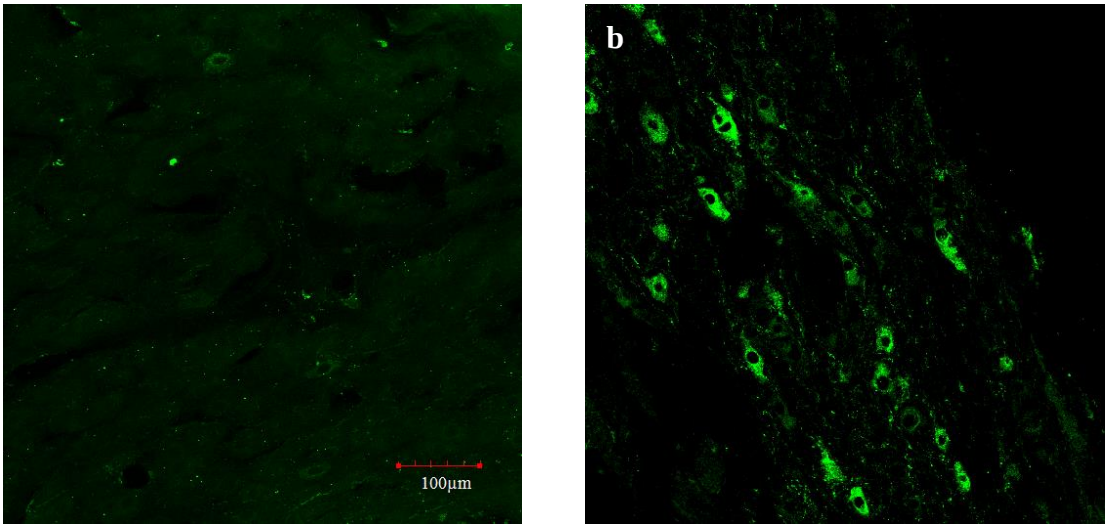

Figure 5.1. Longer survival time following CTb exposure to blood vessels results in fewer, less intensely labeled neurons than a shorter survival time. (a) Out of 3 rats where a segment of mesenteric artery or vein (6 mm) was exposed to CTb, only 1 CG showed a few, weakly labeled neurons after 4 days. (b) A 3 day survival time yields many more, intensely labeled neurons.

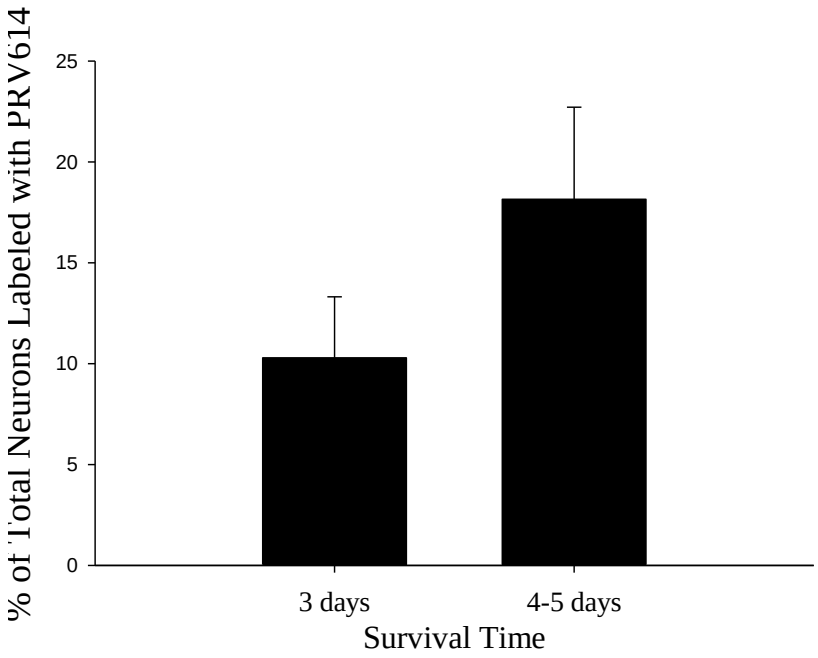

Figure 5.2. More PRV614-labeled neurons on average are measured in the CG after 4-5 days survival time than 3 day survival time. PRV614-labeled neurons in the CG are normalized to the total number of sympathetic postganglionic neurons measured for both the 3 day (n=6 rats) and 4-5 days (n=8 rats) survival time.

Immunohistochemistry

Following appropriate survival times, rats were deeply anesthetized, CGs were dissected, cleaned of fat and excess connective tissue, drop-fixed overnight in 4% PFA, and cryoprotected overnight in 30% sucrose. Tissue was serial sectioned (15 μm) into four series. One of the four series was washed with 3X5 min in tris-buffered saline supplemented with tween 20, blocked for 30 min with normal donkey serum, incubated with rabbit anti-NPY (Immunostar) and goat anti-CTb (List Biological Laboratories) for 48 hr, and incubated with donkey anti-rabbit AF647 (Jackson Immunoresearch Laboratories) and donkey anti-goat AF488 (Jackson Immunoresearch Laboratories) for 2 hr.

CGs dissected after injecting the PRV mixture into the kidney were processed as whole mount and incubated with a chicken anti-GFP (Aves Labs) antibody and a rabbit anti-RFP (Rockland Antibodies and Assays) antibody for 48 hr, and incubated with donkey anti-rabbit AF647 (Invitrogen) and donkey anti-chicken DL405 (Jackson Immunoresearch).

PC-12 Cell Culture

PC-12 cells (American Type Culture Collection) are derived from a rat pheochromocytoma tumor in the adrenal medulla. They were cultured at 37°C in a 95%O_2/5%CO_2 humidified incubator in RPMI 1640 medium supplemented with 10% heat inactivated horse serum, 5% fetal bovine serum, 100 U/ml penicillin, 100 μg/ml streptomycin, and 0.25 μg/ml Fungizone . All reagents for cell culturing were obtained from Invitrogen. To differentiate PC12 cells, 50ng/ml NGF 2.5S (Millipore) was added to the medium for 7 days. In order to test whether differentiated PC12 cells can take up both tracers, a 40 μL mixture of

PRV152 and PRV614 was added to 2 mL of culture media and the cells were incubated for 24 hr. Following incubation period, images were captured of live cells.

Image Analysis

Retrogradely-labeled neurons in the CG were imaged at a confocal microscope (Olympus Fluoview-F1000 Spectral confocal microscope). PMT voltage and gain settings were optimized for each channel prior to collection of sequential Z-stack images. Cell counts and cross-sectional area measurements were obtained from maximum intensity projections of Z-stacks. Cell counts were made for fluorogold-positive, GFP-positive, RFP-positive, NPY-positive, GFP-and-RFP-positive, GFP-positive and NPY-positive, and RFP-positive and NPY-positive neuronal populations. The observer was blind to surgical details on what tracer was applied to what blood vessel type. For cross-sectional area measurements, analysis software (Olympus Fluoviewer) was used to trace the outline of GFP-positive, RFP-positive, and GFP-and-RFP-negative neuronal populations. Area measurements obtained from traced neurons were then compiled and analyzed. Only neurons with visible nuclei were included in cell counts and cross-sectional area measurements.

Intensity-based co-localization analysis was conducted on Fluoview software (Olympus) to quantify amount of co-localization of two signals. This was done with a small sample of randomly selected neurons counted as green (GFP-expressing), red (RFP-expressing), yellow (GFP-and-RFP-expressing), blue (NPY-expressing), blue-green (GFP-and-NPY-expressing), and purple (RFP-and-NPY-expressing) neurons taken from all samples. Intensity thresholds were individually set for each channel of each neuron to distinguish autofluorescence from signal. For each neuron, the distribution of pixels was plotted at various pixel intensities for each selected

fluorescence channel. Data was reported as number of pixels overlapping and as % of pixels overlapping of total pixels for artery-projecting, vein-projecting, and artery and vein-projecting neurons. Data was also reported for artery-projecting NPY+ and NPY- neurons and for vein-projecting NPY+ and NPY- neurons.

Statistics

Student's *t* tests were used to analyze all comparisons. All tests were performed using SPSS 21 (IBM). Statistical significance was set at $p \leq 0.05$. Results are presented as means ± standard error of means.

RESULTS

PRV614/CTb Yields More Double-Labeled Neurons than PRV152/PRV614 in the CG

A mixture of PRV152 and PRV614 when applied to a 6 mm branch of an adjacent pair of both the mesenteric artery and vein resulted in few double-labeled neurons (1.18±1.18% of total neurons) (**Fig. 5.3A**). A mixture of PRV614 and CTb applied similarly resulted in significantly more double-labeled neurons (19.25±4.06% of total neurons) (**Fig. 5.3B, C**). However, in the latter preparation type, fewer PRV labeled neurons were observed than CTb labeled neurons. Hence, data was reanalyzed by normalizing the number of double-labeled neurons to the number of neurons labeled with PRV614. After normalization, the PRV614/CTb mixture still yielded significantly more double neurons as a percentage of neurons labeled with PRV614 (66.45±4.70%) than the PRV152/PRV614 mixture (3.00±3.00) (**Fig. 5.3D**). However, the relative difference between the two tracer combinations changed from 16.3X before normalization to 22.2X after normalization to PRV614-labeled neurons.

PRV Competition Occurs after Application in the Kidney but not in PC12 Cells

A combination of PRV152 and PRV614 was injected into the left kidney to examine whether competition for PRVs in sympathetic postganglionic neurons is exclusive to the mesenteric blood vessel preparation. In addition, antibodies were used against GFP and RFP to reveal any additional labeled neurons that do not exhibit intrinsic fluorescence. However, only 3.5% of double-labeled neurons were observed of neurons labeled with PRV614 (n=1, shown in **Fig. 5.4**).

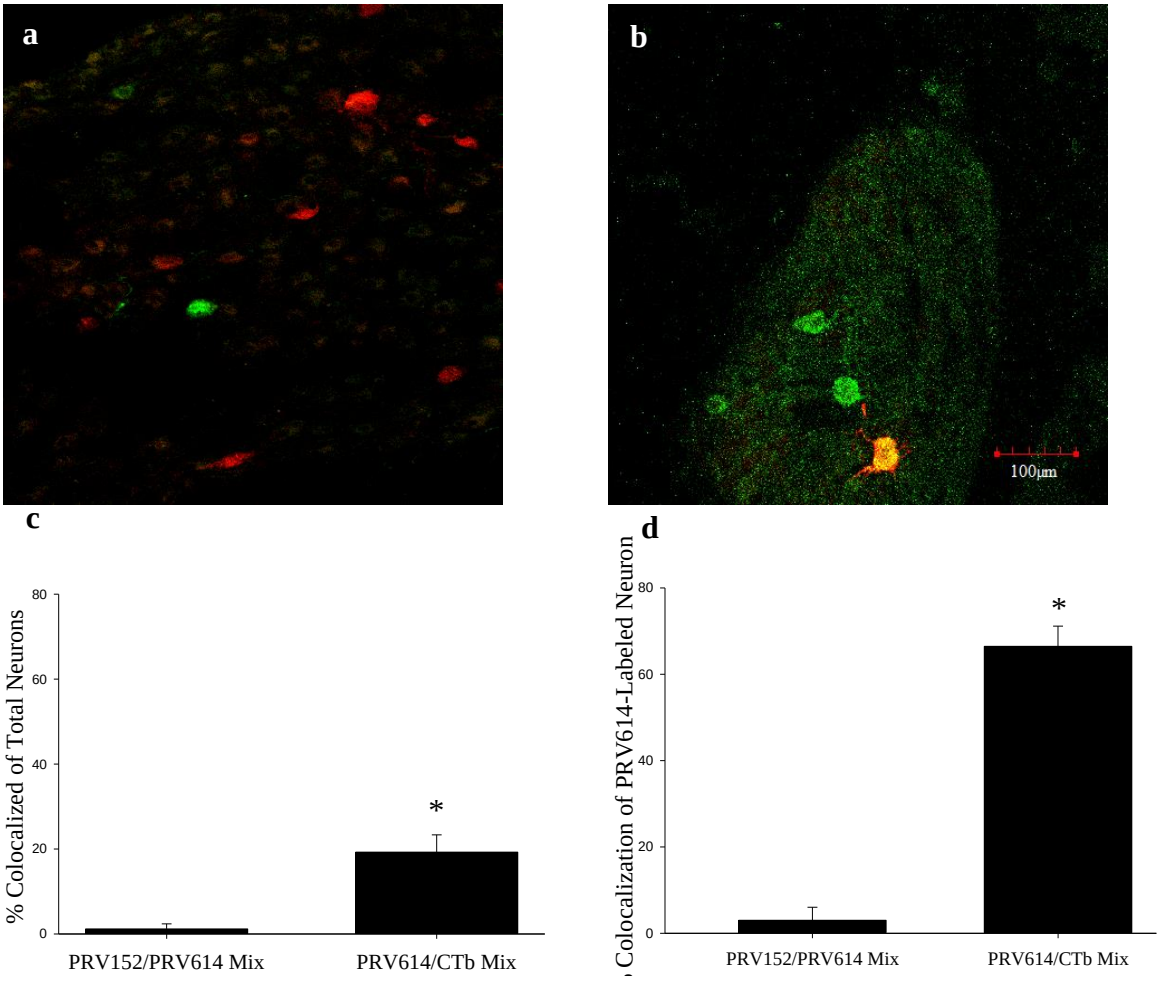

Figure 5.3. A PRV614 and CTb mixture results in more double-labeled neurons in the CG than a PRV152 and PRV614 mixture. (a) PRV152 and PRV614 were mixed and exposed to a 6 mm length of an adjacent pair of mesenteric artery and vein (n=2 rats) resulting in few double-labeled neurons. (b) PRV614 and CTb were mixed and similarly applied (n=2 rats) resulting in more double-labeled neurons. (c) Number of double-labeled neurons for both tracer mixtures is normalized to number of total sympathetic postganglionic neurons. (d) Number of double-labeled neurons for both tracer mixtures is normalized to number of PRV614-labeled neurons. * indicates a significant difference between the PRV152 and PRV614 combination and the PRV614 and CTb combination.

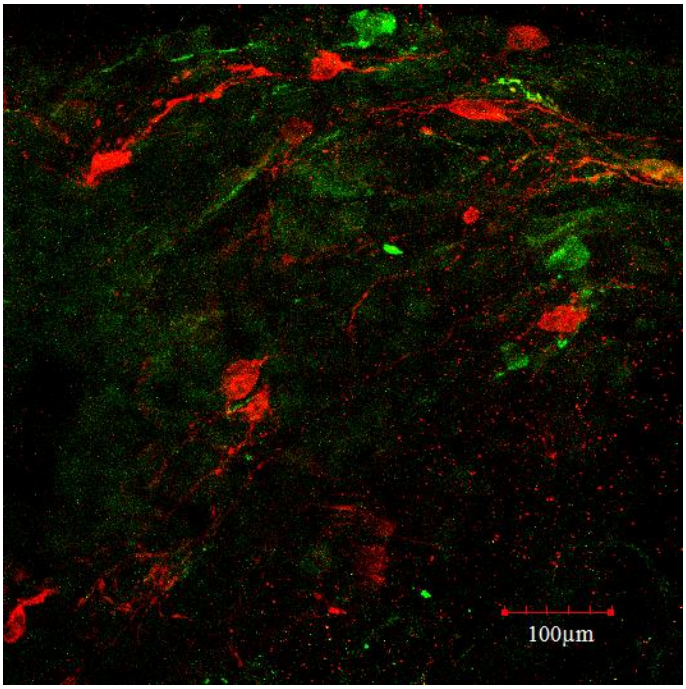

Figure 5.4. A mixture of PRV152 and PRV614 applied to the left kidney yields few double-labeled neurons in the CG. Only 3.5% of neurons were double-labeled in the CG as normalized to the number of neurons labeled with the PRV614 (n=1 rat).

In order to test whether PRV competition also occurred *in vitro*, differentiated PC12 cells were exposed to a mixture of both PRVs for 24 hr. When differentiated PC12 cells were exposed overnight to a mixture of PRV152 and PRV614, ~90% of cells were double-labeled (**Fig. 5.5**).

Artery-and-Vein-Projecting Neuronal Populations in the CG with PRV614/CTb Tracers

Six CGs were examined for retrogradely labeled neurons using the PRV614 and CTb combination of tracers. All CGs showed PRV-and-CTb-labeled neurons (**Fig. 5.6A**). Analysis of cell counts indicated that of 9682 sympathetic postganglionic neurons (labeled with fluorogold), 9.0±2.3% were vein-projecting, 17.1±5.2% were artery-projecting, 3.3±1.3% were artery and vein-projecting, and 70.6±7.8% were unlabeled (**Fig. 5.6B**).

For the same reason discussed above, data for double-labeled neurons was normalized to PRV614-labeled neurons and this reanalyzed data is shown for both PRV152/PRV614 and PRV614/CTb tracer combinations (**Fig. 5.7**). For the PRV152/PRV614 combination, PRV152 was the weakest tracer for 4 of 8 rats and PRV614 was the weakest tracer for the remaining 4 rats. However, for the PRV614/CTb combination, PRV614 was the weakest tracer for 5 of 6 rats and CTb was the weakest tracer for only 1 rat. When reanalyzed after excluding the rat with fewer CTb-labeled neurons than PRV-labeled neurons, the number of double-labeled neurons as a percentage of neurons labeled with PRV614 increased for PRV152/PRV614 preparations to 9.6±2.2% and for PRV614/CTb preparations to 39.2±3.2%. Interestingly, the PRV614/CTb combination gave significantly more double-labeled neurons normalized to PRV614-labeled neurons. After exposing a similar length of blood (regardless of artery or vein) to tracers, a similar number of labeled neurons were counted when using PRV152, PRV614, or CTb (**Fig. 5.8**).

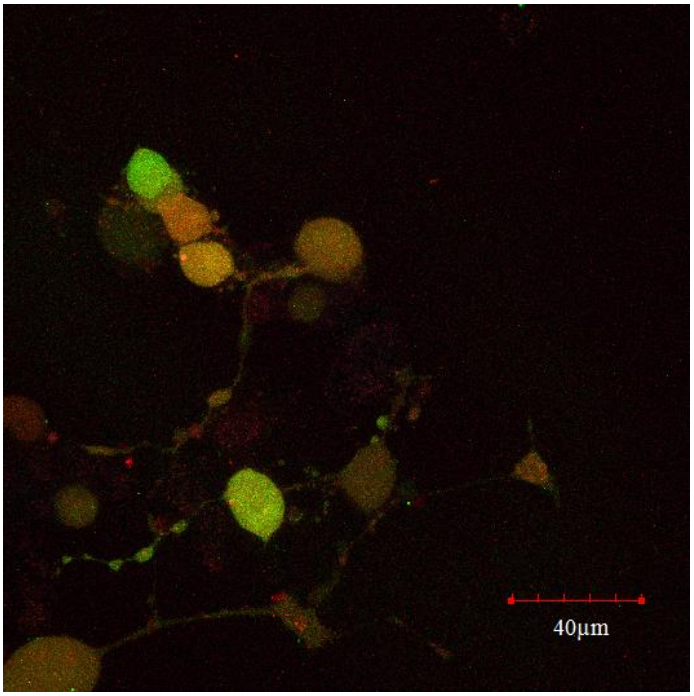

Figure 5.5. Co-infection of both PRV tracers successfully occurs in vitro in differentiated PC12 cells. Differentiated PC12 cells were exposed to a mixture of PRV152 and PRV614 in equal parts and observed 24 hr later. Nearly all PC12 (~90%) cells were double-labeled with both PRV tracers.

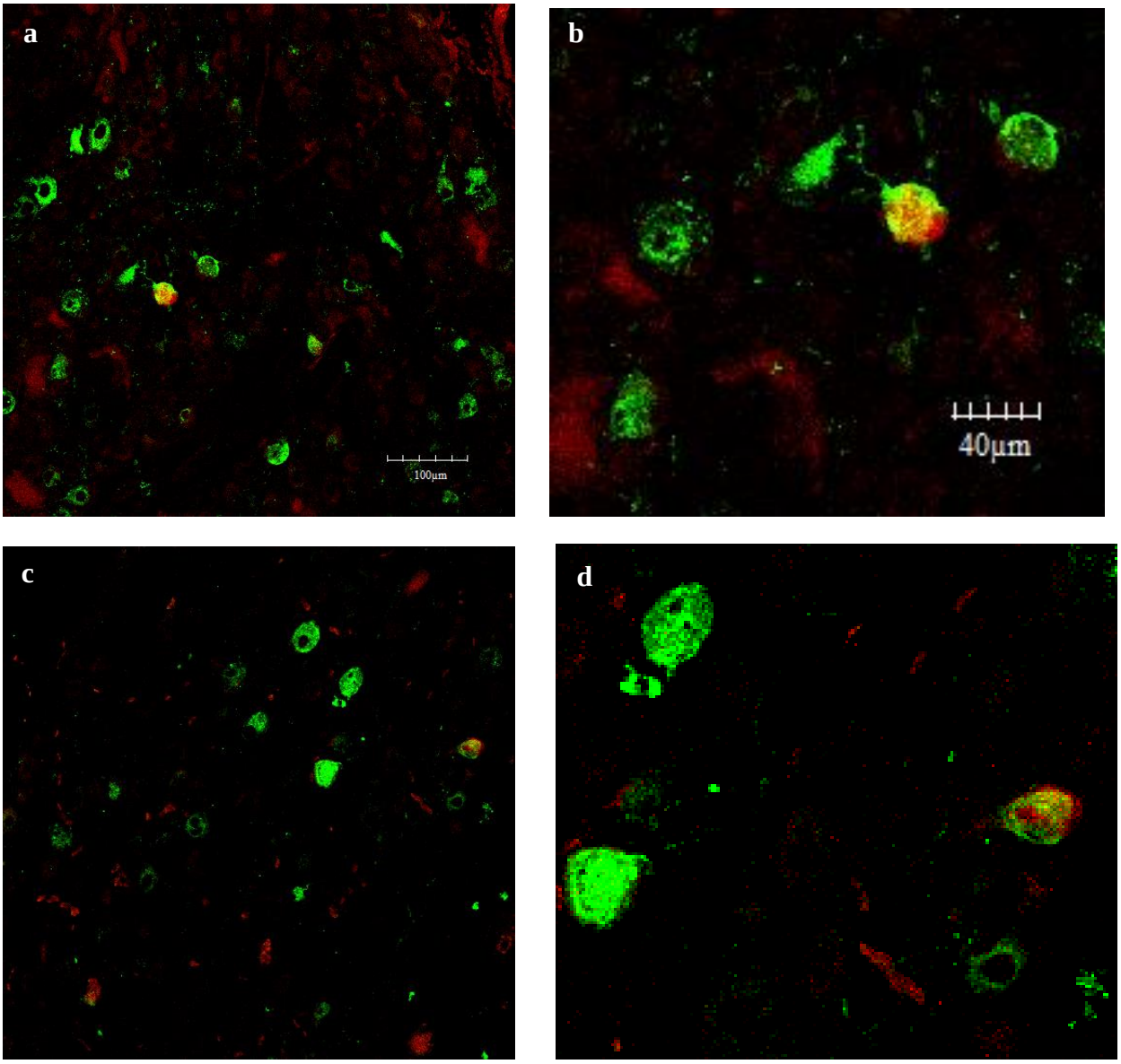

Figure 5.6. There is both distinct and overlapping innervation in the CG to mesenteric arteries and veins. Several images of labeled neurons (A, C, G, E) are shown with a magnified view of these images on the right (B, D, F, H). Many single-labeled (red or green) neurons and few double-labeled (artery and vein-projecting) neurons are visible indicating distinct artery-projecting and vein-projecting sympathetic postganglionic neurons. In A, B, E, F, G, H green indicates artery-projecting neurons and red indicates vein-projecting neurons whereas in C, D green indicates vein-projecting neurons and red indicates green-projecting neurons. (I) Proportions of artery-projecting, vein-projecting, artery and vein-projecting, and unlabeled neuronal populations from 9682 sympathetic postganglionic neurons examined from 6 CGs.

Figure 5.6 (cont'd)

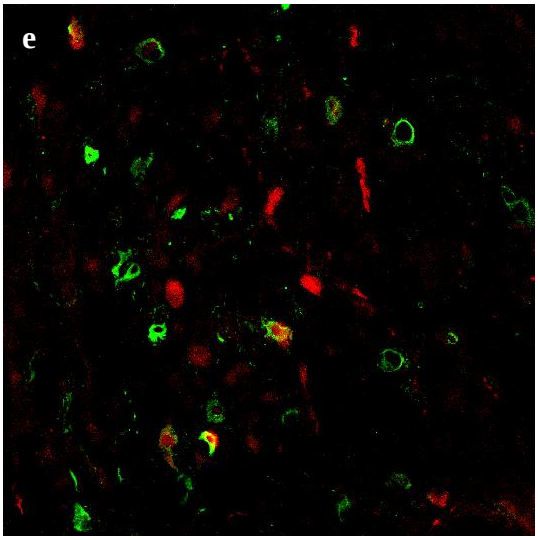

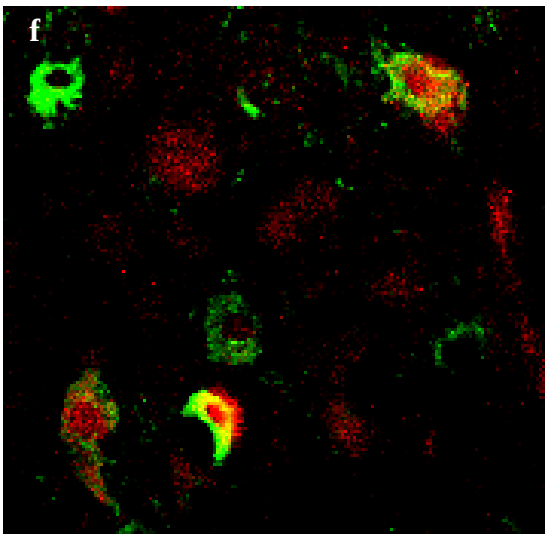

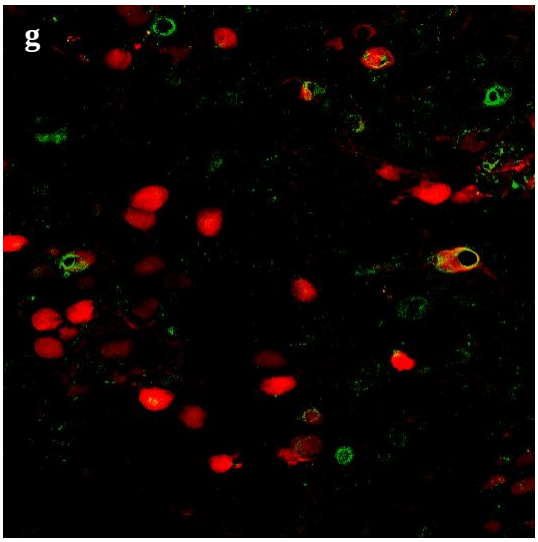

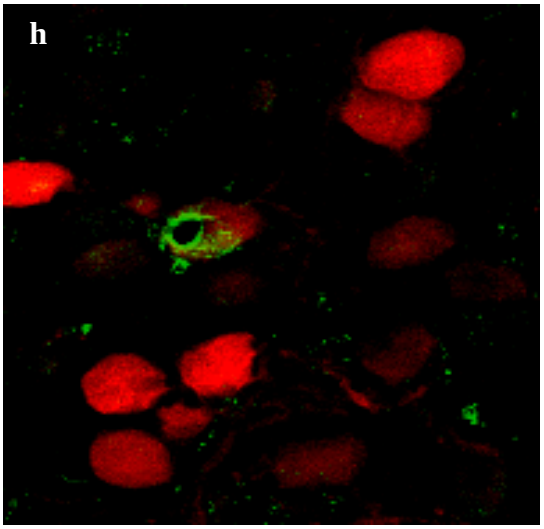

Figure 5.6 (cont'd)

i

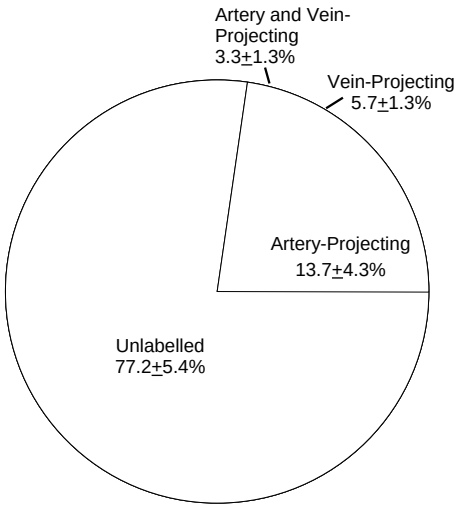

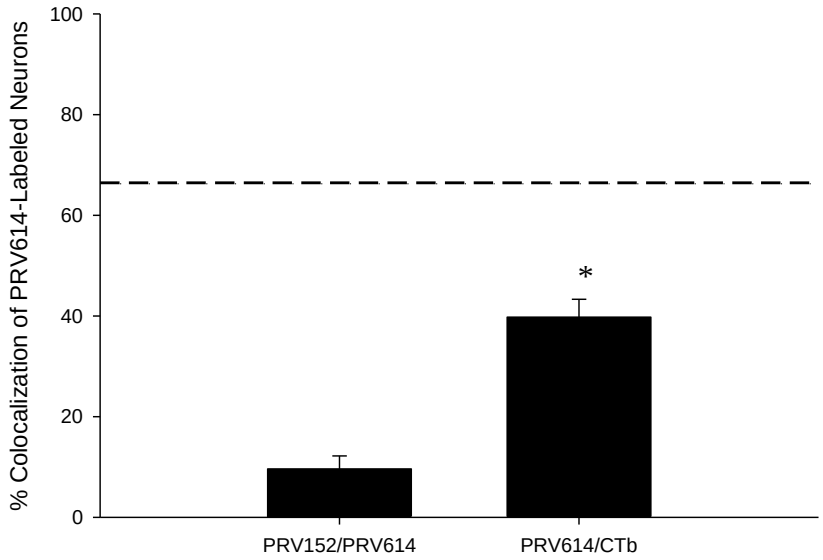

Figure 5.7. The PRV614 and CTb combination of tracers yield significantly more double-labeled neurons after normalizing to neurons labeled with PRV614 than the PRV152 and PRV614 combination. Double-labeled neurons were normalized to number of neurons labeled with PRV614. For the PRV152/PRV614 combination, PRV614 yielded the fewest total number of labeled neurons per CG in only 50% of the preparations but for the PRV614/CTb combination, PRV614 yielded the fewest number of labeled neurons per CG in 83% of the preparations. After reanalysis, the PRV614 and CTb combination yield significantly more double-labeled neurons than the PRV152 and PRV614 combination. * indicates a significant difference between the two tracer combinations. The reference line corresponds to the maximal percentage of double-labeled neurons obtained after mixing PRV and CTb together before applying to mesenteric blood vessels.

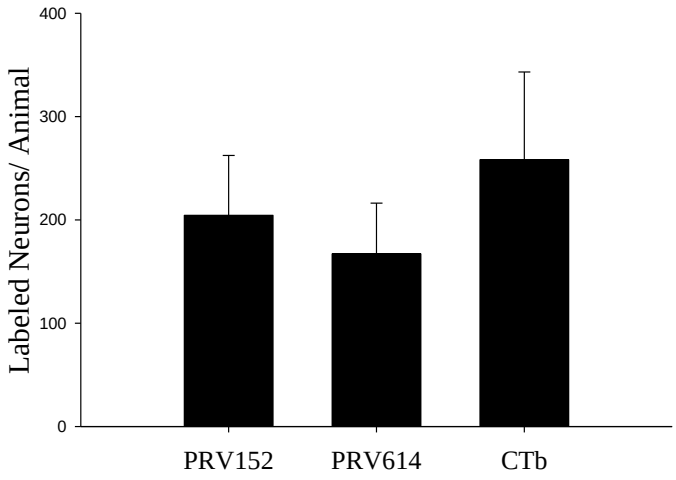

Figure 5.8. Use of PRV152, PRV614, or CTb does not significantly affect number of labeled neurons observed. Data were collapsed together for tracers exposed around arteries and veins to compare both PRV tracers with the non-viral monosynaptic tracer, CTb. There was no significant difference in the number of labeled neurons per rat for any of the tracers used.

Co-localization analysis was conducted to verify that single-labeled neurons (green-or-red-labeled) were visually different from double-labeled neurons (green-and-red-labeled). Representative images of a PRV614-labeled neuron (**Fig. 5.9A**), a CTb-labeled neuron (**Fig. 5.9B**), and a neuron labeled with both CTb and PRV614 (**Fig. 5.9C**) shows that there are differences between each of these neurons in the number of pixels at various levels of intensity in channel 1 (red/PRV614) and 2 (green/CTb). Moreover, there is a significant difference in number of green and red pixels overlapping (**Fig. 5.9D**) and in percent of green and red pixels overlapping of total pixels (**Fig. 5.9E**) between artery-projecting or vein-projecting (ie. single-labeled) and artery and vein-projecting (ie. double-labeled) neurons.

Vascular-Projecting Neurons are Larger in Size than Unlabeled Neurons

In order to compare the sizes of artery-projecting to vein-projecting neurons, the frequency distributions of the cross-sectional areas of all neuronal population were plotted. The frequency distribution histograms were bell curves for artery-projecting (**Fig. 5.10B**), vein-projecting (**Fig. 5.10C**), and unlabeled neurons (**Fig. 5.10D**) but artery-projecting neurons were bimodally. There was no significant difference between mean cross-sectional areas of artery-projecting and vein-projecting neurons. However, the mean areas for artery-projecting and vein-projecting sympathetic postganglionic neurons were significantly larger than unlabeled neurons (**Fig. 5.10A**).

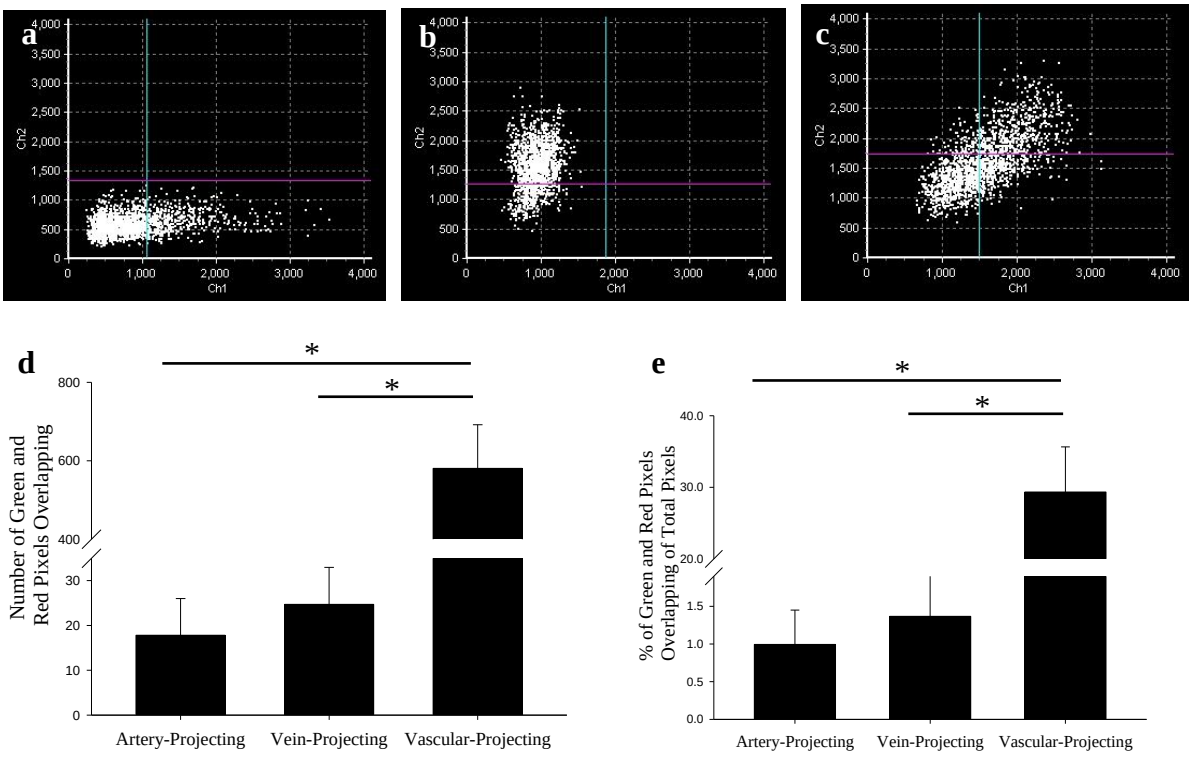

Figure 5.9. Co-localization analysis confirms that artery and vein-projecting neurons are visually different from artery-projecting and vein-projecting neurons. Number of pixels at various levels of intensity is shown for channel 1 (corresponding to RFP) and channel 2 (corresponding to CTb) for a PRV614-labeled neuron (a), a CTb-labeled neuron (b), and a double-labeled neuron (c). There is a significant difference in number of green and red pixels overlapping (d) and n % of green and red pixels overlapping of total pixels (e) between artery-projecting (n=15 neurons from 6 rats) or vein-projecting (n=10 neurons from 6 rats) and artery and vein-projecting (n=8 neurons from 6 rats) neurons.

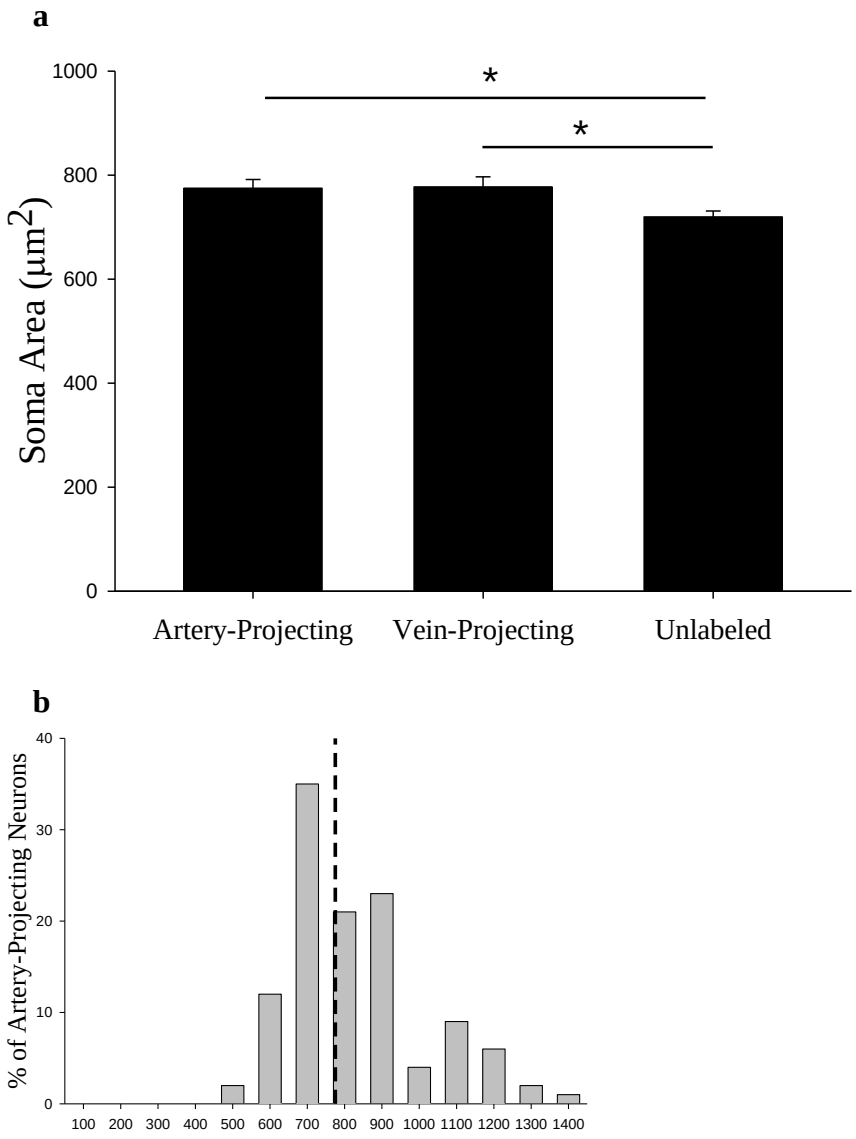

Figure 5.10. Artery-projecting and vein-projecting neurons have a larger cross-sectional area and different frequency-size histograms than unlabeled neurons. (a) cross-sectional areas of artery-projecting (n=115 neurons from 6 rats), vein-projecting (n=92 neurons from 6 rats), and unlabeled neuronal populations (n=266 neurons from 6 rats) in the CG. Frequency-size histograms for artery-projecting (b), vein-projecting (c), and unlabeled (d) sympathetic postganglionic neurons; mean soma size for each population is represented by vertical dotted reference lines.

Figure 5.10 (cont'd)

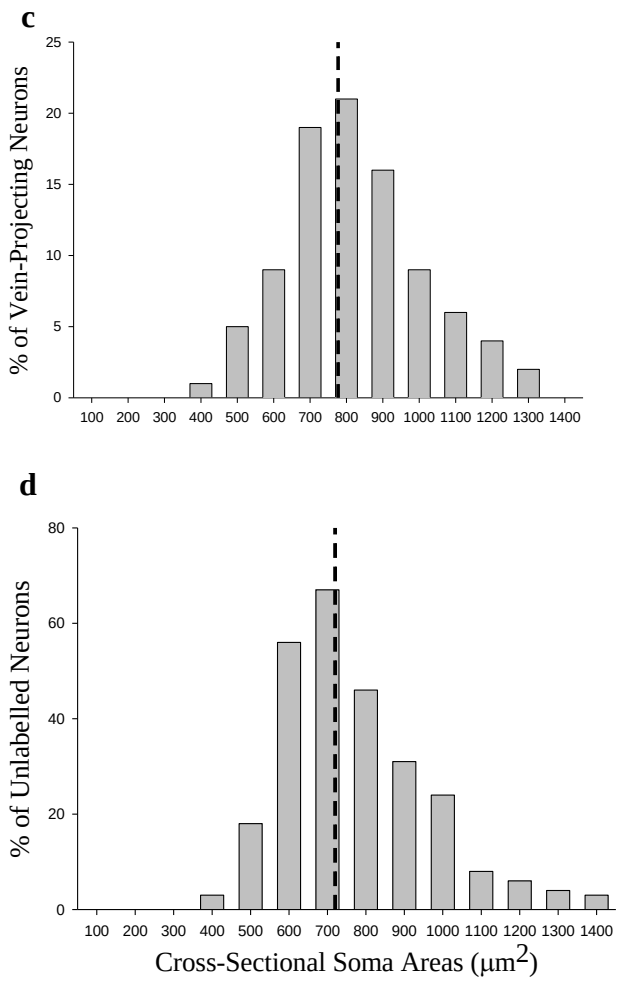

Vascular-Projecting Neurons are not Selectively NPY-Positive

NPY immunofluorescence was measured in artery-projecting, vein-projecting, and unlabeled neuronal populations (**Fig. 5.11A**). No difference was observed in percent of NPY immunofluorescent neurons between the different neuronal populations (**Fig. 5.11B**).

Co-localization analysis was conducted to verify that NPY-immunofluorescent positive (NPY+) neurons were visually different from NPY-immunofluorescent negative (NPY-) neurons. Representative images of a PRV614-labeled, NPY- neuron (**Fig. 5.12A**), a CTb-labeled, NPY- neuron (**Fig. 5.12B**), a PRV614-labeled, NPY+ neuron (**Fig. 5.12C**), and a CTb-labeled, NPY+ neuron (**Fig. 5.12D**) shows that there are differences between each of these neurons in the number of pixels at various levels of intensity in channels 1 (red/PRV614), 2 (green/CTb), and 3 (far red/NPY). Moreover, there is a significant difference in number of green or red and far red pixels overlapping (**Fig. 5.12E**) and in percent of green or red and far red pixels overlapping of total pixels (**Fig. 5.12F**) between NPY+ and NPY- neurons of both artery-projecting and vein-projecting neurons.

Vascular-Projecting Neurons Project Widely

The innervation patterns of artery-projecting and vein-projecting neurons were further investigated by placing tracers on either two arteries, two veins, or proximal and distal segments of the same artery or vein. For proximal/distal and adjacent vessel preparations, the blood vessels targeted were ones that supplied the ileum section of the intestine (**Fig. 5.13 A,B** and **5.14 A,B**) whereas for distant preparations, one of the blood vessels supplied the ileum section of the intestine and the second supplied the jejunum (**Fig. 5.15 A,B**). For each of these three

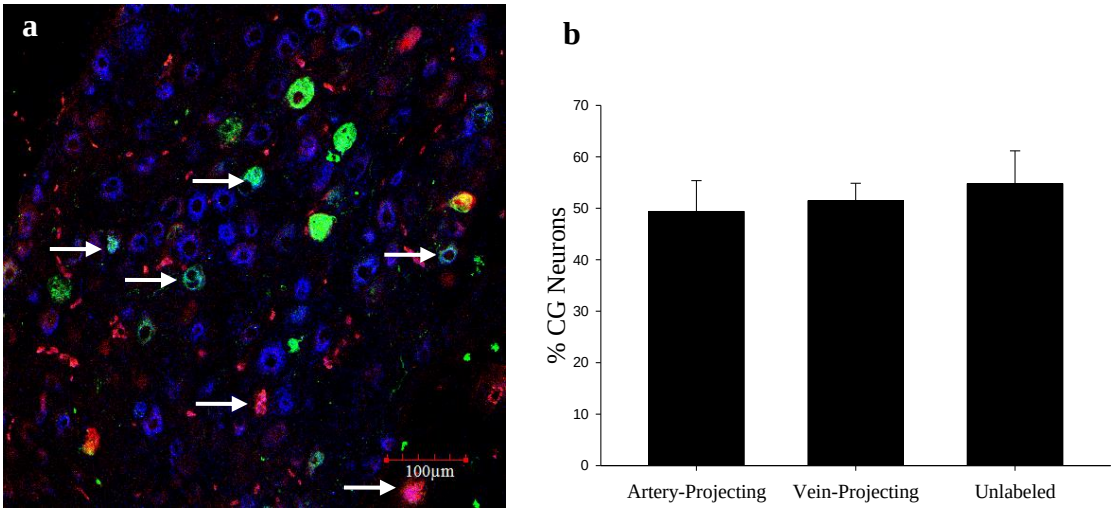

Figure 5.11. NPY is not a selective marker of vascular-projecting neurons. (a) Overlap of NPY immunofluorescence (labeled blue) with artery-projecting (labeled red or magenta when colocalized with NPY) and vein-projecting (labeled green or blue-green when colocalized with NPY) retrogradely labeled neurons in the CG; co-localizations between artery-projecting or vein-projecting neurons and NPY are shown by white arrows. (b) Proportions of NPY immunofluorescent neurons within artery-projecting (n=1695), vein-projecting (n=830), and unlabeled neuronal populations (n=3253) examined in 6 CGs.

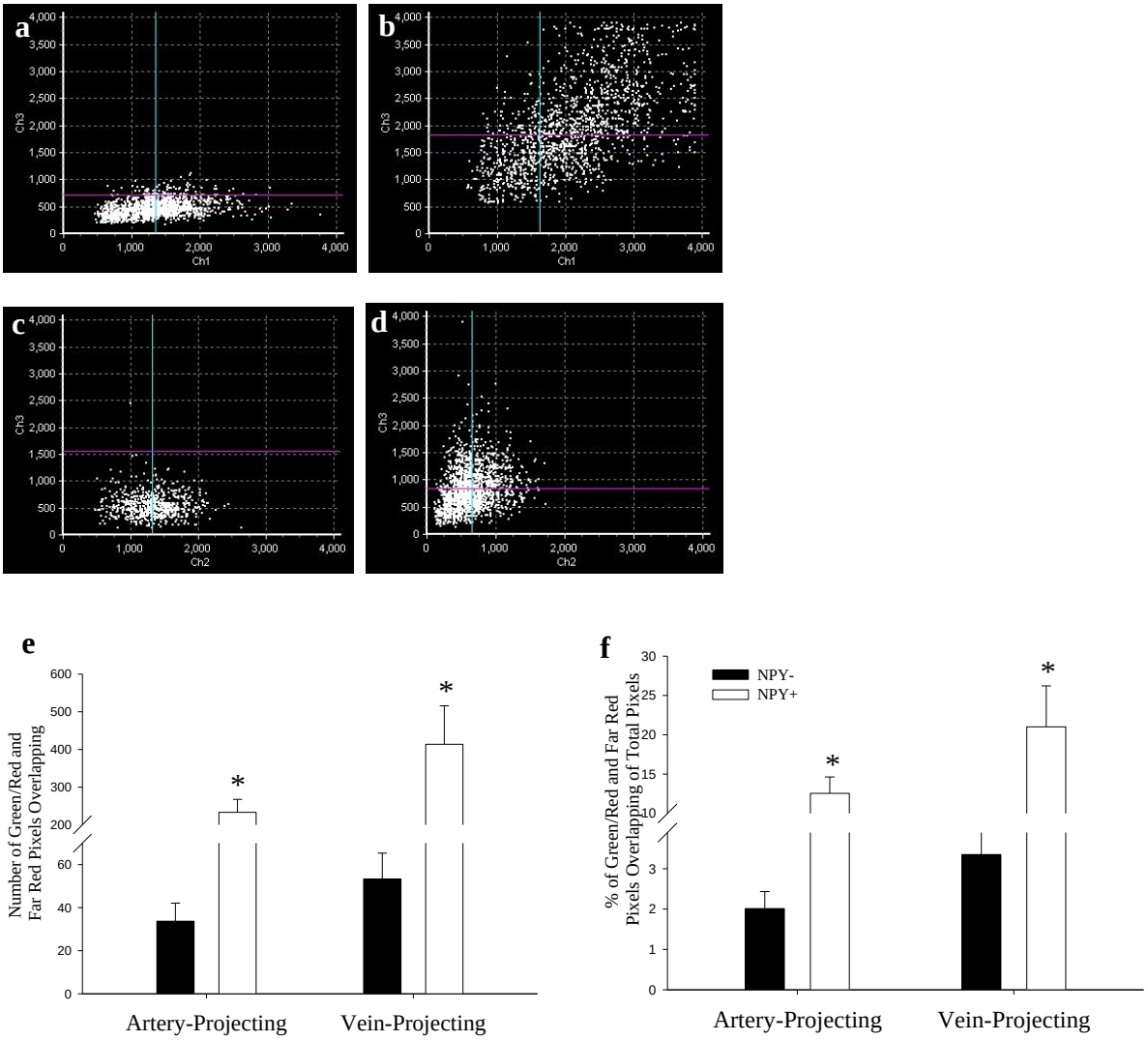

Figure 5.12. Co-localization analysis confirms that NPY immunofluorescent positive (NPY+) neurons are visually different from NPY immunofluorescent negative (NPY-) neurons. Number of pixels at various levels of intensity is shown for channel 1 (corresponding to RFP), channel 2 (corresponding to CTb), and channel 3 (corresponding to NPY) for a PRV614-labeled neuron (a), a CTb-labeled neuron (b), a PRV614-and-NPY-labeled neuron (c) and a CTb-and-NPY-labeled neuron (d). There is a significant difference in number of green or red and blue pixels overlapping (e) and in % of green and red pixels overlapping of total pixels (f) between NPY+ and NPY- neurons for both artery-projecting (n=10 neurons from 6 rats) and vein-projecting neurons (n=11 neurons from 6 rats).

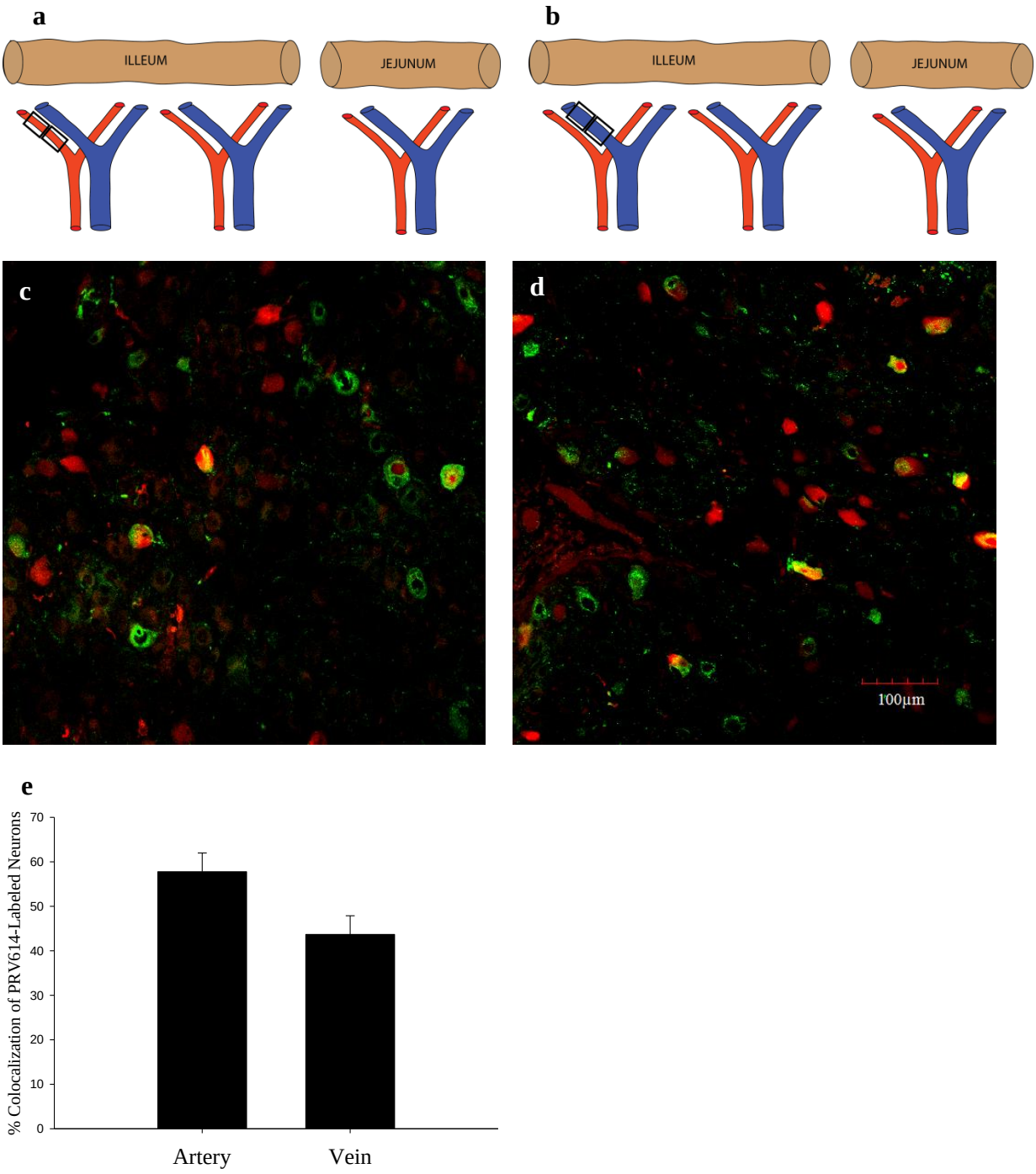

Figure 5.13. There is both distinct and overlapping innervation in the CG to proximal and distal segments of mesenteric arteries or veins. Many green and red labeled neurons and some double-labeled neurons are visible indicating both distinct and overlapping innervation projects to proximal and distal segments of mesenteric arteries (a) and veins (b) (n=3 rats for proximal and distal segments of arteries and n=3 rats for proximal and distal segments of veins). (c) There is no significant difference between arteries and veins in the amount of innervation projecting to both proximal and distal segments of the same vessel.

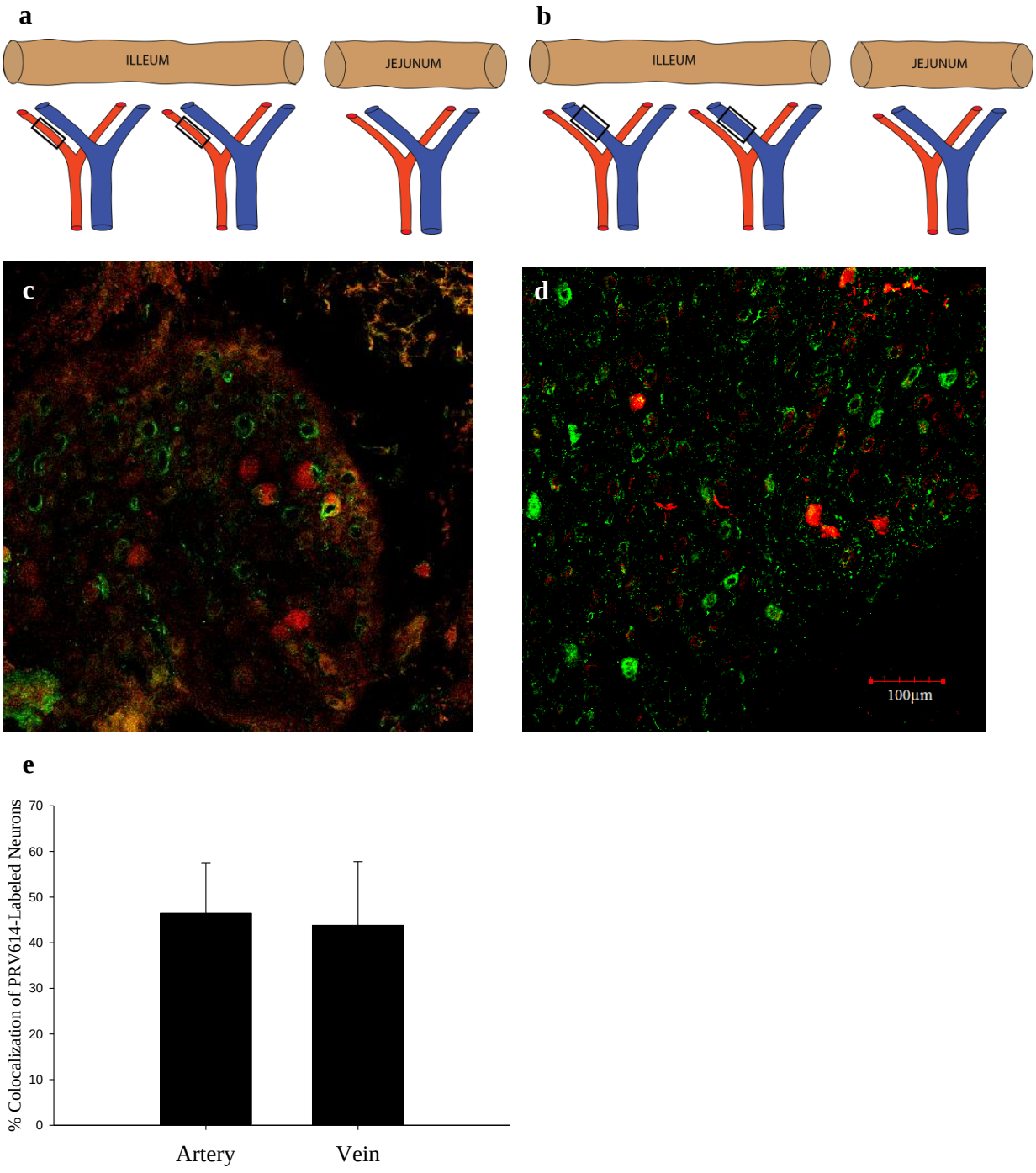

Figure 5.14. There is both distinct and overlapping innervation in the CG to mesenteric arteries or veins that are adjacently located from each other. Many green and red labeled neurons and some double-labeled neurons are visible indicating both distinct and overlapping innervation projects to adjacently located mesenteric arteries (a) and veins (b) (n=3 rats for adjacently located arteries and n=3 rats for adjacently located veins). (c) There is no significant difference between arteries and veins in the amount of innervation projecting to both adjacently located vessels of the same type.

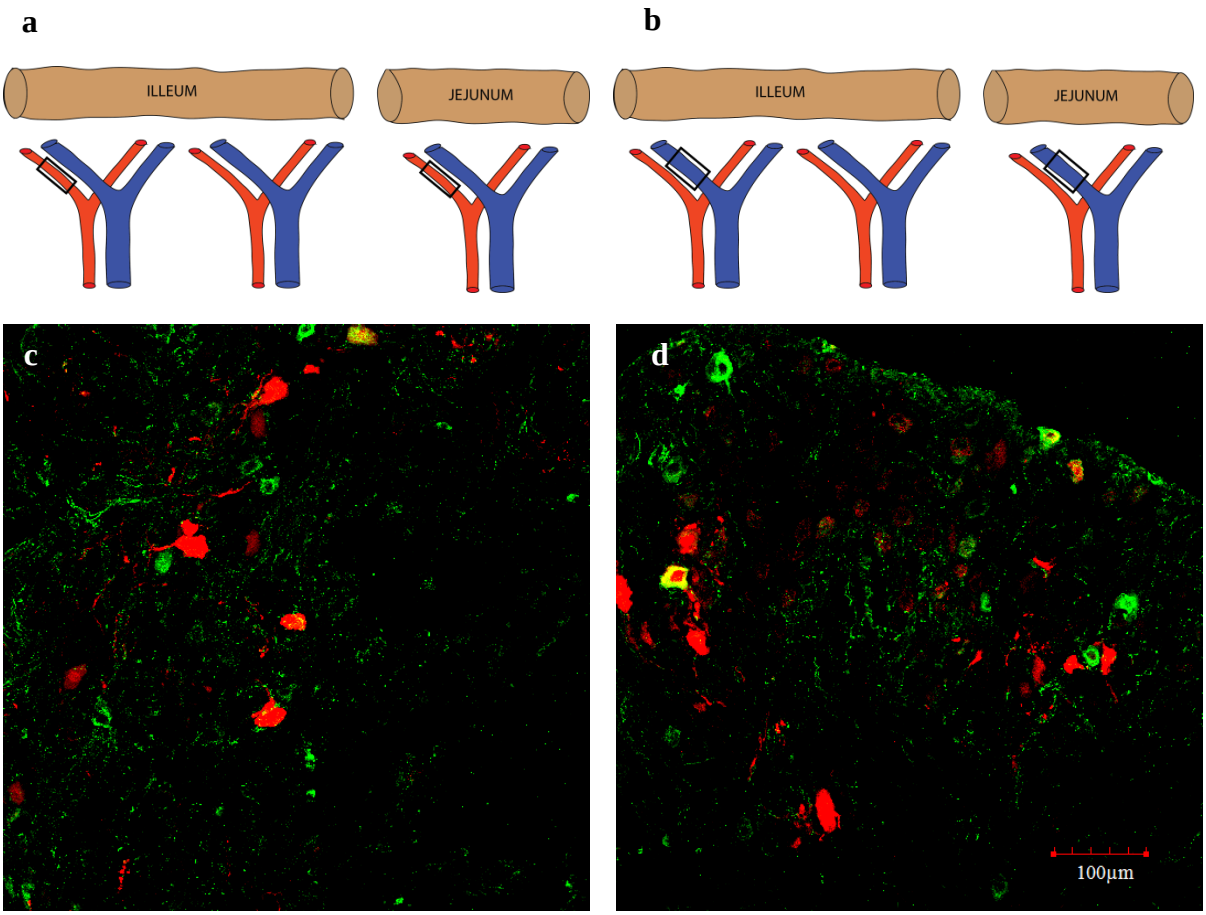

Figure 5.15. There is both distinct and overlapping innervation in the CG to mesenteric arteries or veins that are distantly located from each other. Many green and red labeled neurons and some double-labeled neurons are visible indicating both distinct and overlapping innervation projects to distantly located mesenteric arteries (a) and veins (b) (n=3 rats for distantly located arteries and n=3 rats for distantly located veins). (c) There is no significant difference between arteries and veins in the amount of innervation projecting to both distantly located vessels of the same type.

Figure 5.15 (cont'd)

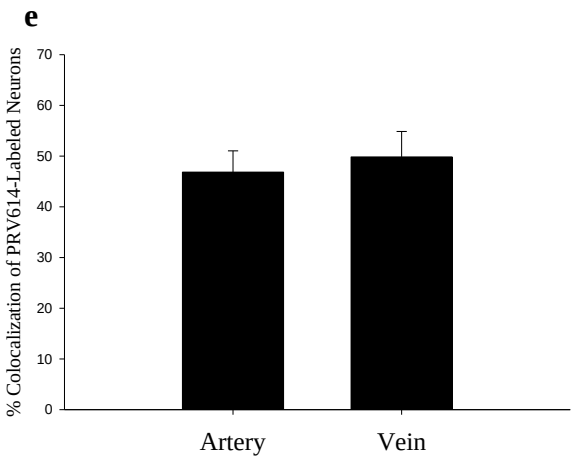

preparation types, the amount of co-localization was similar between artery-projecting (57.8±4.2% for proximal and distal segments, 46.4±11.1% for adjacent vessels, and 46.8±4.2% for distant vessels) and vein-projecting (43.7±4.2% for proximal and distal segments, 43.8±13.9% for adjacent vessels, and 49.8±5.0% for distant vessels) neurons (Fig. 5.13 C-E, Fig. 5.14 C-E, and Fig. 5.15 C-E). In addition, there was no effect of preparation type on amount of co-localization observed when artery-projecting neurons and vein-projecting neuronal groups were lumped together (Fig. 5.16).

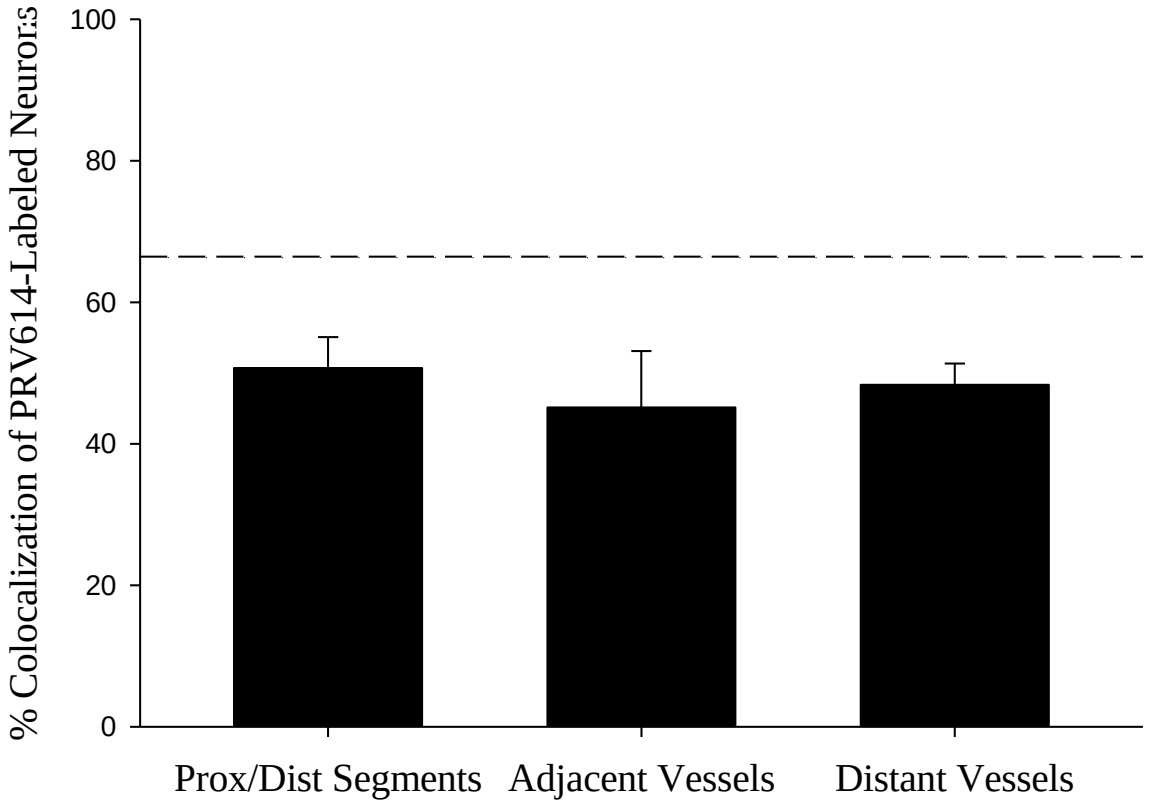

Figure 5.16. Number of double-labeled neurons is not influenced by location where tracers are applied. Application of PRV614 and CTb to proximal or distal segments of the same vessel, or to two adjacent vessels, or to two distantly placed vessels does not affect the number of double-labeled neurons observed. Number of double-labeled neurons is normalized to number of neurons labeled with PRV614. The reference line corresponds to the maximal percentage of double-labeled neurons obtained after mixing PRV and CTb together before applying to mesenteric blood vessels.

DISCUSSION

Key findings of the study are: 1. Co-infection of PRV152 and PRV614 does not occur in sympathetic postganglionic neurons after applying a mixture of PRV152 and PRV614 to mesenteric blood vessels; 2. Mixture of both PRVs into the kidney does not yield a high number of double-labeled neurons; 3. Co-infection of both PRVs does occur *in vitro* in differentiated PC12 cells; 4. A combination of PRV614 and CTb indicates that there is both separate and overlapping sympathetic innervation from the CG to mesenteric arteries and veins; 5. Artery-projecting and vein-projecting neurons both have larger cross-sectional areas than unlabeled neurons; 6. NPY is not a selective marker for vascular-projecting neurons; 7. Vascular-projecting neurons project widely with many neurons innervating widely separated mesenteric blood vessels.

Co-infection of PRV152 and PRV614 is Uncommon in Sympathetic Postganglionic Neurons

A mixture of PRV152 and PRV614 was applied to mesenteric blood vessels and resulted in a large proportion of single-labeled and relatively few double-labeled neurons. Moreover, it is unlikely that this finding is limited to our specific preparation type since injecting a mixture of PRVs into the kidney reproduces the same finding in the CG. Hence, the predominant single labeling from a mixture of PRVs does not vary by terminal field density or peripheral target. This finding is surprising since a mixture of these PRVs injected into the eye yields many double-labeled neurons (~75% of all neurons are double-labeled) in brain regions (Banfield et al., 2003) suggesting that the inability of two PRVs to effectively co-infect the same neuron may be limited to sympathetic ganglia. However, we found that co-infection of both PRVs did occur *in vitro* in differentiated PC12 cells, which are often used as a model of sympathetic neurons.

While the inability of PRVs to effectively co-infect sympathetic postganglionic neurons was an unexpected finding in our studies, it is an important one. Most studies utilizing PRVs inject them into peripheral targets and study labeling patterns in the central nervous system. However, sympathetic ganglia are the first link in the neuronal circuit to take up these tracers and any bias at this level may influence labeling patterns observed in higher order neurons of the circuit.

Previous work indicates that other neuronal populations also respond unexpectedly to PRV. For instance, PRVs were unable to infect neurons in the ventral tegmental area after being injected into the prefrontal cortex although this pathway was labeled by other tracers (Záborszky et al., 2006). This is thought to be due to few efferent terminal fields relative to many afferent terminal fields at the uptake site. In accordance, labeling was observed in the brainstem after injections in the ventral tegmental area. However, in our case, PRV-labeled neurons were observed in all attempted preparations, but the majority of neurons were single-labeled.

Another factor affecting PRV labeling is viral concentration (Banfield et al., 2003). However, we used a similar concentration of both PRVs and saw no preferential labeling from any one PRV. It is possible that both PRVs compete for access into or for productive replication in sympathetic postganglionic neurons. In pseudounipolar sensory neurons, PRVs can enter a latent state of infection in pseudounipolar sensory neurons but can replicate and be transported to the brain in immunosuppressed hosts such as neonates (reviewed in Pomeranz et al., 2005, Muller et al., 2011). The mechanism behind one PRV strain infecting productively and another going into latency is currently unknown and needs to be further investigated in sympathetic postganglionic neurons.

Separate and Overlapping Innervation to Mesenteric Blood Vessels from the CG

Using PRV614 and CTb, we found that there is both separate and overlapping innervation to arteries and veins from the CG. As a percentage of total neurons, 19.4% of neurons are either artery-projecting or vein-projecting while only 3.3% of neurons project to both arteries and veins. However, there was a bias for fewer PRV614 labeled neurons than CTb labeled neurons in almost all cases (5/6 preparations). This is likely due to a short survival time (3 days) used to ensure efficient CTb labeling. To account for this bias, a reanalysis of data was done that normalized the number of double-labeled neurons to the number of PRV614-labeled neurons. Since CTb labeling is maximal at this survival time, this reanalysis provides a conservative measure of how many of the underrepresented PRV614-labeled neurons are also labeled with CTb. After normalization, 39.2% of PRV614-labeled neurons were also observed to be labeled with CTb. This is significantly different from 5.6% of PRV614-labeled neurons that also labeled with PRV152. Hence, while using two PRVs allows us to label artery-projecting and vein-projecting neurons, using PRV614 and CTb allows us to more accurately determine how much separate and overlapping innervation projects to mesenteric arteries and veins.

Use of PRV and CTb indicates that a large portion of sympathetic innervation to mesenteric arteries and veins is overlapping than separate. When considering that a PRV614 and CTb mixture only yields 66.5% of PRV-labeled neurons as double-labeled, 39.2% co-localization represents 58.9% of the maximal co-localization observed. This is similar to the 55% co-localization observed by Hsieh *et al.* (2000) indicating that a majority of sympathetic innervation of mesenteric arteries and veins is overlapping but that there is also separate innervation.

Mesenteric veins constrict at a lower frequency of stimulation than mesenteric arteries (Hottenstein and Kreulen, 1987). One possible explanation for this could be that low frequency stimulation activates neurons selectively projecting to veins whereas higher frequency stimulation recruits neurons selectively projecting to arteries and ones projecting to both arteries and veins. In this way, certain stimuli like reflexive ones can act upon both arteries and veins, whereas other physiological stimuli can act upon either arteries or veins.

Of the single-labeled neurons, we found more artery-projecting (13.7% of total neurons) than vein-projecting (5.7% of total neurons) neurons. This supports previous findings (Hsieh et al., 2000) of more artery-projecting than vein-projecting neurons in the CG projecting to primary branches of the superior mesenteric artery and vein. However, we observed 2.4X more artery-projecting vs. vein-projecting neurons, whereas the previous study found 8.2X more artery-projecting vs. vein-projecting neurons. In general, more artery-projecting neurons may correspond to the higher density of the sympathetic innervation observed around mesenteric arteries compared to veins but there may be differences in innervation patterns between primary (targeted in the previous study) and secondary branches (targeted in the current study) of the superior mesenteric blood vessels.

Dense Innervation of Small Segments of Mesenteric Blood Vessels

There was no significant difference in the number of CTb-labeled neurons, PRV152 -labeled neurons, or PRV614-labeled neurons after exposing each of these tracers on small segments of blood vessels. Each of these tracers resulted in a surprisingly large number of labeled neurons in the CG (~22.7% of all sympathetic neurons) from targeting small segments of blood vessels (~5-10 mm). In contrast, a previous study by Hsieh *et al.* (2000) found that

exposing tracers to 15 mm segments of the primary superior mesenteric artery and vein resulted in retrograde labeling in ~7.4% of all sympathetic neurons. This stark difference in results may be due to the different retrograde tracers used in the two studies. Fast blue and diamidino yellow were used in the previous study (Hsieh et al., 2000) whereas PRV and CTb were used in the current study. Interestingly, when we used fluorogold and fast blue in preliminary studies, there were approximately 100-fold fewer labeled neurons with these retrograde tracers than with PRV and CTb tracers. PRVs and CTb uptake is receptor mediated (reviewed in Kobbert et al., 2000, Pomeranz et al., 2005), which may be more efficient than the pH trapping uptake mechanism of conventional fluorescent tracers (Wessendorf, 1991).

Vascular-Projecting Neurons are Larger than Unlabeled Neurons

Cross-sectional areas of both artery-projecting and vein-projecting neurons were larger than those of unlabeled neurons and there was no significant difference between areas of artery-projecting and vein-projecting neurons. The frequency distribution histograms of all neuronal populations were similarly bell shaped but artery-projecting neurons had a bimodal distribution compared to unimodal distributions for vein-projecting and unlabeled neurons. Using two PRVs, we had previously found that vein-projecting neurons were larger than artery-projecting and unlabeled neuronal populations. However, the PRV and CTb tracer combination is better at accurately identifying artery and vein-projecting neurons than the two PRV tracer combination. Larger soma sizes in sympathetic postganglionic neurons are correlated with larger target size (Voyvodic, 1989). Hence, it is possible that vascular-projecting neurons innervate a broader area or have a denser innervation of their targets than unlabeled neurons.

NPY is not a Selective Marker for Vascular-Projecting Neurons

NPY was not selectively expressed in artery-projecting or vein-projecting neurons relative to unlabeled neurons. This was similar to what we found when using two PRVs, further indicating that NPY is not a selective marker for sympathetic neurons projecting to mesenteric blood vessels. While the 'chemical coding' hypothesis suggests that NPY is present only in vascular-projecting sympathetic neurons due to the high prevalence of NPY in sympathetic nerves forming junctions with arteries and veins (Elfvin et al., 1993), there is now considerable evidence arguing against this hypothesis. Retrograde tracing studies show that only a subset of between ~40-80% of vascular-projecting neurons express NPY depending on the vascular bed being examined (Gibbins and Morris, 1990, Browning et al., 1999).

Vascular-Projecting Neurons Project Widely

This is the first time that the innervation of adjacent and widely separated mesenteric blood vessels was studied. Surprisingly, a similar proportion of separate to overlapping sympathetic innervation was found projecting to two adjacent vessels of the same type and to distantly located vessels of the same type. This suggests that vascular-projecting neurons are not only highly divergent accounting for the many labeled neurons from applying tracers to small segments of blood vessels, but also widely diverging. Also, innervation patterns did not differ between artery-projecting and vein-projecting neurons. While it needs to be further investigated, there may be different subsets of neurons that either project widely or project narrowly and the recruitment order of these subsets may be stimuli-specific. For instance, hemorrhage may require venoconstriction of many mesenteric veins throughout the splanchnic vascular bed; however,

other physiological stimuli may only require regional vasoconstriction or venoconstriction of arteries or veins, respectively, in the splanchnic vascular bed.

A previous study examined innervation patterns of sympathetic postganglionic neurons projecting to the cutaneous vasculature of the guinea pig ear (Gibbins et al., 1998). The authors reported that a single neuron can innervate a wide region of skin as much as 7 mm apart, which must contain many diverging blood vessels. Hence, even for cutaneous vasculature sympathetic postganglionic diverge widely.

Previous electrophysiology studies support our finding that there is some overlapping input to blood vessel segments that are directly proximal or distal to one another. Transmural stimulation resulted in excitatory junction potentials in colonic blood vessels that could be recorded within 7 mm of the stimulation site (Kreulen, 1986). Similarly, stimulation of proximal segments of mesenteric blood vessels also activated distal branches of mesenteric blood vessels indicating that there is at least some overlapping input to proximal and distal segments of mesenteric blood vessels (Hill et al., 1983).

CONCLUSIONS

In this study, we found that using a PRV and CTb mixture on mesenteric blood vessels resulted in more double-labeled neurons than using a mixture of two PRVs. This suggests that the PRVs compete for uptake, or retrograde transport, or productive replication in sympathetic postganglionic neurons. After applying PRV and CTb on small segments of adjacent mesenteric arteries and veins, we found approximately similar numbers of single-labeled as double-labeled neurons. Hence, contrary to what we found with two PRVs, this combination of tracers points to a similar amount of separate and overlapping sympathetic innervation of mesenteric arteries and veins. Also, vascular-projecting neurons had larger soma areas than unlabeled neurons. NPY was not a selective marker of vascular-projecting neurons. Moreover, we found that the majority of sympathetic innervation to both adjacent and widely separated blood vessels of the same is overlapping. This can be explained by a wide divergence of most sympathetic postganglionic neurons but a narrow divergence of others.

CHAPTER SIX: GENERAL DISCUSSION

MAJOR FINDINGS

These studies are the first to examine the 5-HT system (Chapter 2) and patterns of neuronal activation (Chapter 3) in prevertebral ganglia within the DOCA-salt rat model of hypertension and to study vascular-projecting neurons in sympathetic ganglia (Chapters 4 and 5). Key findings of these combined works are: 1) 5-HT and 5-HIAA levels are not different in normotensive and hypertensive CGs but 5-HT synthesis and 5-HT_3 receptor levels are lower in hypertensive CGs; 2) c-fos expression as a marker for neuronal activation is not basally altered in hypertensive sympathetic ganglia; 3) systemic nicotine treatment *in vivo* and continuous preganglionic nerve stimulation *in vitro*, but not 2-DG treatment *in vivo*, results in less c-fos expression in hypertensive sympathetic ganglia relative to normotensive ganglia; 4) two PRVs can label vascular-projecting neurons but they compete for productive replication within any given sympathetic postganglionic neuron; 5) vascular-projecting neurons diverge to innervate many mesenteric blood vessels; 6) use of PRV614 and CTb indicates that there is approximately a similar amount of separate as there is overlapping sympathetic innervation to mesenteric arteries and veins; 7) there is a similar proportion of overlapping input projecting to proximal and distal segments of the same vessels, adjacent blood vessels of the same type, and widely separated vessels of the same type.

NO EVIDENCE OF INCREASED SYMPATHETIC DRIVE IN HYPERTENSIVE SYMPATHETIC GANGLIA

Sympathetic nerve activity is elevated in human patients and in several animal models of hypertension (Esler, 2000, Malpas, 2010). For instance, postganglionic sympathetic nerves in spontaneously hypertensive rats (SHRs) have a higher level of activity than normotensive Wistar Kyoto rats (WKYs) and after a given preganglionic nerve stimulation, postganglionic nerve

activity is enhanced to a greater extent in SHRs than WKYs (Magee and Schofield, 1992). In addition, surgical dissection of the CG leads to a decrease in basal arterial pressure and attenuation in the development of hypertension (King et al., 2007, Kandlikar and Fink, 2011b, Ye et al., 2011).

However, the current studies do not support a higher basal sympathetic drive in hypertensive CGs. 5-HT is shown to activate sympathetic postganglionic neurons and a higher level of 5-HT in sympathetic ganglia would indicate that sympathetic drive is elevated in sympathetic ganglia of hypertensive rats. In contrast, we found that 5-HT and 5-HIAA levels were similar between normotensive and hypertensive CGs. Moreover, gene expressions of the 5-HT synthesis gene tryptophan hydroxylase and of the 5-HT_{3A} receptor gene are both decreased in hypertensive CGs. Less 5-HT synthesis and lower receptor levels suggests that 5-HT contributes less to neuronal excitation in hypertensive CGs than normotensive CGs.

In addition, no basal level of c-fos expression was observed in normotensive or hypertensive CGs. This suggests that there may be no difference in the basal level of activation between normotensive and hypertensive CGs. Although c-fos expression was observed after just 2 Hz of preganglionic nerve stimulation *in vitro*, the basal level of activation in sympathetic ganglia may be lower than this and may not trigger c-fos expression.

Similarly, in a mild DOCA-salt rat model of hypertension, celiac ganglionectomy attenuated the development of hypertension but neither whole-body NE spillover, indicative of systemic sympathetic activity, nor splanchnic-specific NE spillover were higher in ganglionectomized relative to sham rats (Kandlikar and Fink, 2011b). These results suggest that while the CG is a key regulator of hypertension, increased splanchnic sympathetic activity may

not be the underlying mechanism by which the CG contributes to the pathophysiology of hypertension. Instead, increased vascular reactivity of mesenteric blood vessels may be responsible.

DESENSITIZATION OF NICOTINIC RECEPTORS ON SYMPATHETIC NEURONS IN HYPERTENSION

Decreased neuronal activation was observed in sympathetic prevertebral ganglia from hypertensive than normotensive rats after direct stimulation from systemic nicotine treatment and preganglionic nerve stimulation. This result can be explained by factors that affect nicotinic receptors in hypertension. Sympathetic nerve activity is noted to be increased in hypertension (Esler, 2000, Malpas, 2010) and increased preganglionic input to sympathetic ganglia in hypertension may cause a desensitization of nicotinic receptors on postganglionic neurons. (Fig. **6.1**).

Nicotinic receptors are ionotrophic receptors that are highly permeable to Na^+, K^+, and Ca^{2+} (reviewed in Skok, 2002) There are three states for nicotinic receptors: activated or open, desensitized (high agonist affinity), and resting (low agonist affinity). While it was thought that desensitization of these receptors may occur via downregulation of receptors, chronic exposure to nicotine in the brain causes an upregulation of high-affinity receptors that rapidly desensitize and remain inactive after agonist exposure (Wang and Sun, 2005). A similar mechanism may take place in autonomic ganglia as well and needs to be further investigated. Phosphorylation of nicotinic receptors affects rate of desensitization and recovery and dephosphorylation of receptors can induce receptor desensitization (Huganir and Miles, 1989, Dunn and Raftery, 2000); this may be a second mechanism for desensitization in autonomic ganglia. In addition,

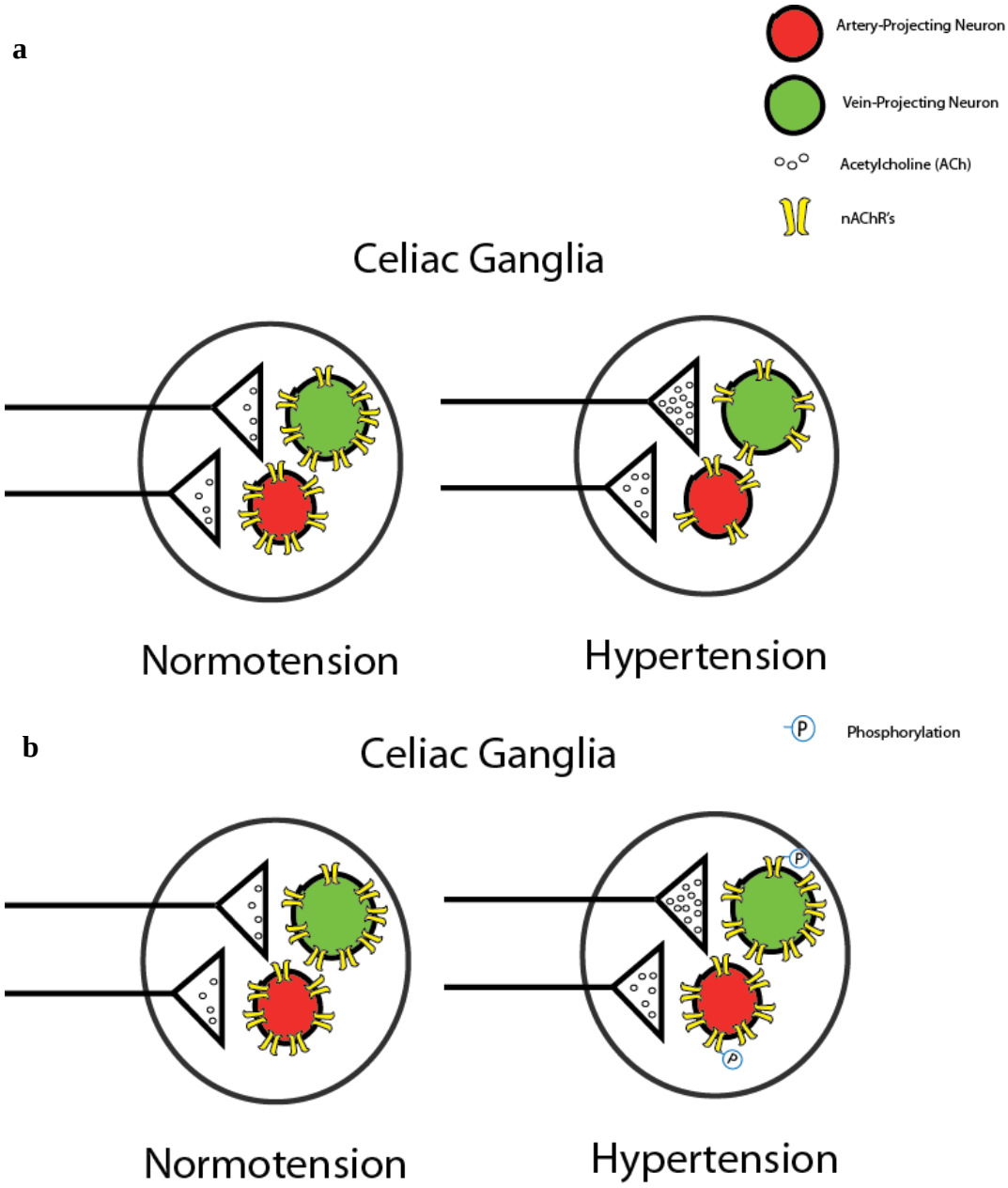

Figure 6.1. Different mechanisms by which desensitization of nicotinic receptors in sympathetic ganglia of hypertension may occur. It is possible that (a) there is a downregulation of nicotinic receptors, or (b) there is phosphorylation of nicotinic receptors, or (c) reactive oxygen species may inhibit the function of nicotinic receptors, or (d) excess glucocorticoids may inhibit nicotinic receptors in hypertensive relative to normotensive CGs.

Figure 6.1 (cont'd)

c

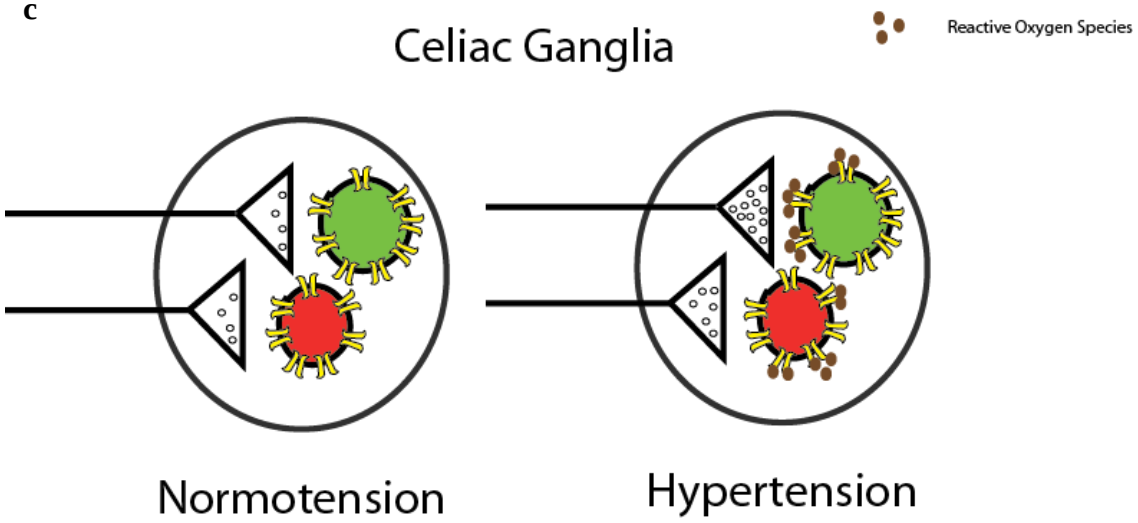

d

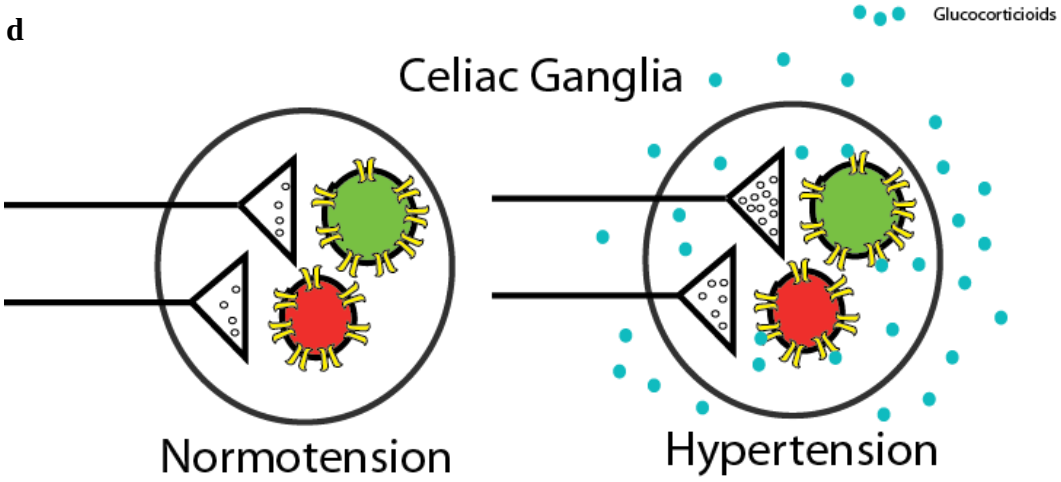

nicotinic receptors in sympathetic ganglia may be functionally altered and inactivated by an excess of reactive oxygen species (Krishnaswamy and Cooper, 2012), which are known to be elevated in prevertebral ganglia of hypertensive rats (Dai et al., 2006, Cao et al., 2007, Cao et al., 2009). Finally, many paracrine and endocrine factors are shown to modulate the functioning of nicotinic receptors and if these factors are elevated in hypertension, then they may have a pronounced influence on nicotinic receptors in hypertensive ganglia. For instance, glucocorticoids have an inhibitory effect on nicotine-induced depolarization in dissociated sympathetic neurons from the superior cervical ganglion, a paravertebral ganglion (Uki et al., 1999). Since hypertension in DOCA-salt rats is induced by administering a high dose of a glucocorticoid, DOCA, it is possible that elevated glucocorticoid levels have an inhibitory effect on nicotine-induced, direct stimulation on sympathetic ganglia. In addition, neuropeptides like substance P and calcitonin gene related peptide are also shown to induce nicotine desensitization (Akasu et al., 1984). This is relevant since the synthesis and release of both these vasoactive peptides is increased in hypertension (Watson et al., 2002).

COMPETITION BETWEEN TWO PRVS IN SYMPATHETIC POSTGANLGIONIC NEURONS

Initially, two PRVs (PRV152 and PRV614) were used for retrograde tracing from mesenteric blood vessels to the CG. These tracers are isogenic strains derived from an attenuated PRV vaccine strain, PRV Becker (reviewed in Pomeranz et al., 2005). When exposed to small segments of adjacent mesenteric arteries and veins, we observed that the vast majority (97.8%) of labeled neurons in the CG were single-labeled corresponding to either PRV152 or PRV614. However, control experiments where both PRVs were mixed together in equal volume and added to the same blood vessels also showed that very few of all labeled neurons were double-labeled

(2.5%). Hence, PRVs may compete for entry, retrograde transport, or productive replication in sympathetic postganglionic neurons.

There is no preferential PRV strain that labeled a large majority of sympathetic neurons. Application of PRV152 and PRV614 was counterbalanced on arteries and veins and overall, neither was found to label more neurons (21.7±5.8% of all neurons were labeled with PRV152 and 17.7±4.5% of all neurons were labeled with PRV614). Hence, both are equally capable of entering sympathetic neurons but entry of one PRV into a neuron may prevent the entry of the second into the neuron. This is probably not due to insufficient axon terminals at the site of blood vessels since this competition was also observed after injection of the PRV mixture into the kidney. While some double-labeled neurons were observed indicating that co-infection of both PRVs is possible in sympathetic neurons, it is an uncommon observance. Due to competition between two PRVs, this combination of tracers can label artery-projecting and vein-projecting neurons but not answer how much sympathetic innervation to blood vessels is separate and overlapping.

Previous work shows that PRV competition does not occur in the central nervous system. For instance, when PRVs were mixed in equal volumes before application to the anterior chamber of the eye, ~75% of neurons were found to be double-labeled in brain regions (Banfield et al., 2003). Hence, competition between PRVs selectively occurs in sympathetic postganglionic neurons. While unexpected, this is an important observation since many studies applied two PRVs into peripheral targets and studied higher order neurons without paying attention to the first order neurons, which are sympathetic postganglionic neurons. However, any bias at the level of first order neurons may influence labeling patterns in higher order neurons.

Competition between viruses occurs between herpes simplex virus (HSV) and adeno associated virus (AAV) (Glauser et al., 2007). Live visualization of the interaction between these two viruses shows that both viruses replicate inside independent replication chambers and that the presence of AAV substantially inhibits formation of the HSV replication chamber. However, competition between strains of the same virus has not been studied in details and needs to be further examined, especially in sympathetic postganglionic neurons.

PRV AND CTB CAN CO-LABEL SYMPATHETIC POSTGANLGIONIC NEURONS

In order to investigate how much sympathetic innervation to blood vessels is separate and overlapping, another previously used combination of tracers (Chen et al., 1999), PRV and unconjugated CTb, was used. Control experiments where both PRV614 and CTb were mixed and applied to the same blood vessels showed significantly more double-labeled neurons with this combination (29.9% of all labeled neurons were double-labeled), relative to what was observed with two PRVs (2.5% of all labeled neurons were double-labeled). However, with the PRV and CTb combination of tracers, we observed that there were fewer PRV614-labeled neurons than CTb-labeled neurons. This is likely because of the 3 day survival time chosen, which was optimal for CTb-labeling but was short for optimal PRV-labeling. In order to correct for this, double-labeled neurons were normalized to the number of PRV614-labeled neurons to get a conservative measure of how many PRV614-labeled neurons were also CTb-labeled. Normalization was done to PRV614-labeled neurons because PRV614-labeled neurons were expected to increase with a longer survival time whereas a maximal number of CTb-labeled neurons was already observed at a 3 day survival time. After reanalysis, again a significantly higher percentage of double-labeled neurons of PRV614-labeled neurons were observed with PRV614 and CTb (66.5%) than with two PRVs (3.0%).

Mixing PRV and CTb together beforehand and applying them to the same blood vessels resulted in co-localization of both tracers in only 66.5% of all neurons and not in all neurons. This was also true of a mixture of both PRVs applied to the anterior chamber of the eye, which only yielded ~75% double-labeled neurons in the brain (Banfield et al., 2003). One of the reasons why both tracers may not be taken up by all neurons is that there is oversaturation of one tracer at some nerve terminals, leading to the selective uptake of that tracer alone. We observed this after applying two PRVs to mesenteric blood vessels followed by a high concentration of fluorogold (1 mL of 0.5% fluorogold injected ip) ~15 min later. In these rats (n=3), no PRV labeling was observed in the CG but all sympathetic postganglionic neurons were labeled with fluorogold. However, in one instance, fluorogold was injected ~1 hr after PRV application, which resulted in many PRV-labeled neurons as well as fluorogold labeling in all sympathetic postganglionic neurons. This indicates that when fluorogold was applied shortly after PRVs, it may have oversaturated all nerve terminals preventing entry and retrograde transport of PRVs. Similarly, the same reason may explain why only 66.5% of all neurons were double-labeled after mixing PRV and CTb and applying them to the same blood vessels.

We are the first to quantify how much co-localization occurs in the CG after mixtures of different tracer combinations. This is important since these tracers are often used for studying labeling patterns in the central nervous system without examination of patterns in the first order neurons, which for many peripheral targets is in sympathetic ganglia.

SEPARATE AND OVERLAPPING SYMPATHETIC INNERVATION OF ARTERIES AND VEINS

Application of PRV614 and CTb to small, adjacent segments of mesenteric arteries and veins indicates that 39.2% of PRV614-labeled neurons were double-labeled. When considering that the maximal amount of co-localization observed after mixing both tracers was 66.5%, 39.2% is 58.9% of that maximal number. This indicates that approximately half of all labeled neurons project to either arteries or veins whereas the half project to both arteries and veins (**Fig. 6.2**). These results are consistent with those of Hsieh *et al.*, (2000), who also found that the majority of labeled neurons in the CG (55%) project to both arteries and veins whereas the remaining labeled neurons project to either arteries or veins. Important differences between these two studies is that the previous study used different retrograde tracers (fast blue and diamidino yellow), targeted primary branches of the superior mesenteric artery and vein, and did not verify that paravascular nerves were dissected.

It may be functionally advantageous to have populations of neurons that innervate either arteries or veins and ones that innervate both arteries and veins. With this organization, it is possible to generate graded control of mesenteric blood vessels via firing rate of individual neurons and also via recruitment of additional neurons. For instance, it is possible that low frequency stimulation leads to constriction of just veins whereas higher frequency stimulation leads to recruitment of neurons projecting just to arteries and neurons projecting to both arteries and veins. This is supported by studies showing that veins constrict at much lower frequency stimulation than arteries (Hottenstein and Kreulen, 1987).

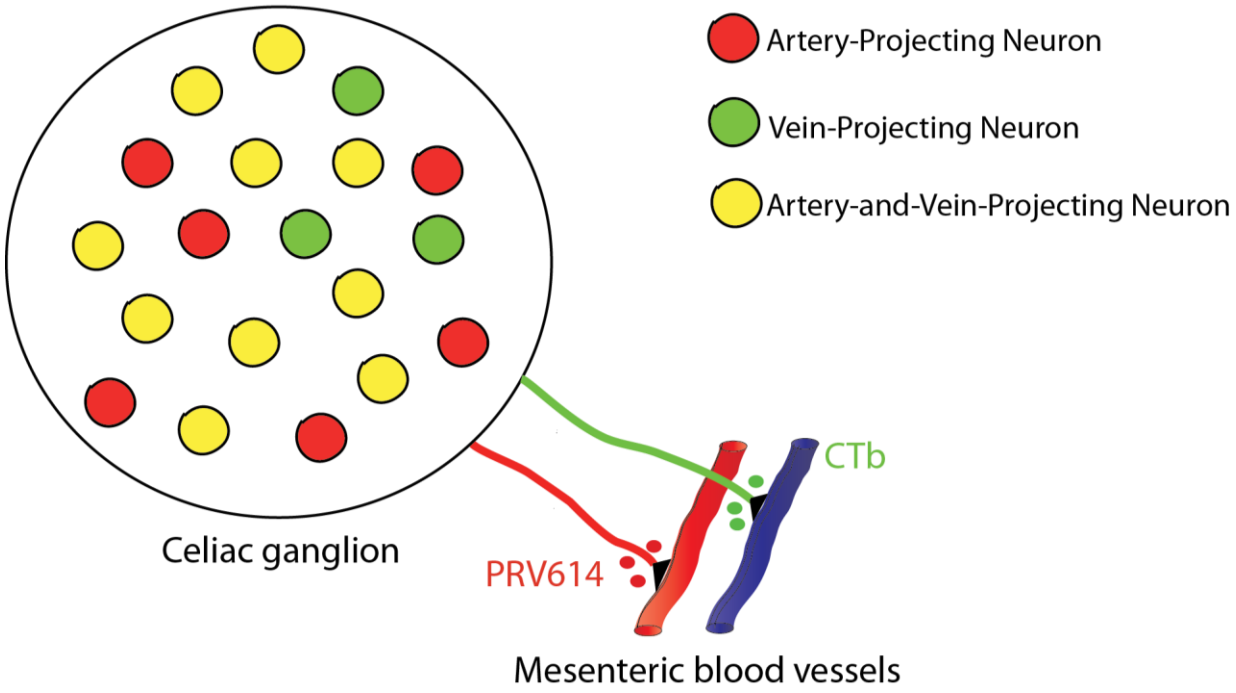

Figure 6.2. Diagram showing the approximate proportion of separate and overlapping sympathetic innervation of mesenteric arteries and veins. The retrograde tracers, PRV614 and CTb, were applied to small segments (~6 mm) of adjacent mesenteric arteries and veins and after 3 days, labeling patterns were observed in the CG. After normalizing to the maximal amount of co-localization observed after mixing tracers and applying to the same blood vessels (66.5%), a majority of PRV614-labeled neurons were also labeled with CTb (59%) and innervated both arteries and veins. The remaining PRV614-labeled neurons were single labeling and only innervated either arteries or veins.

CONVERGENT INPUT TO ARTERIES AND VEINS

A surprising finding was that exposing PRV or CTb tracers to small segments (5-10 mm) of arteries and veins resulted in labeling of large numbers of sympathetic postganglionic neurons (~15% of all CG neurons). This indicates a great deal of converging input to vasculature from sympathetic postganglionic neurons. Alternative explanations for this result may be that the tracers were taken up by nearby paravascular nerves or that the tracers moved transynaptically within the CG across dendrodendritic synapses that are found in sympathetic ganglia (Kondo et al., 1980, Kawai, 1996, Zaidi and Matthews, 1997). However, these explanations were ruled out by controls verifying dissection of paravascular but presence of intact perivascular nerves, and a lack of correlation between number of neurons labeled and survival time. Also, even though CTb is monosynaptic unlike PRV, CTb labeled a similar number of sympathetic neurons after exposing it to small blood vessel segments.

This study sheds new light on the innervation patterns of mesenteric arteries and veins. Dense innervation of splanchnic blood vessels means that recruitment of neurons is an important mechanism in constriction of arteries and veins. It also opens up the possibility that similar to motor neurons, recruitment order of sympathetic postganglionic neurons is physiologically important. According to Henneman's size principle, the recruitment order of motor neurons is from smallest to largest with the smallest neurons innervating the fewest muscle fibers and the largest neurons innervating the most muscle fibers (reviewed in Clamann, 1993). This allows for an exponential rather than a linear increase in force output. Future studies need to investigate whether there is a similar recruitment order for sympathetic postganglionic neurons such that the smallest ones are recruited first and the largest ones are recruited last. Additionally, while there is no difference in soma areas between artery-projecting and vein-projecting neurons, we did not

measure whether there is any difference in artery or vein-projecting neurons and artery and vein-projecting neurons.

DIVERGENCE OF VASCULAR-PROJECTING SYMPATHETIC INNERVATION

We found that there was a similar proportion of separate to overlapping sympathetic innervation to proximal and distal segments of the same blood vessel, adjacent blood vessels of the same type supplying the same segment of the small intestine (ileum), and widely separated blood vessels of the same type supplying different segments of the small intestine (ileum and jejunum). For each of these three preparation types, there is an average of 48.1% of neurons (after normalization to PRV614-labeled neurons) that project to proximal and distal segments of the same blood vessel type, or to two adjacent blood vessels of the same type or to two distant blood vessels of the same type. When considering that the maximal amount of co-localization observed after mixing both tracers was 66.5%, 48.1% of that is 72.3%. Hence, a majority of neurons (72.3%) project widely whereas the remainder project narrowly (**Fig. 6.3**).

The existence of subsets of neurons that diverge widely and ones that diverge narrowly may be functionally advantageous and allow for the activation of many different blood vessels or of a few blood vessels depending on the stimulus. An implication of having a majority of neurons that project widely is that regional differences within splanchnic blood flow are unlikely to occur and indeed, we know of no studies that have examined this question.

Future studies need to examine whether there is a relationship between the size of sympathetic postganglionic neurons and their projection size. Based on previous findings showing a positive correlation between size of the neuron and its target size (Voyvodic, 1989), it is possible that smaller neurons project narrowly while larger neurons project widely. Another

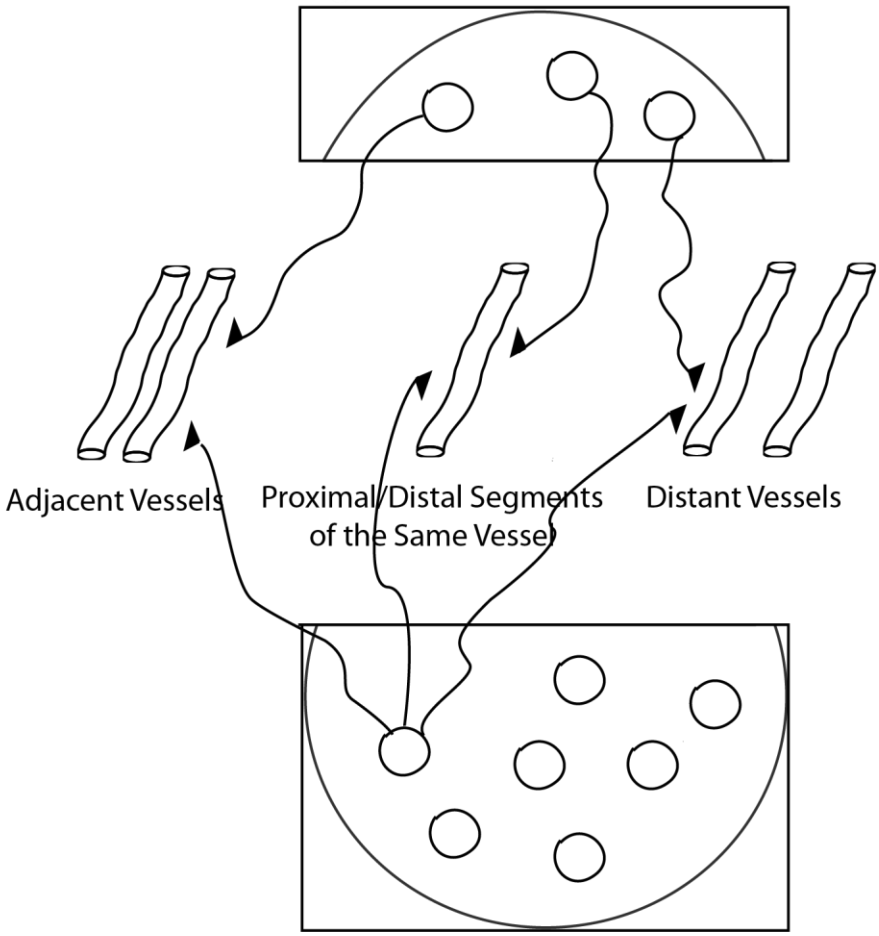

Figure 6.3. Diagram showing the approximate proportion of separate and overlapping sympathetic innervation of proximal and distal segments of the same vessel, adjacent vessels of the same type, and distant vessels of the same type. The retrograde tracers, PRV614 and CTb, were applied to small segments (~8-10 mm) of mesenteric arteries or veins at three locations: 1. Proximal and distal segments of the same blood vessel; 2. Two adjacent blood vessels of the same type; 3. Two distant blood vessels of the same type. All preparations resulted in a similar proportion of PRV614-labeled neurons that were also CTb-labeled. After normalizing to the maximal amount of co-localization observed after mixing tracers and applying to the same blood vessels (66.5%), we found that ~72% of all PRV-labeled neurons projected to proximal and distal segments of a blood vessel, to both adjacent blood vessels, or to both distant blood vessels while the remainder projected to either proximal or distal segments of a blood vessel, to one or the other adjacent blood vessel, or to one or the other distant blood vessel. Based on this, we postulate that the majority of sympathetic postganglionic neurons (shown in the bottom half) project widely to neighboring and widely separated blood vessels while a minority of neurons (shown in the top half) project narrowly to small segments of a single blood vessel.

interesting question to study is whether there is a relationship between the size of the sympathetic postganglionic neuron and its recruitment order. Similar to motor neurons (Clamann, 1993), sympathetic postganglionic neurons may also be recruited according to size, with the smallest ones that project narrowly being recruited first followed by larger neurons that project widely. In addition, the smallest neurons may be ones that selectively project to either arteries or veins whereas larger neurons may be ones that project to both arteries and veins. Such an organization would allow for fine control of arteries or veins at low frequency stimulation and broad control of both arteries and veins at high frequency stimulation.

CONCLUSIONS

This research collectively suggests that instead of an overactive whole sympathetic ganglion, specific pathways within the CG may be activated within hypertension. For instance, 5-HT levels were similar between normotensive and hypertensive CGs and gene expression of genes related to 5-HT synthesis and 5-HT_3 receptors was lower in hypertensive CGs. However, whole ganglia levels may not accurately reflect pathway-specific 5-HT levels and gene expression. Similarly, no difference was found basal neuronal activation measured with c-fos expression between normotensive and hypertensive CGs. However, less neuronal activation was observed after direct stimulation of the CG via preganglionic nerve stimulation and nicotine treatment in hypertensive compared to normotensive CGs. This may be due to desensitization of nicotinic receptors from a higher preganglionic sympathetic drive. Interestingly, a metabolic stimulus, 2-DG, did not result in any difference in c-fos expression between normotensive and hypertensive CGs suggesting that the desensitization of nicotinic receptors may be pathway-specific. Studying sympathetic innervation to mesenteric arteries and veins also uncovered several important insights. Using two PRVs allowed for labeling of artery-projecting and vein-projecting neurons but using a PRV with CTb was better suited for studying whether sympathetic innervation of arteries and veins was separate or overlapping. A majority of neurons in the CG project to both arteries and veins but a large minority project to either arteries or veins. Also, most neurons in the CG projected to two adjacent or two widely separated blood vessels of the same type indicating that while most CG neurons have a wide field of innervation, some neurons have a narrow one.

REFERENCES

REFERENCES

Akasu T, Hirai K, Koketsu K (1981) 5-hydroxytryptamine controls ACh-receptor sensitivity of bullfrog sympathetic ganglion cells. Brain research 211:217-220.

Akasu T, Koketsu K (1986) 5-Hydroxytryptamine decreases the sensitivity of nicotinic acetylcholine receptor in bull-frog sympathetic ganglion cells. The Journal of physiology 380:93-109.

Akasu T, Ohta Y, Koketsu K (1984) Neuropeptides facilitate the desensitization of nicotinic acetylcholine-receptor in frog skeletal muscle endplate. Brain Res 290:342-347.

Alkadhi KA, Salgado-Commissariat D, Hogan YH, Akpaudo SB (1996) Induction and maintenance of ganglionic long-term potentiation require activation of 5-hydroxytryptamine (5-HT3) receptors. The Journal of physiology 496 (Pt 2):479-489.

Amsterdam JD, Garcia-Espana F, Fawcett J, Quitkin FM, Reimherr FW, Rosenbaum JF, Beasley C (1999) Blood pressure changes during short-term fluoxetine treatment. J Clin Psychopharmacol 19:9-14.

Anand BK, Chhina GS, Sharma KN, Dua S, Singh B (1964) Activity of Single Neurons in the Hypothalamic Feeding Centers: Effect of Glucose. The American journal of physiology 207:1146-1154.

Andersson PO (1983) Comparative vascular effects of stimulation continuously and in bursts of the sympathetic nerves to cat skeletal muscle. Acta physiologica Scandinavica 118:343-348.

Banfield BW, Kaufman JD, Randall JA, Pickard GE (2003) Development of pseudorabies virus strains expressing red fluorescent proteins: new tools for multisynaptic labeling applications. J Virol 77:10106-10112.

Barman SM, Orer HS, Gebber GL (2001) The role of the medullary lateral tegmental field in the generation and baroreceptor reflex control of sympathetic nerve discharge in the cat. Annals of the New York Academy of Sciences 940:270-285.

Barnes NM, Hales TG, Lummis SC, Peters JA (2009) The 5-HT3 receptor--the relationship between structure and function. Neuropharmacology 56:273-284.

Bloom SR, Edwards AV, Hardy RN (1978) The role of the autonomic nervous system in the control of glucagon, insulin and pancreatic polypeptide release from the pancreas. The Journal of physiology 280:9-23.

Boyd HD, McLachlan EM, Keast JR, Inokuchi H (1996) Three electrophysiological classes of guinea pig sympathetic postganglionic neurone have distinct morphologies. J Comp Neurol 369:372-387.

Bratton B, Davies P, Janig W, McAllen R (2010) Ganglionic transmission in a vasomotor pathway studied in vivo. The Journal of physiology 588:1647-1659.

Brittle EE, Reynolds AE, Enquist LW (2004) Two modes of pseudorabies virus neuroinvasion and lethality in mice. Journal of virology 78:12951-12963.

Brown J (1962) Effects of 2-deoxyglucose on carbohydrate metablism: review of the literature and studies in the rat. Metabolism 11:1098-1112.

Browning KN, Zheng Z, Kreulen DL, Travagli RA (1999) Two populations of sympathetic neurons project selectively to mesenteric artery or vein. Am J Physiol 276:H1263-1272.

Cajal SR (1995) Histology of the nervous system of man and vertebrates. New York: Oxford University Press.

Cano G, Card JP, Sved AF (2004) Dual viral transneuronal tracing of central autonomic circuits involved in the innervation of the two kidneys in rat. J Comp Neurol 471:462-481.

Cao X, Dai X, Parker LM, Kreulen DL (2007) Differential regulation of NADPH oxidase in sympathetic and sensory Ganglia in deoxycorticosterone acetate salt hypertension. Hypertension 50:663-671.

Cao X, Demel SL, Quinn MT, Galligan JJ, Kreulen D (2009) Localization of NADPH oxidase in sympathetic and sensory ganglion neurons and perivascular nerve fibers. Auton Neurosci 151:90-97.

Card JP, Rinaman L, Lynn RB, Lee BH, Meade RP, Miselis RR, Enquist LW (1993) Pseudorabies virus infection of the rat central nervous system: ultrastructural characterization of viral replication, transport, and pathogenesis. The Journal of neuroscience : the official journal of the Society for Neuroscience 13:2515-2539.

Card JP, Rinaman L, Schwaber JS, Miselis RR, Whealy ME, Robbins AK, Enquist LW (1990) Neurotropic properties of pseudorabies virus: uptake and transneuronal passage in the rat central nervous system. The Journal of neuroscience : the official journal of the Society for Neuroscience 10:1974-1994.

Carlsson A, Lindqvist M (1978) Dependence of 5-HT and catecholamine synthesis on concentrations of precursor amino-acids in rat brain. Naunyn-Schmiedeberg's archives of pharmacology 303:157-164.

Chen S, Yang M, Miselis RR, Aston-Jones G (1999) Characterization of transsynaptic tracing with central application of pseudorabies virus. Brain Research 838:171-183.

Clamann HP (1993) Motor unit recruitment and the gradation of muscle force. Physical therapy 73:830-843.

Conte WL, Kamishina H, Reep RL (2009) The efficacy of the fluorescent conjugates of cholera toxin subunit B for multiple retrograde tract tracing in the central nervous system. Brain Struct Funct 213:367-373.

Costa M, Furness JB (1984) Somatostatin is present in a subpopulation of noradrenergic nerve fibres supplying the intestine. Neuroscience 13:911-919.

Crowcroft PJ, Szurszewski JH (1971) A study of the inferior mesenteric and pelvic ganglia of guinea-pigs with intracellular electrodes. The Journal of physiology 219:421-441.

Curran T, Morgan JI (1995) Fos: an immediate-early transcription factor in neurons. Journal of Neurobiology 26:403-412.

Dai X, Cao X, Kreulen DL (2006) Superoxide anion is elevated in sympathetic neurons in DOCA-salt hypertension via activation of NADPH oxidase. Am J Physiol Heart Circ Physiol 290:H1019-1026.

De Jager S (1886) Experiments and Considerations on Haemodynamics. The Journal of physiology 7:130-215.

De SN (1959) Enterotoxicity of bacteria-free culture-filtrate of Vibrio cholerae. Nature 183:1533-1534.

Dehal NS, Kartseva A, Weaver LC (1992) Comparison of locations and peptide content of postganglionic neurons innervating veins and arteries of the rat hindlimb. Journal of the autonomic nervous system 39:61-72.

Diaz J, Ni W, Thompson J, King A, Fink GD, Watts SW (2008) 5-Hydroxytryptamine lowers blood pressure in normotensive and hypertensive rats. J Pharmacol Exp Ther 325:1031-1038.

Doucet E, Latremoliere A, Darmon M, Hamon M, Emerit MB (2007) Immunolabelling of the 5-HT 3B receptor subunit in the central and peripheral nervous systems in rodents. Eur J Neurosci 26:355-366.

Dun NJ, Kiraly M, Ma RC (1984) Evidence for a serotonin-mediated slow excitatory potential in the guinea-pig coeliac ganglia. The Journal of physiology 351:61-76.

Dunn SM, Raftery MA (2000) Roles of agonist-binding sites in nicotinic acetylcholine receptor function. Biochem Biophys Res Commun 279:358-362.

Eccles RM (1955) Intracellular potentials recorded from a mammalian sympathetic ganglion. The Journal of physiology 130:572-584.

Edmunds ME, Russell GI, Burton PR, Swales JD (1990) Vascular capacitance in rats subjected to chemical renal medullectomy. Hypertension 15:576-582.

Eich RH, Peters RJ, Cuddy RP, Smulyanh, Lyons RH (1962) The hemodynamics in labile hypertension. Am Heart J 63:188-195.

Elfvin LG, Lindh B, Hokfelt T (1993) The chemical neuroanatomy of sympathetic ganglia. Annu Rev Neurosci 16:471-507.

Enquist LW, Card JP (2003) Recent advances in the use of neurotropic viruses for circuit analysis. Current Opinion in Neurobiology 13:603-606.

Esler M (2000) The sympathetic system and hypertension. Am J Hypertens 13:99S-105S.

Esler M, Jennings G, Biviano B, Lambert G, Hasking G (1986) Mechanism of elevated plasma noradrenaline in the course of essential hypertension. J Cardiovasc Pharmacol 8 Suppl 5:S39-43.

Esler M, Jennings G, Korner P, Blombery P, Burke F, Willett I, Leonard P (1984) Total, and organ-specific, noradrenaline plasma kinetics in essential hypertension. Clin Exp Hypertens A 6:507-521.

Esler M, Lambert E, Schlaich M (2010) Rebuttal from Esler, Lambert, and Schlaich. J Appl Physiol 109:2000-2001.

Esler M, Lambert G, Jennings G (1989) Regional norepinephrine turnover in human hypertension. Clin Exp Hypertens A 11 Suppl 1:75-89.

Fenster CP, Hicks JH, Beckman ML, Covernton PJ, Quick MW, Lester RA (1999) Desensitization of nicotinic receptors in the central nervous system. Annals of the New York Academy of Sciences 868:620-623.

Fernstrom JD (1983) Role of precursor availability in control of monoamine biosynthesis in brain. Physiological reviews 63:484-546.

Fink GD (2009) Arthur C. Corcoran Memorial Lecture. Sympathetic activity, vascular capacitance, and long-term regulation of arterial pressure. Hypertension 53:307-312.

Fink GD, Johnson RJ, Galligan JJ (2000) Mechanisms of increased venous smooth muscle tone in desoxycorticosterone acetate-salt hypertension. Hypertension 35:464-469.

Fluckiger JP, Gremaud G, Waeber B, Kulik A, Ichino A, Nussberger J, Brunner HR (1989) Measurement of sympathetic nerve activity in the unanesthetized rat. J Appl Physiol 67:250-255.

Foss JD, Fink GD, Osborn JW (2013) Reversal of genetic salt-sensitive hypertension by targeted sympathetic ablation. Hypertension 61:806-811.

Friedman PA, Kappelman AH, Kaufman S (1972) Partial purification and characterization of tryptophan hydroxylase from rabbit hindbrain. The Journal of biological chemistry 247:4165-4173.

Gale JD, Cowen T (1988) The origin and distribution of 5-hydroxytryptamine-like immunoreactive nerve fibres to major mesenteric blood vessels of the rat. Neuroscience 24:1051-1059.

Gibbins IL (1992) Vasoconstrictor, vasodilator and pilomotor pathways in sympathetic ganglia of guinea-pigs. Neuroscience 47:657-672.

Gibbins IL, Hoffmann B, Morris JL (1998) Peripheral fields of sympathetic vasoconstrictor neurons in guinea pigs. Neuroscience letters 248:89-92.

Gibbins IL, Jobling P, Morris JL (2003) Functional organization of peripheral vasomotor pathways. Acta Physiol Scand 177:237-245.

Gibbins IL, Morris JL (1990) Sympathetic noradrenergic neurons containing dynorphin but not neuropeptide Y innervate small cutaneous blood vessels of guinea-pigs. J Auton Nerv Syst 29:137-149.

Gibbins IL, Morris JL (2006) Structure of peripheral synapses: autonomic ganglia. Cell and tissue research 326:205-220.

Glauser DL, Strasser R, Laimbacher AS, Saydam O, Clement N, Linden RM, Ackermann M, Fraefel C (2007) Live covisualization of competing adeno-associated virus and herpes simplex virus type 1 DNA replication: molecular mechanisms of interaction. Journal of virology 81:4732-4743.

Gothert M, Kollecker P, Rohm N, Zerkowski HR (1986) Inhibitory presynaptic 5-hydroxytryptamine (5-HT) receptors on the sympathetic nerves of the human saphenous vein. Naunyn Schmiedebergs Arch Pharmacol 332:317-323.

Guyenet PG (2006) The sympathetic control of blood pressure. Nat Rev Neurosci 7:335-346.

Hanani M (2010) Satellite glial cells in sympathetic and parasympathetic ganglia: in search of function. Brain Res Rev 64:304-327.

Happola O (1988) 5-Hydroxytryptamine-immunoreactive neurons and nerve fibers in the superior cervical ganglion of the rat. Neuroscience 27:301-307.

Hill CE, Hendry IA, Sheppard A (1987) Use of the fluorescent dye, fast blue, to label sympathetic postganglionic neurones supplying mesenteric arteries and enteric neurones of the rat. J Auton Nerv Syst 18:73-82.

Hill CE, Hirst GD, van Helden DF (1983) Development of sympathetic innervation to proximal and distal arteries of the rat mesentery. The Journal of physiology 338:129-147.

Hoobler SW, Manning JT, Paine WG, Mc CS, Helcher PO, Renfert H, Jr., Peet MM, Kahn EA (1951) The effects of splanchnicectomy on the blood pressure in hypertension; a controlled study. Circulation 4:173-183.

Hottenstein OD, Kreulen DL (1987) Comparison of the frequency dependence of venous and arterial responses to sympathetic nerve stimulation in guinea-pigs. J Physiol 384:153-167.

Hsieh NK, Liu JC, Chen HI (2000) Localization of sympathetic postganglionic neurons innervating mesenteric artery and vein in rats. J Auton Nerv Syst 80:1-7.

Huganir RL, Miles K (1989) Protein phosphorylation of nicotinic acetylcholine receptors. Critical reviews in biochemistry and molecular biology 24:183-215.

Itoyama Y, Sekizawa T, Openshaw H, Kogure K, Goto I (1991) Early loss of astrocytes in herpes simplex virus-induced central nervous system demyelination. Annals of neurology 29:285-292.

Janig W, McLachlan EM (1992a) Characteristics of function-specific pathways in the sympathetic nervous system. Trends in Neurosciences 15:475-481.

Janig W, McLachlan EM (1992b) Specialized functional pathways are the building blocks of the autonomic nervous system. J Auton Nerv Syst 41:3-13.

Joshi S, Levatte MA, Dekaban GA, Weaver LC (1995) Identification of spinal interneurons antecedent to adrenal sympathetic preganglionic neurons using trans-synaptic transport of herpes simplex virus type 1. Neuroscience 65:893-903.

Julius S, Esler M (1975) Autonomic nervous cardiovascular regulation in borderline hypertension. Am J Cardiol 36:685-696.

Kandlikar SS, Fink GD (2011a) Mild DOCA-salt hypertension: sympathetic system and role of renal nerves. Am J Physiol Heart Circ Physiol 300:H1781-1787.

Kandlikar SS, Fink GD (2011b) Splanchnic sympathetic nerves in the development of mild DOCA-salt hypertension. Am J Physiol Heart Circ Physiol 301:H1965-1973.

Karhula T, Soinila S, Lakomy M, Majewski M, Kaleczyk J, Happola O (1995) 5-Hydroxytryptamine-immunoreactive nerve fibers in the rat and porcine prevertebral sympathetic ganglia: effect of precursor loading and relation to catecholaminergic neurons. Neurosci Lett 194:85-88.

Karim F, Hainsworth R (1976) Responses of abdominal vascular capacitance to stimulation of splachnic nerves. The American journal of physiology 231:434-440.

Karlsson S, Ahren B (1991) Contribution of adrenergic nerves and the adrenals to 2-deoxy-D-glucose-induced insulin and glucagon secretion in the mouse. Int J Pancreatol 10:207-215.

Kawai Y (1996) Ultrastructure of neuronal circuitry in sympathetic ganglia. Microscopy Research and Technique 35:146-156.

Kawai Y, Senba E (1997) Noradrenaline-mediated lateral inhibition in the sympathetic ganglion. Neuroscience letters 238:87-89.

Keast JR, McLachlan EM, Meckler RL (1993) Relation between electrophysiological class and neuropeptide content of guinea pig sympathetic prevertebral neurons. J Neurophysiol 69:384-394.

Kielian T (2008) Glial connexins and gap junctions in CNS inflammation and disease. Journal of neurochemistry 106:1000-1016.

King AJ, Novotny M, Swain GM, Fink GD (2008) Whole body norepinephrine kinetics in ANG II-salt hypertension in the rat. Am J Physiol Regul Integr Comp Physiol 294:R1262-1267.

King AJ, Osborn JW, Fink GD (2007) Splanchnic circulation is a critical neural target in angiotensin II salt hypertension in rats. Hypertension 50:547-556.

Kiraly M, Ma RC, Dun NJ (1983) Serotonin mediates a slow excitatory potential in mammalian celiac ganglia. Brain research 275:378-383.

Knoper SR, Matsumoto SG, Kreulen DL (1992) Response to 5-hydroxytryptamine on neurons of guinea pig celiac and inferior mesenteric ganglia in primary culture. Life Sci 51:703-710.

Kobbert C, Apps R, Bechmann I, Lanciego JL, Mey J, Thanos S (2000) Current concepts in neuroanatomical tracing. Prog Neurobiol 62:327-351.

Koistinaho J (1991) Nicotine-induced fos-like immunoreactivity in rat sympathetic ganglia and adrenal medulla. Neuroscience Letters 128:47-51.

Kondo H, Dun NJ, Pappas GD (1980) A light and electron microscopic study of the rat superior cervical ganglion cells by intracellular HRP-labeling. Brain Research 197:193-199.

Kreulen DL (1984) Integration in autonomic ganglia. Physiologist 27:49-55.

Kreulen DL (1986) Activation of mesenteric arteries and veins by preganglionic and postganglionic nerves. The American journal of physiology 251:H1267-1275.

Kreulen DL (2003) Properties of the venous and arterial innervation in the mesentery. J Smooth Muscle Res 39:269-279.

Kreulen DL, Szurszewski JH (1979a) Nerve pathways in celiac plexus of the guinea pig. The American journal of physiology 237:E90-97.

Kreulen DL, Szurszewski JH (1979b) Reflex pathways in the abdominal prevertebral ganglia: evidence for a colo-colonic inhibitory reflex. The Journal of physiology 295:21-32.

Krishnaswamy A, Cooper E (2012) Reactive oxygen species inactivate neuronal nicotinic acetylcholine receptors through a highly conserved cysteine near the intracellular mouth of the channel: implications for diseases that involve oxidative stress. J Physiol 590:39-47.

Kuhn DM, Wolf WA, Lovenberg W (1980) Review of the role of the central serotonergic neuronal system in blood pressure regulation. Hypertension 2:243-255.

Lacroix JS, Stjarne P, Anggard A, Lundberg JM (1988) Sympathetic vascular control of the pig nasal mucosa: (I). Increased resistance and capacitance vessel responses upon stimulation with irregular bursts compared to continuous impulses. Acta physiologica Scandinavica 132:83-90.

Langley JN (1893) The Arrangement of the Sympathetic Nervous System, based chiefly on Observations upon Pilo-motor Nerves. The Journal of physiology 15:176-248 121.

Langley JN, Anderson HK (1895) On the Innervation of the Pelvic and Adjoining Viscera: Part I. The Lower Portion of the Intestine. The Journal of physiology 18:67-105.

LaVail JH, Carter SR, Topp KS (1993) The retrograde tracer Fluoro-Gold interferes with the infectivity of herpes simplex virus. Brain research 625:57-62.

Lazartigues E, Brefel-Courbon C, Bagheri H, Costes S, Gharib C, Tran MA, Senard JM, Montastruc JL (2000) Fluoxetine-induced pressor response in freely moving rats: a role for vasopressin and sympathetic tone. Fundam Clin Pharmacol 14:443-451.

Li M, Galligan J, Wang D, Fink G (2010) The effects of celiac ganglionectomy on sympathetic innervation to the splanchnic organs in the rat. Autonomic neuroscience : basic & clinical 154:66-73.

London GM, Safar ME, Simon AC, Alexandre JM, Levenson JA, Weiss YA (1978) Total effective compliance, cardiac output and fluid volumes in essential hypertension. Circulation 57:995-1000.

Lookingland KJ, Shannon NJ, Chapin DS, Moore KE (1986) Exogenous tryptophan increases synthesis, storage, and intraneuronal metabolism of 5-hydroxytryptamine in the rat hypothalamus. Journal of neurochemistry 47:205-212.

Lovenberg W, Kuhn DM (1982) Substrate regulation of serotonin synthesis. Adv Biochem Psychopharmacol 34:73-83.

Lundgren O (1983) Role of splanchnic resistance vessels in overall cardiovascular homeostasis. Fed Proc 42:1673-1677.

Luo M, Hess MC, Fink GD, Olson LK, Rogers J, Kreulen DL, Dai X, Galligan JJ (2003) Differential alterations in sympathetic neurotransmission in mesenteric arteries and veins in DOCA-salt hypertensive rats. Auton Neurosci 104:47-57.

Ma RC, Horwitz J, Kiraly M, Perlman RL, Dun NJ (1985) Immunohistochemical and biochemical detection of serotonin in the guinea pig celiac-superior mesenteric plexus. Neuroscience letters 56:107-112.

Magee JC, Schofield GG (1992) Neurotransmission through sympathetic ganglia of spontaneously hypertensive rats. Hypertension 20:367-373.

Malpas SC (2010) Sympathetic nervous system overactivity and its role in the development of cardiovascular disease. Physiological Reviews 90:513-557.

Martin DS, Rodrigo MC, Appelt CW (1998) Venous tone in the developmental stages of spontaneous hypertension. Hypertension 31:139-144.

May CN (1996) Prolonged systemic and regional haemodynamic effects of intracerebroventricular angiotensin II in conscious sheep. Clinical and experimental pharmacology & physiology 23:878-884.

May CN (2006) Differential regional haemodynamic changes during mineralocorticoid hypertension. Journal of Hypertension 24:1137-1146.

McFerran JB, Dow C (1975) Studies on immunisation of pigs with the Bartha strain of Aujeszky's disease virus. Research in veterinary science 19:17-22.

McLachlan EM (ed.) (1995) Autonomic Ganglia. Luxembourg: Harwood Academic Publishers GmbH.

McLean IW, Nakane PK (1974) Periodate-lysine-paraformaldehyde fixative. A new fixation for immunoelectron microscopy. J Histochem Cytochem 22:1077-1083.

Meehan AG, Kreulen DL (1991) Electrophysiological studies on the interaction of 5-hydroxytryptamine with sympathetic transmission in the guinea pig inferior mesenteric artery and ganglion. J Pharmacol Exp Ther 256:82-87.

Mei Q, Mundinger TO, Kung D, Baskin DG, Taborsky GJ, Jr. (2001) Fos expression in rat celiac ganglion: an index of the activation of postganglionic sympathetic nerves. American journal of physiology Endocrinology and metabolism 281:E655-664.

Milner WR (1990) Cardiovascular Physiology. New York: Oxford University Press.

Minson J, Arnolda L, Llewellyn-Smith I, Pilowsky P, Chalmers J (1996) Altered c-fos in rostral medulla and spinal cord of spontaneously hypertensive rats. Hypertension 27:433-441.

Morris JL (1995) Distribution and peptide content of sympathetic axons innervating different regions of the cutaneous venous bed in the pinna of the guinea pig ear. Journal of vascular research 32:378-386.

Muller T, Hahn EC, Tottewitz F, Kramer M, Klupp BG, Mettenleiter TC, Freuling C (2011) Pseudorabies virus in wild swine: a global perspective. Arch Virol 156:1691-1705.

Niijima A (1975) The effect of 2-deoxy-D-glucose and D-glucose on the efferent discharge rate of sympathetic nerves. The Journal of physiology 251:231-243.

Niijima A (1989) Neural mechanisms in the control of blood glucose concentration. J Nutr 119:833-840.

Nilsson H, Ljung B, Sjoblom N, Wallin BG (1985) The influence of the sympathetic impulse pattern on contractile responses of rat mesenteric arteries and veins. Acta physiologica Scandinavica 123:303-309.

Norgren RB, Jr., Lehman MN (1998) Herpes simplex virus as a transneuronal tracer. Neurosci Biobehav Rev 22:695-708.

Oomura Y, Kimura K, Ooyama H, Maeno T, Iki M, Kuniyoshi M (1964) Reciprocal Activities of the Ventromedial and Lateral Hypothalamic Areas of Cats. Science 143:484-485.

Osborn JW, Fink GD, Kuroki MT (2011) Neural mechanisms of angiotensin II-salt hypertension: implications for therapies targeting neural control of the splanchnic circulation. Curr Hypertens Rep 13:221-228.

Palkovits M (1973) Isolated removal of hypothalamic or other brain nuclei of the rat. Brain research 59:449-450.

Pang CC (2001) Autonomic control of the venous system in health and disease: effects of drugs. Pharmacology & Therapeutics 90:179-230.

Park J, Galligan JJ, Fink GD, Swain GM (2010) Alterations in sympathetic neuroeffector transmission to mesenteric arteries but not veins in DOCA-salt hypertension. Auton Neurosci 152:11-20.

Pascoe WS, Smythe GA, Storlien LH (1989) 2-deoxy-D-glucose-induced hyperglycemia: role for direct sympathetic nervous system activation of liver glucose output. Brain Research 505:23-28.

Perko MJ, Nielsen HB, Skak C, Clemmesen JO, Schroeder TV, Secher NH (1998) Mesenteric, coeliac and splanchnic blood flow in humans during exercise. The Journal of physiology 513 (Pt 3):907-913.

Pomeranz LE, Reynolds AE, Hengartner CJ (2005) Molecular biology of pseudorabies virus: impact on neurovirology and veterinary medicine. Microbiol Mol Biol Rev 69:462-500.

Price HL, Deutsch S, Marshall BE, Stephen GW, Behar MG, Neufeld GR (1966) Hemodynamic and metabolic effects of hemorrhage in man, with particular reference to the splanchnic circulation. Circulation Research 18:469-474.

Rinaman L, Card JP, Enquist LW (1993) Spatiotemporal responses of astrocytes, ramified microglia, and brain macrophages to central neuronal infection with pseudorabies virus. The Journal of neuroscience : the official journal of the Society for Neuroscience 13:685-702.

Rinaman L, Schwartz G (2004) Anterograde transneuronal viral tracing of central viscerosensory pathways in rats. The Journal of neuroscience : the official journal of the Society for Neuroscience 24:2782-2786.

Rosas-Ballina M, Ochani M, Parrish WR, Ochani K, Harris YT, Huston JM, Chavan S, Tracey KJ (2008) Splenic nerve is required for cholinergic antiinflammatory pathway control of TNF in endotoxemia. Proceedings of the National Academy of Sciences of the United States of America 105:11008-11013.

Rothe CF (1983) Reflex control of veins and vascular capacitance. Physiol Rev 63:1281-1342.

Rowell LB (1973) Regulation of splanchnic blood flow in man. The Physiologist 16:127-142.

Samar RE, Coleman TG (1979) Whole body response of the peripheral circulation following hemorrhage in the rat. The American journal of physiology 236:H206-210.

Sanchez J, Holmgren J (2011) Cholera toxin - a foe & a friend. Indian J Med Res 133:153-163.

Skok VI (2002) Nicotinic acetylcholine receptors in autonomic ganglia. Autonomic neuroscience : basic & clinical 97:1-11.

Smith GP, Epstein AN (1969) Increased feeding in response to decreased glucose utilization in the rat and monkey. The American journal of physiology 217:1083-1087.

Song CK, Enquist LW, Bartness TJ (2005) New developments in tracing neural circuits with herpesviruses. Virus Res 111:235-249.

Sripairojthikoon W, Wyss JM (1987) Cells of origin of the sympathetic renal innervation in rat. The American journal of physiology 252:F957-963.

Sved AF, Ito S, Sved JC (2003) Brainstem mechanisms of hypertension: role of the rostral ventrolateral medulla. Current hypertension reports 5:262-268.

Taborsky GJ, Jr., Ahren B, Havel PJ (1998) Autonomic mediation of glucagon secretion during hypoglycemia: implications for impaired alpha-cell responses in type 1 diabetes. Diabetes 47:995-1005.

Takeshita A, Mark AL (1979) Decreased venous distensibility in borderline hypertension. Hypertension 1:202-206.

Tanaka K, Chiba T (1996) Microvascular organization of sympathetic ganglia, with special reference to small intensely-fluorescent cells. Microsc Res Tech 35:137-145.

Tang YW, Mitchell PS, Espy MJ, Smith TF, Persing DH (1999) Molecular diagnosis of herpes simplex virus infections in the central nervous system. J Clin Microbiol 37:2127-2136.

Ten Tusscher MP, Klooster J, Vrensen GF (1989) Satellite cells as blood-ganglion cell barrier in autonomic ganglia. Brain research 490:95-102.

Turner SL, Jenkins FJ (1997) The roles of herpes simplex virus in neuroscience. J Neurovirol 3:110-125.

Uki M, Nabekura J, Akaike N (1999) Suppression of the nicotinic acetylcholine response in rat superior cervical ganglionic neurons by steroids. J Neurochem 72:808-814.

Vanhoutte PM (ed.) (1985) Serotonin and the Cardiovascular System. New York: Raven Press.

Veenstra-VanderWeele J, Cook EH, Jr. (2003) Knockout mouse points to second form of tryptophan hydroxylase. Mol Interv 3:72-75, 50.

Vollmer RR, Balcita JJ, Sved AF, Edwards DJ (1997) Adrenal epinephrine and norepinephrine release to hypoglycemia measured by microdialysis in conscious rats. The American journal of physiology 273:R1758-1763.

Voyvodic JT (1989) Peripheral target regulation of dendritic geometry in the rat superior cervical ganglion. The Journal of neuroscience : the official journal of the Society for Neuroscience 9:1997-2010.

Wang H, Sun X (2005) Desensitized nicotinic receptors in brain. Brain research Brain research reviews 48:420-437.

Watson RE, Supowit SC, Zhao H, Katki KA, Dipette DJ (2002) Role of sensory nervous system vasoactive peptides in hypertension. Brazilian journal of medical and biological research = Revista brasileira de pesquisas medicas e biologicas / Sociedade Brasileira de Biofisica [et al] 35:1033-1045.

Weiss P, Hiscoe HB (1948) Experiments on the mechanism of nerve growth. J Exp Zool 107:315-395.

Wessendorf MW (1991) Fluoro-Gold: composition, and mechanism of uptake. Brain research 553:135-148.

Whitley RJ, Roizman B (2001) Herpes simplex virus infections. Lancet 357:1513-1518.

Widgren BR, Berglund G, Wikstrand J, Andersson OK (1992) Reduced venous compliance in normotensive men with positive family histories of hypertension. Journal of Hypertension 10:459-465.

Widimsky J, Fejfarova MH, Fejfar Z (1957) Changes of cardiac output in hypertensive disease. Cardiologia 31:381-389.

Yamamoto J, Goto Y, Nakai M, Ogino K, Ikeda M (1983) Circulatory pressure-volume relationship and cardiac output in DOCA-salt rats. Hypertension 5:507-513.

Yang M, Card JP, Tirabassi RS, Miselis RR, Enquist LW (1999) Retrograde, transneuronal spread of pseudorabies virus in defined neuronal circuitry of the rat brain is facilitated by gE mutations that reduce virulence. Journal of virology 73:4350-4359.

Ye ZY, Li DP, Li L, Pan HL (2011) Protein kinase CK2 increases glutamatergic input in the hypothalamus and sympathetic vasomotor tone in hypertension. J Neurosci 31:8271-8279.

Yoshimoto M, Miki K, Fink GD, King A, Osborn JW (2010) Chronic angiotensin II infusion causes differential responses in regional sympathetic nerve activity in rats. Hypertension 55:644-651.

Young DB, Murray RH, Bengis RG, Markov AK (1980) Experimental angiotensin II hypertension. The American journal of physiology 239:H391-398.

Záborszky L, Wouterlood FG, Lanciego JL (2006) Neuroanatomical Tract-Tracing: Molecules, Neurons, and Systems. New York: Springer.

Zaidi ZF, Matthews MR (1997) Exocytotic release from neuronal cell bodies, dendrites and nerve terminals in sympathetic ganglia of the rat, and its differential regulation. Neuroscience 80:861-891.

Zheng ZL, Travagli RA, Kreulen DL (1999) Patterns of innervation of sympathetic vascular neurons by peptide-containing primary sensory fibers. Brain Res 827:113-121.